Geological Survey of Finland 2020

Natural stone exploration in the classic Wiborg rapakivi granite batholith of southeastern Finland – new insights from integration of lithological, geophysical and structural data

Paavo Härmä

Bulletin 411 • Monograph: Academic Dissertation

GTK

Geological Survey of Finland, Bulletin

The Bulletin of the Geological Survey of Finland publishes the results of scientific research that is thematically or geographically connected to Finnish or Fennoscandian geology, or otherwise related to research and innovation at GTK. Articles by researchers outside GTK are also welcome. All manuscripts are peer reviewed.

Instructions for authors available from the Scientific Editor.

GEOLOGICAL SURVEY OF FINLAND

Bulletin 411

Natural stone exploration in the classic Wiborg rapakivi granite batholith of southeastern Finland – new insights from integration of lithological, geophysical and structural data

by

Paavo Härmä

ACADEMIC DISSERTATION

Department of Geosciences and Geography, University of Helsinki

To be presented, with the permission of the Faculty of Science of the University of Helsinki, for public examination in a remote event that will be streamed from room P673, Porthania campus on 27 May 2020, at 12 o'clock noon.

Unless otherwise indicated, the figures have been prepared by the author of the publication.

https://doi.org/10.30440/bt411

Layout: Elvi Turtiainen Oy
Printing house: Edita Prima Oy

Espoo 2020

Supervisors

Docent Olavi Selonen
Åbo Akademi University
Department of Natural Sciences
Geology and Mineralogy
Turku, Finland

Professor O. Tapani Rämö
University of Helsinki
Department of Geosciences and Geography
Helsinki, Finland

Pre-examiners

Dr Vitali Shekov
Deputy Director of the Institute of Geology of the Karelian Research Center
Russian Academy of Sciences
Petrozavodsk, Russian Federation

Docent Pekka Vallius
CEO of Geopex Oy
Kouvola, Finland

Opponent

Docent Pekka Ihalainen
University of Turku
Department of Geography and Geology
Turku, Finland

Härmä, P. 2020. Natural stone exploration in the classic Wiborg rapakivi granite batholith of southeastern Finland – new insights from integration of lithological, geophysical and structural data. *Geological Survey of Finland, Bulletin 411,* 90 pages, 57 figures and 3 tables.

The main objective of this doctoral research was to examine the surficial weathering of rapakivi granites and to develop a revised exploration process for natural stone, more suited to the weathered granites in the classic Wiborg batholith of southeastern Finland. The study area covers the Wiborg batholith, excluding the satellite intrusions of Ahvenisto and Suomenniemi and the Russian part of the batholith. The lithology, fracturing and outcrop weathering of the batholith were defined. In addition, the applicability of new geophysical methods to natural stone exploration, such as electrical resistivity tomography (ERT) and induced polarization (IP), was tested in detecting weathered zones. The potentiality of the different rapakivi granite types of the Wiborg batholith for natural stone extraction was also evaluated.

The lithological assemblage of the Wiborg rapakivi granite batholith is divided into seven main granite types: wiborgite, dark wiborgite, pyterlite, porphyritic rapakivi granite, even-grained rapakivi granite, dark rapakivi granite and aplitic rapakivi granite. The fracture pattern in the rapakivi granite types is mainly orthogonal. In the southeastern part of the batholith, diagonal patterns are found. As observed on outcrops, subhorizontal fractures are dominant in all rapakivi granite types, but subvertical fractures sporadically prevail. The fracture orientation of N30°W is prevalent in all of the rapakivi granites types. Fractures in the direction SW–NE have at least two maxima: N55°E and N75°E.

The coarse-grained rapakivi types in the Wiborg batholith (wiborgite, dark wiborgite, pyterlite and porphyritic rapakivi granite) are weathered with varying intensity. The upper parts of the outcropping granites can be weathered down to a depth of 1–2 metres. Weathering can also be found along random subhorizontal and subvertical fractures deeper in the bedrock. The colour of the weathered and stained surface parts of the granite does not represent the real colour of the fresh rock. In addition, the soundness of the rock is diminished.

Because of the surface weathering of the outcrops, subsurface quality assessment methods should always be used in the Wiborg batholith. Diamond core drilling is an essential method for determining the colour and soundness of the rock, but it is the most costly one. Hence, less expensive and light drilling equipment for shallow core sampling should be utilised. The ERT and the IP methods successfully exposed a ca. 1-m-thick weathered surficial zone of rapakivi granites. A few subvertical open fracture zones were also discovered. ERT and IP are affordable and fast-to-use methods and should be applied in exploration in the Wiborg batholith.

This study demonstrated that the natural stone potential for future quarrying in the Wiborg batholith is good. Prospects may especially be found in areas dominated by wiborgite and pyterlite. Based on the results of this study, a revised exploration process for natural stone is proposed that is especially suited to the weathered rapakivi granites in the Wiborg batholith. It is comprised of a comprehensive set of desk study steps, regional mapping and detailed target studies.

Keywords: natural stone, dimension stone, building stone, exploration, petrography, lithology, geophysics, fracturing, bedrock, rapakivi granite, Wiborg batholith, Finland

Paavo Härmä
Geological Survey of Finland
P.O. Box 96
FI-02151 Espoo
Finland

E-mail: paavo.harma@gtk.fi

ISBN 978-952-217-405-5 (pdf)
ISBN 978-952-217-406-2 (paperback)
ISSN 0367-522X (print)
ISSN 2489-639X (online)

CONTENTS

PART I PRELUDE

1 INTRODUCTION

According to the European standard, "natural stone" is defined as a piece of naturally occurring rock (EN 12670, 2019). A natural stone product is a worked piece of naturally occurring rock used in building and for monuments. In the industry sector, "dimension stone", "facing stone", and also "building stone" are terms used synonymously for natural stone used for architectural purposes. The definition of natural stone does not include "aggregates" or man-made construction products such as concrete or brick.

In natural stone production, blocks of stone (Fig. 1) are quarried from solid bedrock by drilling and blasting, or by cutting with a wire saw, chain saw or blade saw. The blocks are then cut into slabs, tiles and other products that are mechanically finished, e.g. by polishing. Natural stone applications include construction products such as slabs and tiles (Fig. 2), memorial stones and monuments, as well as various small items. Natural stone types that have been produced in Finland include granite, soapstone, schist and marble. At present, granite and soapstone are the main stone types extracted, with ca. 80% of production by volume being granite and 20% soapstone.

The Finnish natural stone industry is comprised of ca. 200 small and medium-sized enterprises. Finland plays an active role in the international natural stone market, exporting to ca. 40 countries. In 2018, exports totalled ca. 210 000 tons with a value of ca. €18 M (Olavi Selonen, personal communication, September 2019). Approximately half of the natural stone quarried was exported. The main export countries were China, Poland, Italy and Spain. The global production of natural stone has grown steadily during the last few decades. China is currently the main marketplace for natural stone.

Rapakivi granites are the most important raw material for granitic natural stone in Finland, as almost 70% of all granite produced in Finland consists of rapakivi granite (Olavi Selonen, personal communication, September 2019). The main production area is the Wiborg rapakivi granite batholith in southeastern Finland. The batholith is a source of mostly brown and red coarse-grained granites with the characteristic texture of large round K-feldspar crystals. *Carmen Red*/*Karelia Red* and *Eagle Red* are red rapakivi granites and *Baltic Brown* is a brown variety extracted from the batholith. The granites are exported globally and used in exteriors and interiors, as well as for monuments. They have gained a reputation in the global stone market as being classical Finnish materials, often used in projects requiring large amounts of homogeneous stone.

The Wiborg batholith represents a unique production area in the world; there are also rapakivi granites in other parts of the globe, but their extraction is very modest compared to Finnish production. The batholith is also one of the main locations for the production of brown granite in the world. Being anorogenic and undeformed, the rapakivi granites are highly potential for natural stone, and the demand for new stone qualities from rapakivi areas is continuous.

While the produced granite is sound and intact, a typical feature of rapakivi granite is the distinct surface weathering of outcrops, termed "grusification". This special type of weathering can extend so deep into the rock that the first couple of metres down from the rock surface can, in the worst case, be unusable as natural stone. The weathering also has a crucial impact on exploration for natural stone in the batholith by changing the surficial colour and soundness of the granite, thus making prospecting more challenging than in unweathered rock areas. In this doctoral study, I addressed this problem by integrating lithological, geophysical and structural data in order to create a new revised exploration process especially suited to the rapakivi granites of the Wiborg batholith.

Fig. 1. The product of a natural stone quarry is a dimensioned and classified stone block. Blocks of *Karelia Red* in Ala-Pihlaja, Virolahti. Photo: Paavo Härmä.

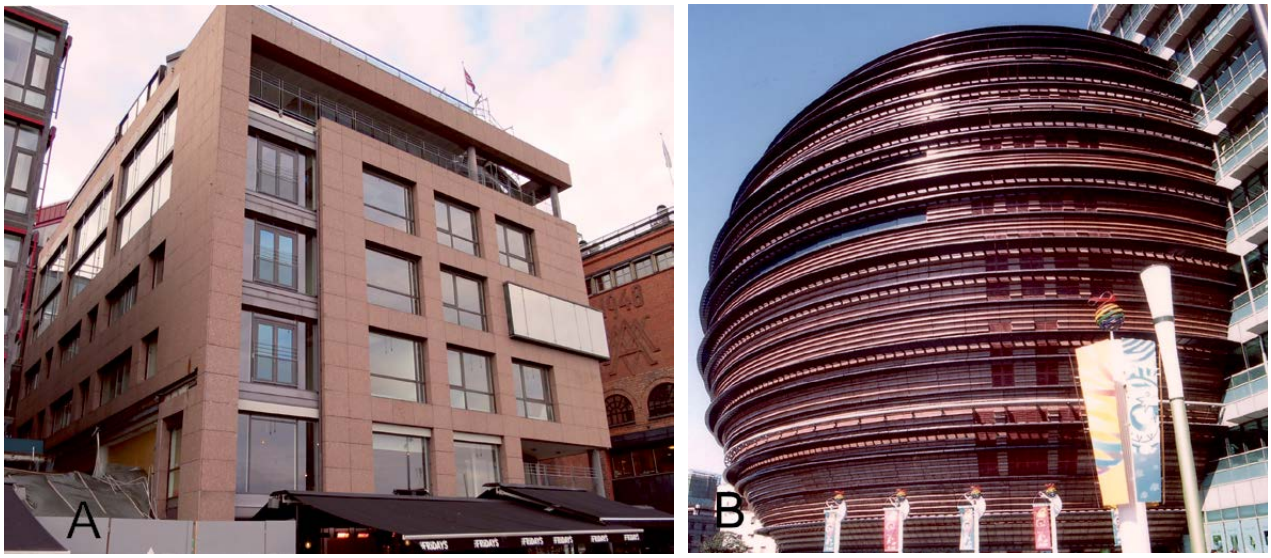

Fig. 2. Typical uses of natural stone products. A. An office building in Åger Brygge, Oslo, Norway, faced by slabs of *Carmen Red* from Virolahti. Photo: Olavi Selonen. B. The Core Pacific building in Taipei, Taiwan, covered by slabs of *Eagle Red* from Kotka. Photo: Palin Granit Oy.

1.1 Research process and dissertation structure

This doctoral thesis is based on my field observations during exploration carried out by the Geological Survey of Finland (GTK) in the Wiborg batholith during four periods: 1997–2002, 2006–2007, 2013–2014 and 2017–2019. The objective of the explorations was to discover reserves for the well-known natural stone qualities and to find new qualities for the natural stone market. The projects were carried out according to an exploration process including the individual steps of desk study, field mapping and detailed examination of the prospect (cf. Chapter 2.2). Altogether, 1135 observations were recorded from rapakivi granite outcrops and from active or abandoned quarries.

It was observed almost immediately during the fieldwork that the real colour, or occasionally even the texture of rapakivi granites was not possible to reliably determine from the outcrops, even with shallow sampling, due to the intensive surficial weathering. In particular, the most interesting and most potential rock types for natural stone, the coarse-grained granite types, were the most weathered.

The common exploration methods did not apply well in the batholith due to the surficial weathering layer of the granites. Many solutions to this challenge were tested, including sampling with various types of equipment such as a hand-held diamond saw or a mini-drill focused on those areas where there had been a soil cover, but which had been later excavated, such as ditches beside forest roads. Nevertheless, the results of the sampling were not acceptable, as ca. 75% of the samples were broken down or had a false colour, or were densely fractured down to 10 cm depth. The only method that yielded good results was diamond core drilling, but this is an expensive method and cannot be applied everywhere because of, for instance, topographical conditions.

From an economic point of view, it is important to be able to evaluate the amount of weathering on outcrops during exploration. Consequently, weathering plays a central role in exploration and quality evaluation in rapakivi areas, especially regarding assessment of the appearance and soundness of the stone.

Therefore, my own interest and the challenges in exploration led to this study of the characteristics of rapakivi granite weathering: what happens in rocks during weathering, how common is weathering in the Wiborg batholith, how can the weathering on outcrops and in deeper parts be specified and using which methods? My interest was in finding evaluation methods that could be put into practise in the exploration process.

The data gathered for this doctoral thesis during the exploration projects are arranged in three topical parts (II, III, IV): In Part II "Lithological and structural data" (Chapter 5), the geological features of the rock types, as well as the appearance, fracturing and potentiality of rock types in the Wiborg batholith are described. Rapakivi weathering is demonstrated in Part III "Rapakivi weathering" (Chapter 6), including a description of the weathering of the main rock types at selected sites and outcrops. In Part IV "Geophysical and morphological methods" (Chapter 7), the new methods applied in exploration are described. The doctoral thesis is also comprised of an introductory Part I "Prelude" (Chapters 1–4) and Part V "Discussion and conclusions", including discussion of the results of the study (Chapter 8), as well as the presentation of conclusions (Chapter 9).

1.2 Objectives and study area

The main objectives of this doctoral research were to characterize the surficial weathering of the different rapakivi granite types, consider the influence of this weathering on exploration for natural stone in weathered areas, and develop a revised exploration process for natural stone, more suited to the weathered granites in the Wiborg batholith of southeastern Finland.

The applicability of the selected geophysical methods for detecting the weathered surface of rapakivi granites was tested at a selected site. Detailed mapping of the rock types and structural features of the Wiborg batholith was carried out. The potentiality of the different rapakivi granite types of the batholith for natural stone extraction was also evaluated.

The study area covers the Wiborg rapakivi granite batholith, excluding the satellite intrusions of Ahvenisto and Suomenniemi and the Russian part of the batholith (Fig. 3). The study was carried out as batholith-scale fieldwork and as detailed site investigations at selected locations.

1.3 Author's contribution to the topical parts of the doctoral thesis

For Part II, I mapped the rock types, made observations on the fracturing and participated in taking shallow samples from the entire Wiborg batholith area.

For Part III, I selected the studied weathered sites, planned the location of the investigation traverses, and mapped in detail the selected weathered outcrops and traverses. I also took part in sampling with a hand-held diamond saw and studied the impregnated thin sections.

For Part IV, I was involved in planning the geophysical survey and the location of the investigation traverses. I mapped the cleaned traverses in detail while geophysical measurements were carried out by the geophysical unit of GTK. I further participated in the interpretation of the results of the geophysical survey. The petrophysical measurements were conducted in the petrophysical laboratory of GTK.

2 NATURAL STONE EVALUATION

2.1 Criteria for feasible natural stone

The two most important criteria for feasible natural stone are the appearance and soundness of the stone (e.g. Shadmon 1996, Selonen 1998, Selonen et al. 2000, Lorenz & Gwosdz 2003, Bradley et al. 2004, Romu 2014, Luodes 2015).

2.1.1 Appearance of stone

The aesthetic properties of stone are essential when selecting natural stone for architectonic purposes (Bradley et al. 2004). The appearance of stone is defined by its colour, texture, pattern and structure (e.g. Bradley et al. 2004). Natural stones can be monochromatic, i.e. composed of one colour, or polychromatic, comprising several colours. Monochromatic stones (the most common colours being red, brown and grey) include rapakivi granites and other granitic stones, while multi-coloured stones include migmatites, gneisses or gneissose granites, and marbles with a vivid and strong design. The structure of natural stones varies from even grained or porphyritic to migmatitic. Natural stones are priced by colour, the rarer colours such as blue, yellow and black being the most highly priced.

The colour of monochromatic stones such as rapakivi granites must be homogeneous throughout the deposit (Fig. 4). All types of colour variations, stripes, inclusions, clusters of minerals, or veins are regarded as defects (Fig. 5) and are not accepted in first-class stone. In contrast, a suitable variation in colour is sought after in polychromatic stones, and more variation in appearance is accepted. The slightest variations in the appearance of rock can be decisive in whether the stone has economic value (Selonen et al. 2011). The same feature can be seen in the collection of commercial granites of the Wiborg batholith (see Chapter 4.2). At first glance, certain stones can look very similar, but they are nevertheless identified by the stone market as individual stone qualities. The main aspect is that a deposit of natural stone must be homogeneous enough to be specified as one and the same product.

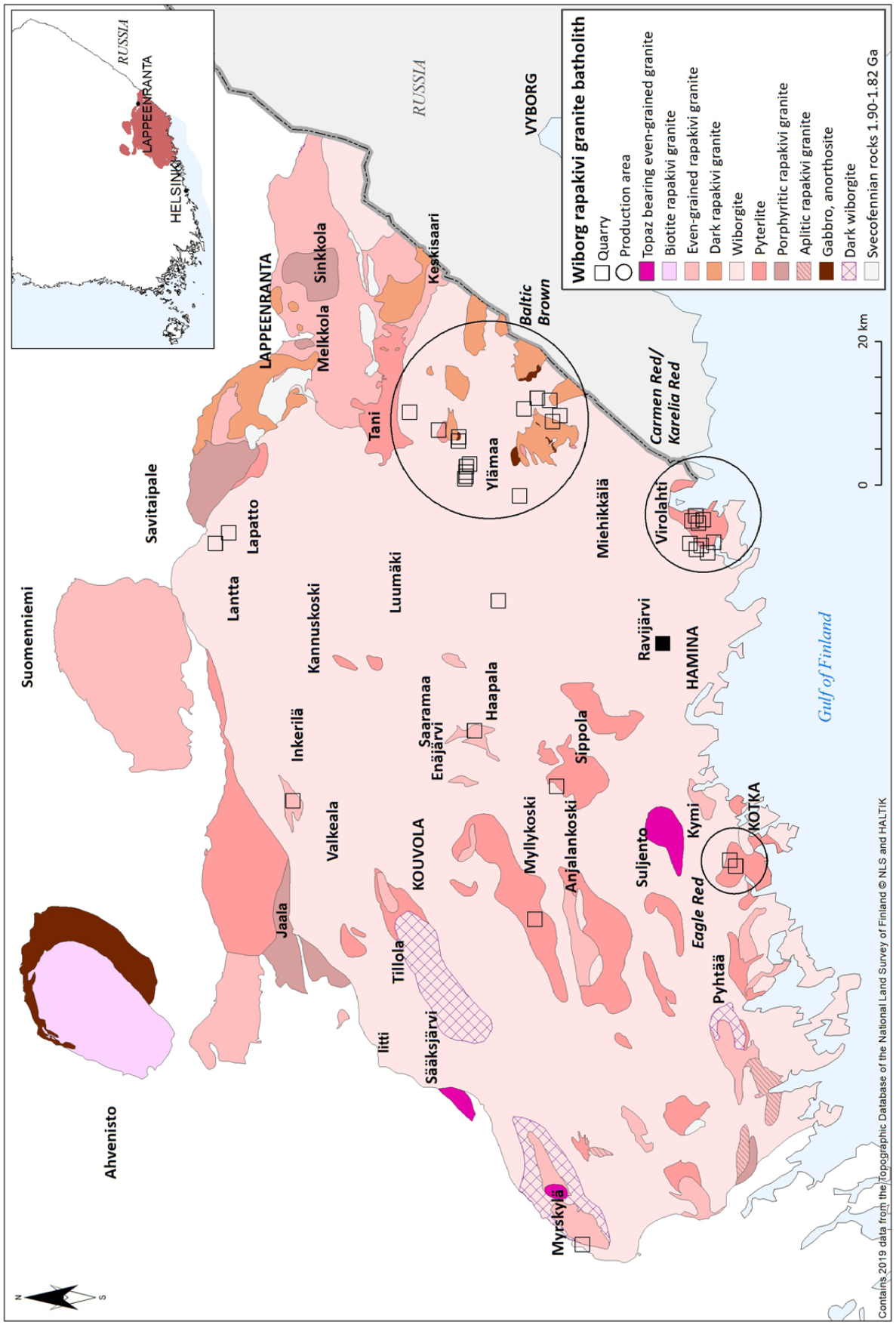

Fig. 3. Geological map of the Wiborg rapakivi granite batholith in southeastern Finland, showing the study area of the dissertation. The main current production areas for natural stone are indicated by circles. Modified from Härmä et al. (2015).

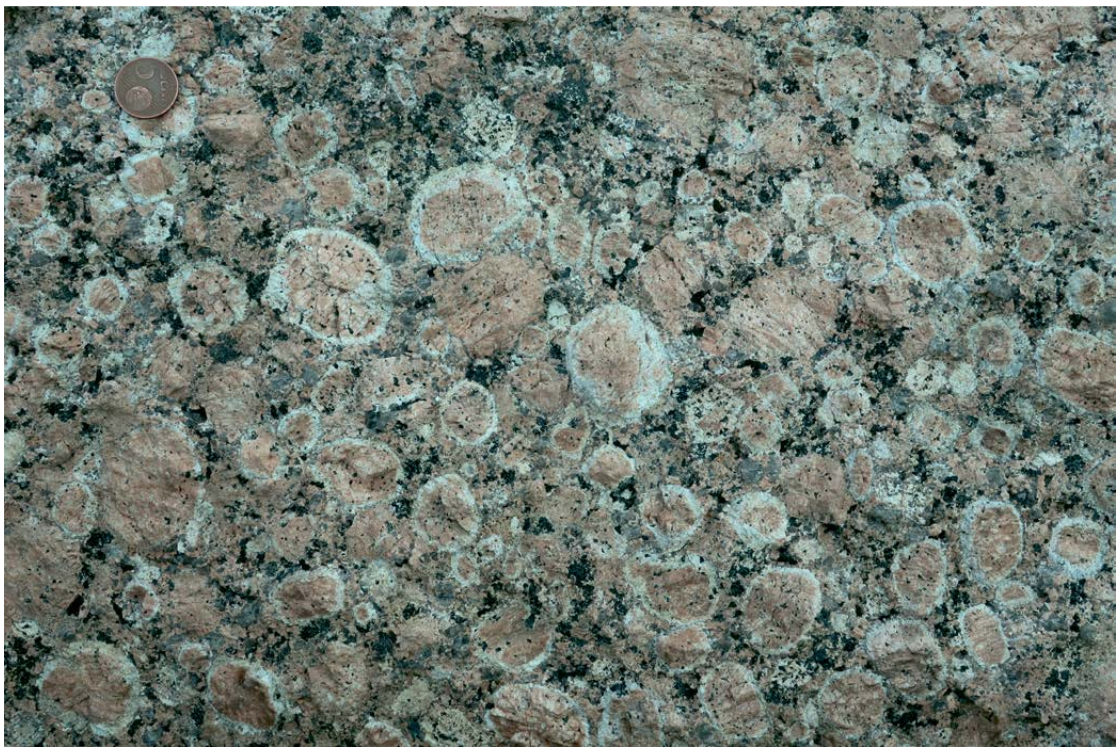

Fig. 4. Typical homogeneous rapakivi granite texture and colour on an outcrop. The coin in the upper left corner is 2 cm in diameter. Location: Lantta, Savitaipale. (Coordinates: x=6773920 and y=527160 EUREF FIN TM35FIN). Photo: Paavo Härmä.

Fig. 5. A cross-cutting granitic vein and an inclusion of even-grained granite are regarded as defects in the commercial appearance of a rapakivi granite. The length of the hammer handle is 70 cm. Location: Ravijärvi, Virolahti. (Coordinates: x=6720845 and y=525645 EUREF FIN TM35FIN). Photo: Paavo Härmä.

2.1.2 Soundness of stone

A prospect for natural stone must have a feasible pattern and spacing of fractures in order to be an object for extraction (Luodes et al. 2000, Härmä et al. 2001, Luodes 2015). It has to be economically feasible to quarry, which means that it has to be sound enough to allow the extraction of stone blocks of a suitable size. The required fracture spacing is defined by the future use of the stone and by the block size constrained by the processing machinery. For instance, a suitable size of quarry blocks for modern gang saws varies as follows: 2.40–3.45 m (length) x 0.80–2.40 m (height) x 1.30–1.95 m (width). This implies that the spacing of the natural fractures on an outcrop must be more than 2–3 m and the extracted block should be at least 3 m^3 in size to be used in production.

The character of the fracturing is also important when assessing the soundness of stone, with the orthogonal fracture pattern being preferred (Figs. 6 and 7). This criterion is especially important for rapakivi granites, because they are typically produced on a large scale with large block sizes.

Besides this, the macroscopic fracturing must be sparse enough for extraction, and the stone itself must be internally intact and free from cracks and microfractures. When used in the construction industry, the stone must satisfy strict physical and mechanical durability requirements, and the mechanical and physical properties have to meet an acceptable level. The mineralogy has to be suitable to cause no problems in the planned use of the stone. In outdoor use, it is important that the stone does not contain easily weathering minerals, or minerals that can cause undesirable discolouration or weakening of the mechanical properties of the rock. These properties, including microscopic soundness, are measured in certified laboratories using standardised methods (e.g. EN standards inside the European Economic Area, EEA) (Ihalainen 1994, Siegesmund & Snethlake 2014, Selonen et al. 2018, Luodes et al. 2019).

Fig. 6. Well-developed orthogonal fracturing in a rapakivi outcrop. The spacing between the fractures here is over 3 m, being rather optimal for the extraction of natural stone. Location: Hujakkala, Ylämaa. (Coordinates: x=6731570 and y=553140 EUREF FIN TM35FIN). Photo: Paavo Härmä.

Fig. 7. Orthogonal fracturing in a rapakivi granite outcrop. The spacing between the subhorizontal fractures (sheeting) here is too dense to be feasible for natural stone production. Location: Pentinkylä, Ylämaa. (Coordinates: x=6744260 and y=556440 EUREF FIN TM35FIN). Photo: Paavo Härmä.

2.1.3 Other criteria

Only those natural stones that have a colour and general textural outlook that is considered commercially attractive are quarried. The market demand indicates whether the stone has value in the international marketplace for stone. Even if the stone would otherwise be suitable for production, it will have no value without an appreciation from the market, which in turn depends on the prevailing architectural style and fashion. Fashions and preferences in the natural stone market change quite rapidly, and there is also considerable variation between countries with regard to the demand for certain stone types and colours.

However, in exploration, prospects with low immediate economic interest should not be rejected, because they can later become interesting due changes in fashion and demand.

2.2 Exploration process

The process of natural stone exploration is often referred as a stepwise regional study aimed at identifying new deposits of natural stone (Heldal & Lund 1995, Shadmon 1996, Selonen 1998, Luodes et al. 2000, Selonen et al. 2000, Loorents 2000, Luodes 2003, Heldal & Arvanitides 2003, Selonen & Heldal 2003, Härmä et al. 2005, Härmä et al. 2006, Ashmole & Motloung 2008, Carvalho et al. 2008, Luodes et al. 2014, 2015, Selonen et al. 2014, Luodes 2015, Härmä et al. 2017, Vartiainen 2017). The process includes the individual stages of desk study, field mapping and detailed examination of prospects (Selonen et al. 2000, Ashmole & Motloung 2008, Luodes 2015) (Fig. 8).

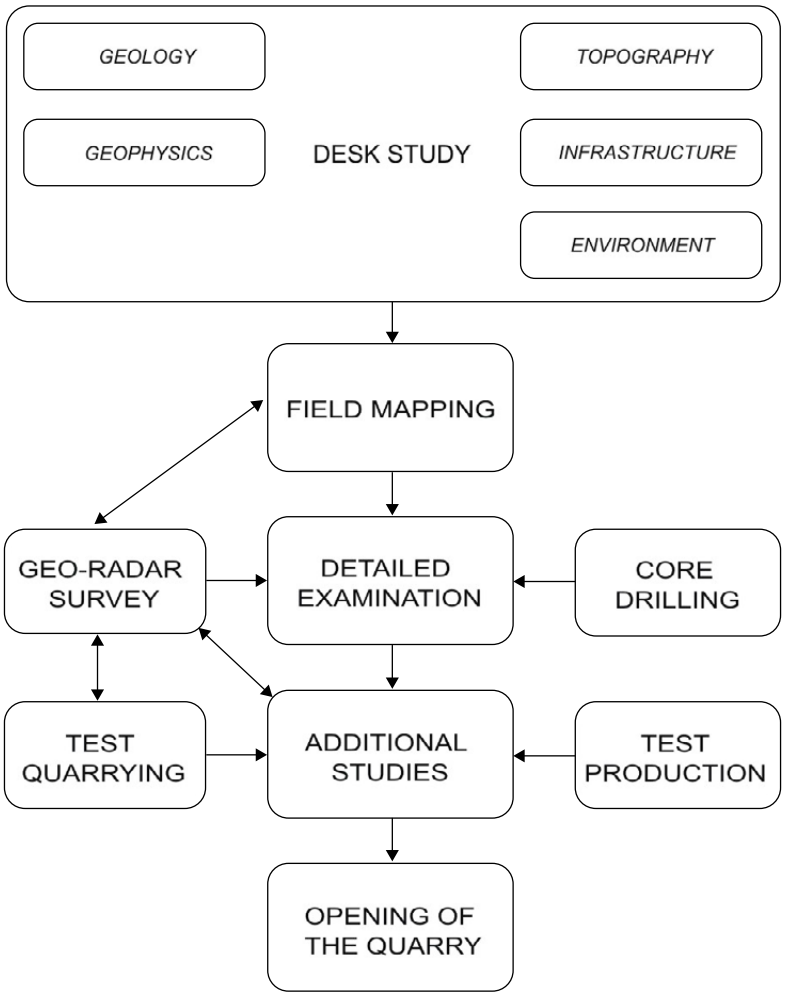

Fig. 8. Exploration process for natural stone according to Luodes (2015). Environmental aspects are omitted.

2.2.1 Desk stage

The preliminary evaluation of the exploration area is carried out during the desk stage with geological, geophysical and topographical data. A geological model and a geological exploration model of the target area are prepared (e.g. Selonen et al. 2011, 2014).

In the natural stone exploration process, it is beneficial to define the geological setting of the exploration area at both a regional and a detailed scale (Selonen et al. 2000, Arponen et al. 2009, Selonen et al. 2011, 2012, 2014). A geological model on a regional scale gives an overall concept of the geological and lithological environment, as well as the structural evolution of the area. The location of natural stone deposits is determined by the regional geological evolution of the bedrock, a fact that can be applied to target selection in the exploration process (Selonen et al. 2000, Arponen et al. 2009, Selonen et al. 2011, 2012, 2014).

Generalized geophysical data can be used in assessing the bedrock and its potential areas for natural stone. Different types of geophysical data reflect the different properties of the bedrock and help in the discovery of geological units, especially in covered areas (Luodes et al. 2014) (see Chapter 7).

Analysis of topographical data can reveal geological structures and large tectonic features, especially in areas where the soil cover is thin or the bedrock is exposed. This is a typical environment, for instance, for the glacially washed rocks in southern Finland. From the topographical features, prognoses of suitable targets for natural stone can be inferred (Selonen et al. 2014). For LiDAR, see Chapter 7.2.3.

Infrastructural factors, such as access to the prospect, are important when estimating the economic possibilities of a prospect (Luodes et al. 2014). A challenging location and high initial cost can prevent the setting up of a quarry. Hence, the road infrastructure and logistic possibilities (e.g. roads, railroads and waterways) are assessed during

the desk study. Environmentally sensitive regions and protected areas are also noted and excluded from further studies.

2.2.2 Field mapping

Field mapping is carried out after evaluation of the existing data. Target selection is largely based on the geological exploration model (Selonen et al. 2014). Evaluation is carried out on outcrops.

The field mapping is focused on visual observations of rock characteristics such as texture, soundness, fracturing (e.g. type, spacing) and homogeneity (e.g. Luodes et al. 2014). In addition, colour variations are observed. In the most promising prospects, sampling can be carried out. Shallow sampling from rock outcrops with a mini-drill or a hand-held diamond saw are routine methods. The size of the prospect is evaluated.

2.2.3 Detailed examination of the prospect

When a target studied during field mapping is considered to have potential for natural stone, a detailed examination of the prospect is commenced (e.g. Luodes et al. 2000, Härmä et al. 2001, 2017, Vartiainen 2017).

During the detailed examination, investigation traverses are prepared in suitable locations covering the entire prospect (Fig. 9A). The texture, structure and colour of the rock are assessed by detailed mapping (at a scale of 1:100). The traverses are mapped in detail to quantify and qualify the spacing and density of joints and fractures of different dimensions. Nowadays, observations of fracture orientations are usually carried out by using the Virtual Reference Station Global Positioning System (VRS GPS), which allows easy handling of digital data after measurements (Fig. 9B).

Sampling is an essential part of the detailed examination of a prospect (e.g. Luodes 2008, Ashmole & Motloung 2008). Samples taken with a hand-held diamond saw (Fig. 10A) or with a mini-drill are used in evaluating the colour, texture and mineralogy of the rock. For evaluation of the aesthetic properties and homogeneity of the rock, as well as for laboratory tests, large block samples are extracted by drilling and wedging (Fig. 10B). Samples with a different surface finishing can also be produced to show the variation in the characteristics and commercial potential of the rock.

The main geophysical method applied during the detailed examination is ground penetrating radar (GPR) (e.g. Luodes & Sutinen 2011, Luodes 2015). Horizontal and subhorizontal fractures clearly appear in radargrams, while vertical and subvertical fractures are more challenging to interpret (Luodes 2015). Other geophysical methods can include magnetic ground measurements, electromagnetic VLF-R and EM31, seismic ground survey

Fig. 9. A. Mr Pentti Toivanen (GTK) is cleaning the investigation traverses with water. B. Detailed mapping on traverses with the Virtual Reference Station Global Positioning System (VRS GPS). Mr Paavo Härmä (GTK) (left) and Mr Heikki Pirinen (GTK) (right) are mapping the subvertical fractures. Photos: Hannu Luodes.

Fig. 10. A. Sampling with a hand-held diamond saw yields samples with a length of 25 cm and a width of 10–15 cm. Mr Markku Putkinen (GTK) is taking the sample. B. Block samples are extracted from the homogeneous parts of rocks to manufacture slabs for aesthetic evaluation. Mr Rasmus Nyman (GTK) is hitting the wedges. Photos: Paavo Härmä.

methods and microgravimetric methods (Elo 2006, Carvalho et al. 2008, Luodes et al. 2014, Vartiainen 2017) (see Chapter 7).

Diamond core drilling provides invaluable information on the quality of the prospect by producing a drill core in which the variation in colour, mineralogy and fracturing of the rock can be observed at depth (Leinonen 2005, Vartiainen 2017). However, the correct placement of vertical or inclined drill holes is very important (Leinonen 2005, Luodes et al. 2014). The depth of core drilling in natural stone exploration is commonly down to 20 m and the core diameter is ca. 76 mm. Fractures can also be monitored by video camera in core drill holes; this method is suited to confirming observations made from the drill cores (Vartiainen 2017).

The detailed examination can be associated with test quarrying in which a few hundred cubic metres (≤1000 m^3) are typically extracted (Luodes et al. 2014). In this process, the quarrying properties (extractability/drillability) of the rock are documented. The extracted material is processed into final products to determine the production properties such as sawability, flaming ability, honability and polishing ability.

The technical properties of the rocks are measured using internationally accepted standardized tests (e.g. Selonen et al. 2018, Luodes et al. 2019). Environmental considerations, such as licencing, the use of leftover stone and the status of land use planning, are assessed on the basis of currently available information (Luodes 2015).

3 RAPAKIVI GRANITES

3.1 Geological setting

The Finnish word "rapakivi" has been internationally accepted as a term for a definite type of granite. Centuries ago, Finnish geologists noted how red granites sharply cut the structures of the adjacent deformed rocks. In some cases, the rock surface was weathered, forming a gravel-like surface called rapakivi ("crumbly stone") by the local people. The name was internationally introduced and defined by the famous Finnish geologist J.J. Sederholm in 1891 (Sederholm 1891).

Nowadays, rapakivi granites are defined as "A-type granites characterized by the presence, at least in the larger batholiths, of granite varieties showing rapakivi texture" (Haapala & Rämö 1992). They have been identified in several areas, including Sweden, the Baltic countries, Russia, Ukraine, Greenland, Canada, the United States, Brazil, Venezuela, Botswana and Australia (Rämö & Haapala 2005, Müller 2007). Rapakivi granites are found as discordant intrusions, cutting through an older deformed metamorphic bedrock, and are not, in most cases, affected by subsequent ductile deformation. The majority of rapakivi granites are of Proterozoic age (ca. 1800–1000 Ma), but also Archaean (ca 2800 Ma) and Phanerozoic (400–10 Ma) rapakivi suites are known (Calzia & Rämö 2005, Rämö & Haapala 2005).

Incipient or aborted rifting has been suggested as the tectonic environment for many anorogenic granitic suites (Rämö & Haapala 1995, 2005). An extensional tectonic setting prevailed during the emplacement of the rapakivi granites, as indicated by the associated dyke rocks and previous shear zones.

Rapakivi granite magmatism is typically bimodal (Rämö 1991, Eklund 1993, Rämö & Haapala 1995, 2005). Diabases, gabbros and anorthosites are found together with rhyolite, granite and syenite. Magmatic underplating is a probable mechanism for the generation of the silicic-mafic association (Rämö & Haapala 1995, 2005). This involves partial melting of the upper mantle and lower crust in response to thermal perturbations associated with underplating. The partial fusion and upwelling of mantle material caused partial melting of the crust, producing rapakivi granite magmas (Rämö & Haapala 1995, 2005).

3.2 Rapakivi texture

The rapakivi texture *sensu stricto* consists of plagioclase-mantled alkali feldspar megacrysts (ovoids) and two generations of quartz and feldspar (Vorma 1971) (Fig. 4). The formation of the rapakivi texture has been studied since the late 19th century (Sederholm 1891, Vorma 1971, Rämö & Haapala 2005, Vernon 2016). Several models have been proposed for the generation of the texture, including subsolidus reorganization of feldspar components (Dempster et al. 1991, 1994), magma mixing (Hibbard 1981, Stimac & Wark 1992, Wark & Stimac 1992) and sub-isothermal polybaric crystallization in a decompressing system (Nekvasil 1991, Eklund & Shebanov 1999, Elliott 2001).

Recently, Heinonen et al. (2017) demonstrated that the ovoids probably crystallized over a prolonged period of time and possibly under different conditions compared to the matrix material. Heinonen et al. (2017) concluded that ovoids in the rock types of the Wiborg batholith most probably represent several separate batches of magmas that were individually emplaced and evolved at mid- to upper crustal levels at ca. 1635 to 1628 Ma. The fully or nearly fully crystallized ovoid materials were subsequently remobilized by later granitic magmas that crystallized the matrix during the final emplacement of the granites ca. 1628 Ma ago.

3.3 The Wiborg rapakivi granite batholith

The Proterozoic rapakivi granites of Finland are found as four major batholiths (Åland, Laitila, Vehmaa and Wiborg) and as several smaller batholiths and stocks in southern Finland (Rämö & Haapala 2005) (Fig. 11).

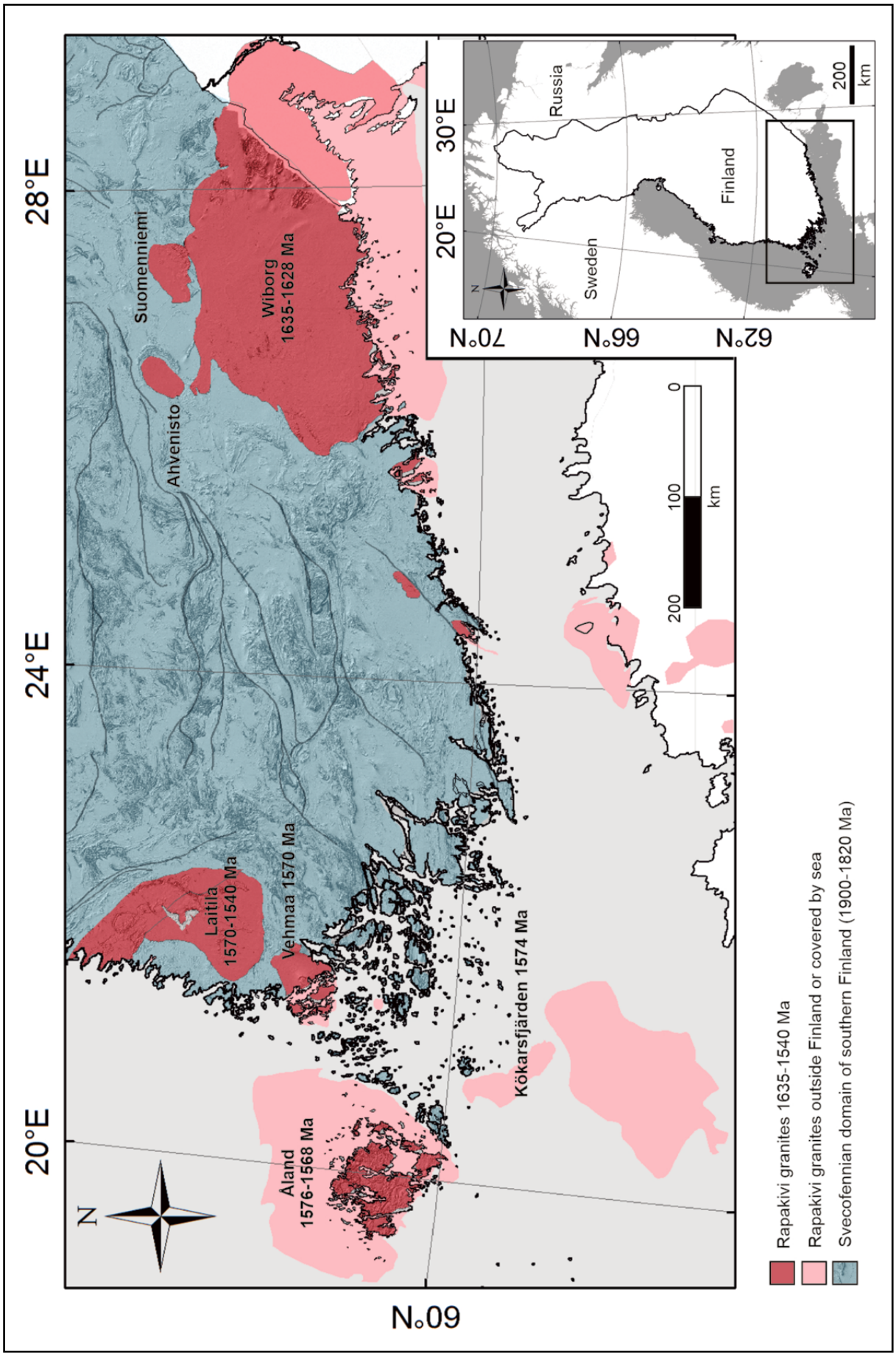

Fig. 11. Major rapakivi granite batholiths in Finland. Modified from Karell (2013).

The total area of the Wiborg rapakivi granite batholith is ca. 18 000 km^2. The batholith covers an area of 12 000 km^2 in southeastern Finland, shown on the Finnish geological map sheets 3014, 3021, 3022, 3023, 3024, 3041, 3042, 3044, 3111, 3113, 3114, 3131, 3132, 3133, 3134, 4111 and 4112 (Laitakari & Simonen 1963, Lehijärvi 1964, Vorma 1965, Lehijärvi & Tyrväinen 1969, Simonen & Tyrväinen 1981, Laitala 1984, Simonen 1973, Simonen 1987, Nykänen & Meriläinen 1991). A comprehensive explanation for the map sheets has been published by Simonen (1987). The batholith extends in the east to the western part of the Karelian Isthmus in Russia and in the south beneath the Gulf of Finland. Satellite plutons of Ahvenisto and Suomenniemi are found in the northern part of the Wiborg batholith (Fig. 3).

As defined in this this study, the Wiborg batholith consists of seven main granite types: wiborgite, dark wiborgite, pyterlite, porphyritic rapakivi granite, even-grained rapakivi granite, dark rapakivi granite and aplitic rapakivi granite (Fig. 1) (see Chapter 5.2). The wiborgite covers the main part of the area of the batholith in Finland, whereas the other rapakivi varieties mainly occur as rather small intrusions.

The age of the granites in the Wiborg batholith is 1635–1628 Ma (Heinonen et al. 2016, 2017), indicating ages older than those of the rapakivi batholiths in southwestern Finland. The Wiborg batholith has sharply intruded the older, ca. 1900–1830 Ma deformed and metamorphosed country rocks, which include migmatitic mica schists, amphibolites and quartz-feldspar gneisses, as well as gabbros, granodiorites and potassium-rich granites (Simonen 1987). Country rocks can be found inside the batholith as inclusions and roof pendants, e.g. in the northeastern parts of the batholith (Simonen 1987, Harju et al. 2010).

Different models have been presented for the form and the formation depth of the Wiborg batholith (e.g. Simonen 1987). It has been interpreted as a sheet-like laccolite or a diapiric batholith-like intrusion. According to Simonen (1987), the wide extent and depth of the intrusion and the sharp, outward-dipping contacts against the country rocks are characteristic features for a diapiric batholith intrusion. Roof pendants and smaller cupola-like intrusions fit well with the model of the batholith (Simonen 1987).

Wahl (1925) stated that the Wiborg batholith is a sheet-like intrusion with a thickness of only 1 km, emplaced along subhorizontal fractures. Later, the geophysical data of Laurén (1970) and Luosto et al. (1990) confirmed that the batholith is a relatively thin, ca. 10-km-thick sheet-like body. Furthermore, according to Elo & Korja (1993) and Korja et al. (1993), the crust is 15–20 km thinner below the Wiborg batholith than in the surrounding areas based on the interpretation of seismic and gravity data. The areal extension of the batholith in the SW–NE direction was noted by Elo & Korja (1993). The granites intruded in pulses (Selonen et al. 2005, Karell et al. 2009, 2014, Rämö et al. 2014, Heinonen et al. 2017), possibly along earlier subhorizontal structures. The final emplacement took place through different intrusion mechanisms (Rämö & Haapala 2005, Selonen et al. 2005, Lukkari 2007, Karell 2013).

As a result of the intrusion of the Wiborg batholith, there is a 5-km-wide zone of contact metamorphic alterations in the surrounding country rocks (Vorma 1972, Simonen 1987, Villar 2017). The contact metamorphism has occurred under pyroxene-hornfels facies, and the microcline in the host rocks has been altered into orthoclase because of the heat from the rapakivi intrusion. According to Vorma (1972), the emplacement temperature of the rapakivi was more than 800 °C.

Besides natural stone, the Wiborg batholith is also a resource for other economic commodities. The rapakivi granites are associated with a variety of types of mineralization, such as the occurrence of topaz, Li–Fe mica and albite, high F, Li, Rb, Ga, In, Sn and Nb, and low Mg, Ti, Zr, Ba, Sr and Eu (Al-Ani 2015). The Kymi stock (Fig. 3) is bounded by a marginal stockscheider pegmatite that hosts minor topaz gemstone mineralizations and rare-element mineralization that has so far been non-economic (e.g. Haapala 1995, Lukkari et al. 2009, Berni et al. 2017, Al-Ani et al. 2018). In addition, abundant subeconomic (Pb-Zn-Cu-As-W-Sn) quartz veins are found around the Kymi stock. Many indium-bearing polymetallic veins of different styles and metal associations have been discovered in the westernmost parts of the Wiborg batholith (e.g. Sundblad et al. 2008, Cook et al. 2011, Valkama et al. 2016, Valkama 2019). REE-bearing minerals have also been discovered (e.g. Al-Ani 2015, Al-Ani et al. 2018). The Wiborg batholith is also a source of gemstone occurrences, e.g. at Ylämaa (spectrolite) and Luumäki (beryl) (Kinnunen 2017). In addition, reserves of crushed rock aggregates have been explored all over the batholith (e.g. Vallius 1995),

and there is an open database of rock aggregates at GTK (Bedrock aggregate). The country rocks (roof pendants) of the Wiborg batholith are quarried, for instance, for limestone (e.g. Lunden 1979, Lehtinen 1995).

4 PRODUCTION OF NATURAL STONE IN THE WIBORG BATHOLITH

4.1 Historical aspects of quarrying in the Wiborg batholith

4.1.1 Churches and fortresses

During the Middle Ages, local granites were used in the construction of "grey-stone" churches in the Wiborg batholith (Hiekkanen 2018). These include the medieval churches of Hamina and Pyhtää, as well as the sacristy of the church in Virolahti (from ca. 1500–1530).

At the end of the 18th century, fortresses were built in eastern Finland by the Empire of Russia and the Kingdom of Sweden (e.g. Paajanen 2014). In the area of the Wiborg batholith, the Russian fortifications include the fortresses in the city of Kotka, i.e. Ruotsinsalmi (1790–1808) (Fig. 12) and Kyminlinna (1791–1792 and the beginning of the 19th century), the fortress in the city of Hamina (1722–1809) and the fortress in the city of Lappeenranta (from the beginning of the 1790s) (Muinonen 2014). The Swedish fortresses include Svartholma (1748–1760s) and Loviisa (main phase 1747–1775) (Enqvist & Suhonen 2004, Suhonen 2007, 2011) (Fig. 13). The construction material for the fortresses was mainly local granite quarried near the building locations, but brick and wood were also used.

Fig. 12. The fortress of Ruotsinsalmi in Kotka was built during 1790–1808 on the order of the Russian General Aleksandr Suvorov. The granitic stones used in the construction are mostly wiborgite and pyterlite quarried nearby. Photo: Olavi Selonen.

Fig. 13. The fortress in Loviisa (including the Rosen and Ungern bastions). This Swedish fortress was under the construction during 1747–1775, but was never finished. Local even-grained and porphyritic rapakivi granites were mostly used in the construction of the fortress. Photo: Paavo Härmä.

4.1.2 Construction of St Petersburg, Russia

The most important period in the history of using the granites in the Wiborg batholith was the construction of the Russian city of St Petersburg at the end of the 18th century (e.g. Hirn 1963, Heldal & Selonen 2003, Bulakh et al. 2010, Bulakh & Abakumova 2014, Kaukiainen 2016). Because no hard rocks were available near the building site, the material was taken, among other places, from the Wiborg batholith. There, the main quarry areas were situated both along the shoreline and in the archipelago of Virolahti and Hamina in present-day Finland, and areas near the city of Vyborg in present-day Russia.

Granite was extracted in Virolahti, e.g. in Pyterlahti (Hevonniemi), Hämeenkylä, Korpisaari, Karhusaari and Hailniemi (Enqvist 2007), while in Hamina, quarry locations included the island of Kuorsalo (Pitkä-Kotka) (Kaukiainen 2016).

Granite from Virolahti and Hamina was extensively utilized in the wall and canal structures of the Neva River, the supporting structures of bridges and quays, the foundations of buildings as well as in street paving in St Petersburg. The two most famous objects constructed of Finnish granite in St Petersburg are St Isaac's Cathedral (1818–1858) (Fig. 14A) and the Alexander I Column (1829–1834) (Fig. 14B). In St Isaac's Cathedral, there are 112 monolithic red granite columns quarried from the shores of the Gulf of Finland (Bulakh et al. 2010). The Alexander I Column mainly consists of a monolith of red rapakivi granite extracted from the Pyterlahti (Hevonniemi) quarry in Virolahti. The monolith has a diameter of ca. 3.5 m and a height of 25.6 m (Bulakh et al. 2010).

Stone extraction and processing for the construction of St Petersburg continued in southeastern Finland up to the early 1900s. The total amount of stone exported was over one million cubic metres (Kaukiainen 2016).

Fig. 14. A. Columns of St Isaac's Cathedral (1818–1858). B. The Column of Tsar Alexander I (1829–1834). The rock type in the columns is pyterlite. Photos: Paavo Härmä.

4.1.3 Modern industrial quarrying

During the period from the beginning of the 1900s up to the 1970s, granite was quarried in the Wiborg batholith in localised areas for the domestic markets and for export. Modern industrial scale quarrying of granite in the Wiborg batholith started in the 1970s, when the production potential of the brown wiborgite granite (*Baltic Brown*) in the Ylämaa area in the eastern part of the batholith was discovered. See Puntanen & Talka (1999) for further information.

From the 1970s, other important industrial quarrying sites in the Wiborg batholith have included Kotka (*Eagle Red*), Virolahti (*Carmen Red, Karelia Red*), Anjalankoski (*Carmen Red, Karelia Red*) and Savitaipale (*Karelian Brown, Baltic Brown*, finished).

4.2 Current production

Wiborgite and pyterlite are currently the main granite types used as natural stone in the Wiborg batholith, produced in the eastern and southeastern parts of the batholith (e.g. Selonen & Härmä 2003). Also see Fig. 3 for the main production areas.

4.2.1 Baltic Brown

Baltic Brown is a brown wiborgite extracted from several quarries in the eastern part of the Wiborg batholith (Figs. 15 and 16A). It is suitable for all interior and outdoor uses, including large projects. The stone is mostly exported to China, but also to Italy, Spain and Egypt.

4.2.2 Carmen Red/Karelia Red

Carmen Red/Karelia Red is a red pyterlite quarried from several quarries in the southeastern part of the Wiborg batholith (Figs. 16B and 16C). The granite is suitable for all interior and outdoor uses and is regularly stocked for the world market, especially in China, Taiwan and Spain. The granite is also well suited to large projects.

Fig. 15. Natural stone quarry for wiborgite (*Baltic Brown*) in Hujakkala, Ylämaa. (Coordinates: x=6731570 and y=553140 EUREF FIN TM35FIN). Photo: Paavo Härmä.

4.2.3 Eagle Red

Eagle Red is a red pyterlite quarried from two quarries in the southern part of the Wiborg batholith (Fig. 16D). It is suitable for all interior and outdoor uses, including large projects. The granite is produced as large blocks for the export market in Europe (mainly Italy).

4.2.4 Baltic Green

Baltic Green is a green pyterlite (partly wiborgitic) extracted from two quarries in the eastern part of the Wiborg batholith (Fig. 16E). The granite is suitable for all interior and outdoor uses. The stone is exported, for example, to Poland, Russia and the Baltic countries.

4.2.5 New Balmoral

New Balmoral is a red even-grained rapakivi granite. The fine-grained granite is suitable for all interior and outdoor uses, mainly for small and medium-scale projects, as well as for monuments in the domestic and export markets (Fig. 16F). The granite is quarried from one quarry.

4.2.6 Myrskylä Red

Myrskylä Red is an even and fine-grained red rapakivi granite. It is mainly applied as paving stone, kerbstone, gravestone and environmental stone in the domestic market (Fig. 16G). *Myrskylä Red* is a traditional Finnish paving stone quality.

4.2.7 Kymen Brown

Kymen Brown is a brown pyterlite (sporadically wiborgite). The granite is suitable for all interior and outdoor uses (Fig. 16H). The granite is quarried from one quarry for domestic and foreign markets (the Baltic countries).

4.2.8 Kymen Red

Kymen Red is an even and fine-grained red rapakivi granite (Fig. 16I). It is well suited, for example, to monuments and as a building material for both indoor and outdoor applications, mainly in the domestic markets. The granite is quarried from one quarry.

4.2.9 Other stone qualities

Karelia Beige is a reddish or beige porphyritic rapakivi granite (Fig. 16J). The granite is suitable for all interior and outdoor uses. It is mainly used in the domestic markets.

Brownhill is an orbicular granite, consisting of orbs in a medium-grained granitic matrix (Fig. 16K). Applications for the granite include small tabletops (1 x 2 m), bowls, dishes and other small objects. The colour of the stone varies from grey to light grey-brown. It is a special stone quality with limited availability.

Spectrolite is a coarse-grained deep grey or black anorthosite with iridescent spectrolite (plagioclase) crystals (Fig. 16L). *Spectrolite* is a well-known gem-

stone type all over the world, but is also used as natural stone, especially for tabletops and in interior decoration.

For the technical properties of the produced stones, see Härmä & Selonen (2018).

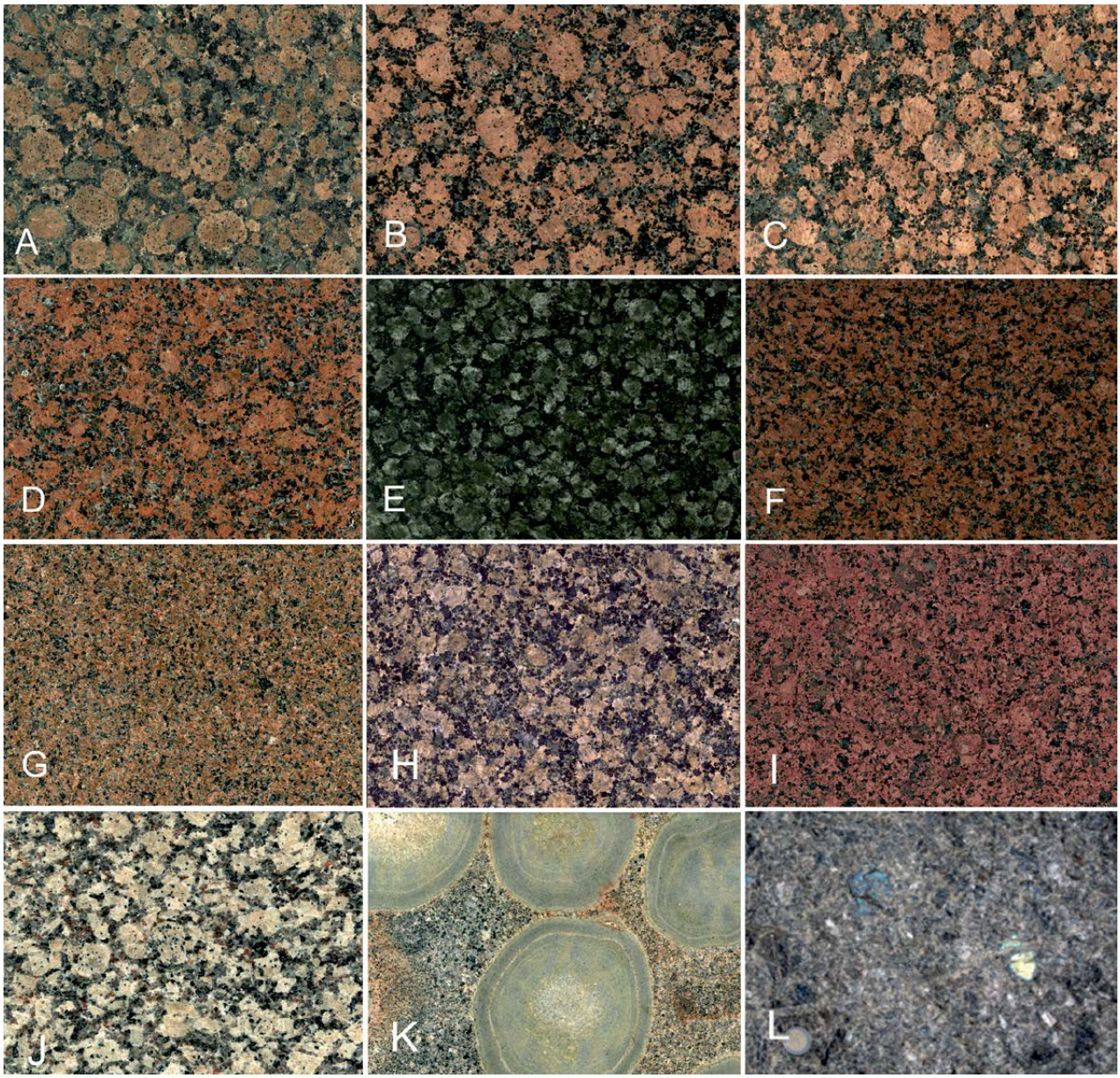

Fig. 16. Commercial stone qualities produced in the Wiborg batholith. A. *Baltic Brown.* B. *Carmen Red.* C. *Karelia Red.* D. *Eagle Red.* E. *Baltic Green.* F. *New Balmoral.* G. *Myrskylä Red.* H. *Kymen Brown.* I. *Kymen Red.* J. *Karelia Beige.* K. *Brownhill.* L. *Spectrolite*. Source: Kivi ry (KIVI - Stone from Finland) Suomessa louhittavat kivilajit (Stones quarried in Finland).

PART II LITHOLOGICAL AND STRUCTURAL DATA

5 LITHOLOGY AND FRACTURING OF THE WIBORG BATHOLITH

5.1 Study methods

Studies on rock types and structural features were carried out as field mapping covering the entire Wiborg batholith. The potentiality of the rock types for natural stone was also defined during mapping. The mapping focused on the definition of the rapakivi granite types as well as the colour, texture, appearance, homogeneity and their variations in the granites. Special attention was paid to wiborgite, pyterlite, even-grained rapakivi granites and dark rapakivi granites, as they are the most widespread rapakivi varieties.

The soundness of the granites was defined by measuring the spacing of the subvertical and subhorizontal macroscopic fractures on outcrops. The orientation of a total of 874 subvertical fractures was recorded (Table 1) and compiled as rose diagrams. A total of 341 samples were taken with a hand-held diamond saw during the field mapping. These samples were used to determine the rock types and to evaluate the appearance of the rocks, although the samples had mostly been broken down by weathering. Larger block samples (over 40) were extracted by drilling and wedging to evaluate the aesthetic properties and homogeneity of the rock. Slabs with different surface finishing were produced to show the variation in the outlook characteristics of the rock. Finally, samples for thin section analysis were taken during the block sampling. The modal mineralogy of the rock types was studied under a polarizing microscope in order to specify the rock type. All the observations were saved in the natural stone database of GTK.

Table 1. Number of observations of subvertical fractures (fracture planes dipping between 45° and 90°) during field mapping.

Rock type	Number of observations
Wiborgite	390
Pyterlite	266
Even-grained granites	147
Dark rapakivi granites	40
Other rapakivi granite types	31
Total	874
Quarry A (case study in Chapter 5.5)	155
Quarry B (case study in Chapter 5.5)	144

5.2 Rock types in the Wiborg batholith

In this study, seven main types of rapakivi granite were defined in the Wiborg batholith, consisting of wiborgite, dark wiborgite, pyterlite, porphyritic rapakivi granite, even-grained rapakivi granite, dark rapakivi granite and aplitic rapakivi granite (Fig. 3). Furthermore, areas having distinct colours and textural appearances were defined within the individual rapakivi types.

The approximate abundances of the different rapakivi types in the Finnish side of the Wiborg batholith, based on the GIS software calculations by the author, are as follows: wiborgite 75%, pyterlite 6%, even-grained rapakivi granites 6%, dark rapakivi granites 6%, porphyritic rapakivi granites 3% and other rock types 4%.

5.2.1 Wiborgite

Wiborgite, the traditional rapakivi, is the main rapakivi granite variety in the Wiborg batholith. It has the widest areal distribution and extends as large areas across the batholith (Fig. 3).

The wiborgite has a typical rapakivi texture with K-feldspar megacrysts (ovoids) mantled by a plagioclase rim (Fig. 17A), but the megacrysts occasionally lack the plagioclase rim. The thickness of the plagioclase rim varies from 1–5 mm. The ovoids are mostly evenly distributed, but can occasionally be rather scarce.

The megacrysts vary from 1–10 cm in diameter, with an average size of 1–4 cm. In places, the size distribution of the ovoids is bimodal, with large (7–10 cm) and small (1–2 cm) ovoids existing together, the smaller being more common than the larger ones. In the central part of the batholith, between the villages of Kaipiainen and Luumäki, there are large homogeneous areas of wiborgite with evenly dispersed, 1–2 cm K-feldspar ovoids. The matrix between the ovoids generally amounts to ca. 10–30% of the rock, but variations are found, and the volume of the matrix can in cases even exceed 50% (Fig. 17B). The main minerals of wiborgite include quartz, K-feldspar, plagioclase and hornblende. Inclusions of aplitic rapakivi granite and even-grained biotite rapakivi granite are found in the wiborgite.

The main colours of the wiborgite are dark brown, brown and light brown, as well as dark green, but the colour can locally also be reddish brown or greenish brown. Distinctly uniform areas of dark green wiborgite can be found around the villages of Lemi, Lahnajärvi, Sammalinen, Hovi and Leino.

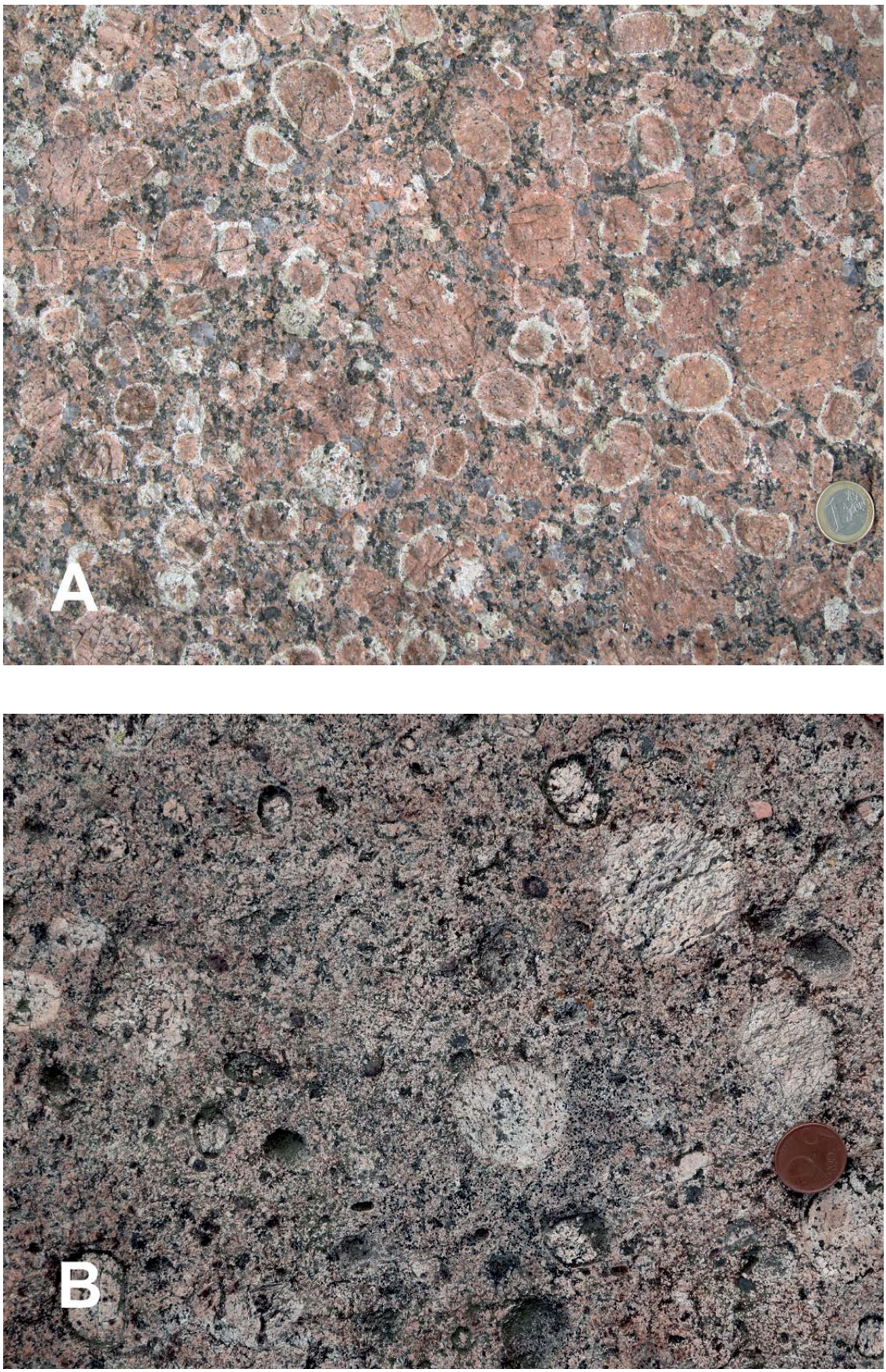

Fig. 17. A. Wiborgite with a typical rapakivi texture. K-feldspar megacrysts (ovoids) are mantled by a plagioclase rim. The coin is 2.5 cm in diameter. Location: Muhniemi, Kouvola. (Coordinates: x=6728030, y=482555 EUREF FIN TM35FIN). B. The matrix amounts to over 50% in this type of wiborgite. The coin is 2 cm in diameter. Location: Elimäki, Kouvola. (Coordinates: x=6737375, y=472185 EUREF FIN TM35FIN). Photos: Paavo Härmä.

5.2.2 Dark wiborgite

Dark wiborgite is a variety of wiborgite carrying K-feldspar megacrysts (ovoids), occasionally mantled with plagioclase, as well as angular plagioclase crysts of andesine composition (1–5 cm in diameter) in a dark-coloured matrix (Fig. 18).

The main colours of the rock are dark brown and black, with occasional shades of dark greenish brown. The main minerals are K-feldspar, quartz, plagioclase and hornblende. In addition, fayalitic olivine, magnetite and biotite are found as accessory minerals. According Simonen (1987), the dark-coloured wiborgite contains more plagioclase and hornblende than the normal wiborgite. Dark wiborgite is mostly found in the western and northwestern parts of the batholith (Fig. 3).

5.2.3 Pyterlite

Pyterlite is the second most abundant rapakivi granite type and is found as scattered intrusions in the Wiborg batholith (Fig. 3). It is a rapakivi granite variety with rounded, densely dispersed K-feldspar megacrysts (ovoids) having a diameter of 1–4 cm (Fig. 19A), but the size can vary from 1 to 10 cm. For example, the ovoids in the Virolahti pyterlite intrusion (2–4 cm) are larger than in the Kotka intrusion (1–2 cm). The megacrysts lack the rim of plagioclase and they are only occasionally mantled. Angular megacrysts are randomly present.

There are usually many ovoids in pyterlite, and they are evenly distributed, but ovoids can occasionally be scarce. A uniform area of brown pyterlite with evenly dispersed, 1–2 cm K-feldspar ovoids can be found to the southwest of the city of Lappeenranta (Fig. 19B). The amount of matrix can be over 50%, but ca. 20% of matrix is the average. The matrix is usually medium grained. The main minerals are K-feldspar, plagioclase, quartz and biotite.

The main colours of the pyterlite are red, brown and dark green. Distinct uniform areas of dark green pyterlite can be found around the villages

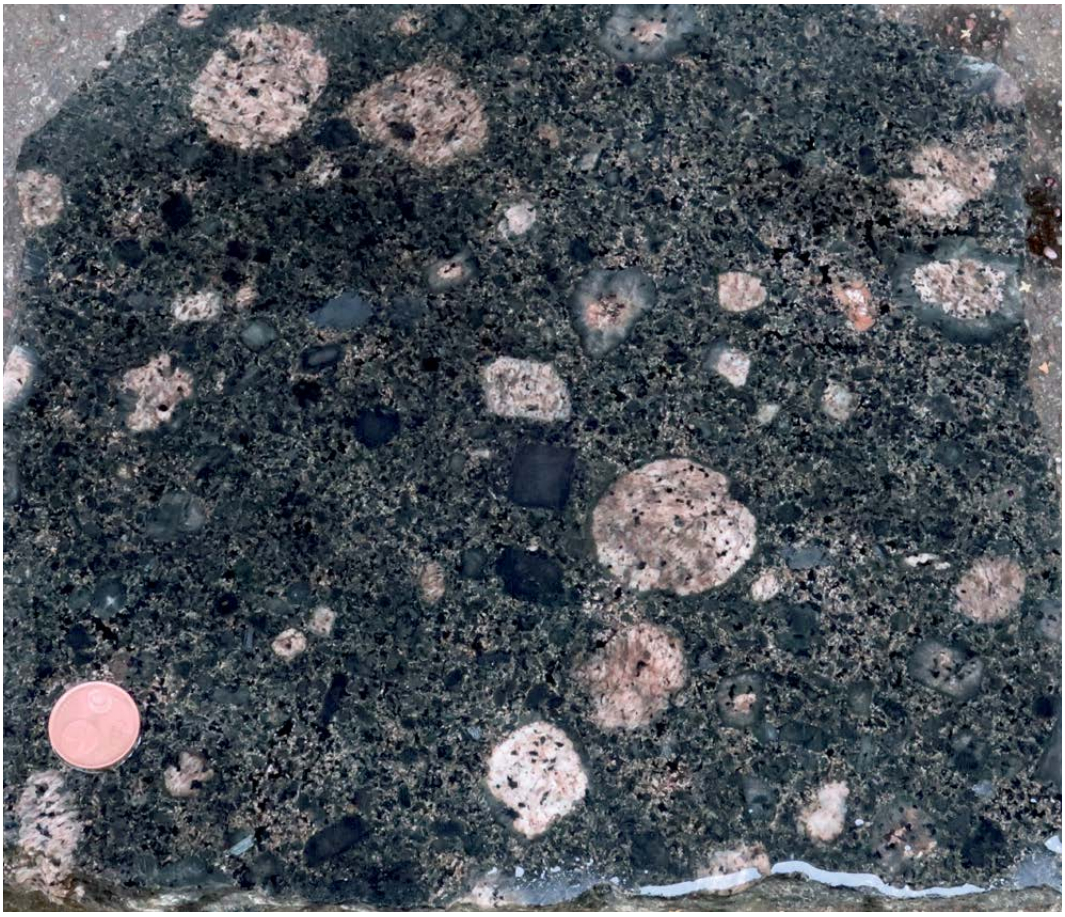

Fig. 18. A slab of dark wiborgite. Angular and euhedral dark plagioclase crystals are clearly visible on the sawed and wet surface. The coin is 2 cm in diameter. Location: Tillola, Kouvola. (Coordinates: x=6748463, y=474335 EUREF FIN TM35FIN). Photo: Paavo Härmä.

of Rantamäki, Sirkjärvi and Raippo. Transitions of pyterlite to wiborgite and to porphyritic rapakivi granite are common. The observed contacts between the wiborgite and pyterlite are usually in a subhorizontal position. Enclaves of even and medium-grained rapakivi granite are also found in the pyterlite.

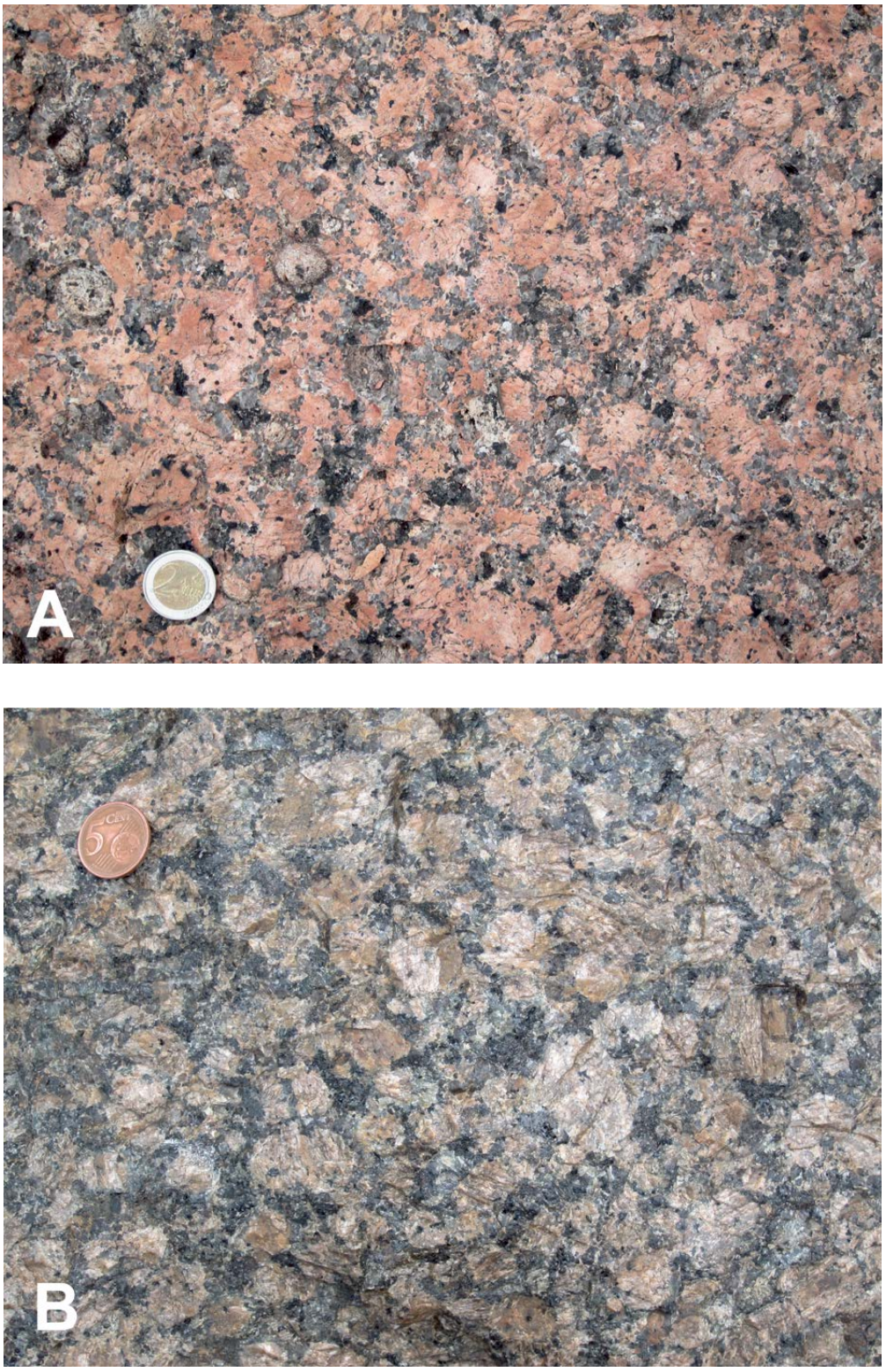

Fig. 19. A. Megacrysts (ovoids) (1–3 cm in diameter) are mostly without a plagioclase rim in pyterlite. The coin is 3 cm in diameter. Location: Pyterlahti, Virolahti. (Coordinates: x=6712626, y=535225 EUREF FIN TM35FIN). B. Homogeneous brown pyterlite with evenly dispersed, 1–2 cm K-feldspar ovoids. The coin is 2 cm in diameter. Location: Monola, Lappeenranta. (Coordinates: x=6712626, y=535225 EUREF FIN TM35FIN). Photos: Paavo Härmä.

5.2.4 Porphyritic rapakivi granites

Three varieties of porphyritic rapakivi granite were defined in this study. Porphyritic rapakivi granites are often found as relatively small bodies associated with pyterlite, even-grained rapakivi granites and wiborgite, mainly in the northern parts of the batholith (Fig. 3).

The typical porphyritic rapakivi granite consists of angular K-feldspar megacrysts (1–3 cm) in a medium-grained matrix. In addition, rounded megacrysts are randomly present. The main minerals are K-feldspar, plagioclase, quartz and biotite. The colour of the typical porphyritic rapakivi granite in the Jaala area (Fig. 3) is mainly red with light blue-coloured, droplet-shaped quartz grains (Fig. 20A). Transitions from porphyritic rapakivi granite to pyterlite and even-grained rapakivi granite are observed in places.

The porphyritic rapakivi granite in the Savitaipale municipality (Fig. 3), in the northeastern part of the batholith, consists of angular and rounded K-feldspar megacrysts (1–2 cm) in a medium-grained matrix (Fig. 20B). The colour is beige or occasionally pale red.

The porphyritic Sinkko granite (Hackman 1934, Simonen 1987) in the eastern part of the batholith (Fig. 3) is usually grey in colour, but can occasionally be pale reddish grey. The granite consists of angular K-feldspar megacrysts with a size of ca. 1–2 cm, but can include a few rounded megacrysts (Fig. 20C).

5.2.5 Even-grained rapakivi granites

Three main types of even-grained rapakivi granites are delineated here: biotite granite, hornblende granite and topaz-bearing even-grained granite. The even-grained biotite rapakivi granite is found as relatively small intrusions throughout the batholith, but larger areas are located in the western and northern parts of the batholith, e.g. in the municipalities of Pyhtää, Myrskylä and Valkeala (Fig. 3). The red-coloured, fine to medium-grained biotite granite is texturally rather homogeneous, as around the Tani and Enäjärvi villages (Fig. 3), but might also contain random K-feldspar megacrysts, 1–2 cm in diameter with a plagioclase rim, and as well as angular feldspar megacrysts (Fig. 21A). The mineralogical composition of the red even-grained biotite rapakivi granite is similar to that of the pyterlite, with the main minerals being K-feldspar, quartz, plagioclase and biotite.

The even-grained hornblende rapakivi granite, known as the Lappee granite (Hackman 1934, Simonen 1987), is found in the northeastern part of the Wiborg batholith. The brown or occasionally reddish-brown granite is texturally rather homogeneous (Fig. 21B), but contains sporadic mantled or unmantled K-feldspar megacrysts in places. It has hornblende and biotite as the main mafic minerals.

The topaz-bearing, even-grained granites are found in the western part of the batholith, for example as a part of the well-known Kymi granite stock (Haapala 1974, Lukkari 2007). The Kymi stock (Fig. 3) is composed of a topaz-bearing porphyritic rapakivi granite in the central part and a grey even-grained rapakivi granite along the margins of the stock (Simonen 1987, Haapala & Lukkari 2005). The even-grained granite contains more plagioclase than the biotite rapakivi granite. The topaz-bearing fine-grained Sääksjärvi granite (Fig. 21C) and the even-grained Artjärvi granite also belong to this lithological group (Lukkari 2007).

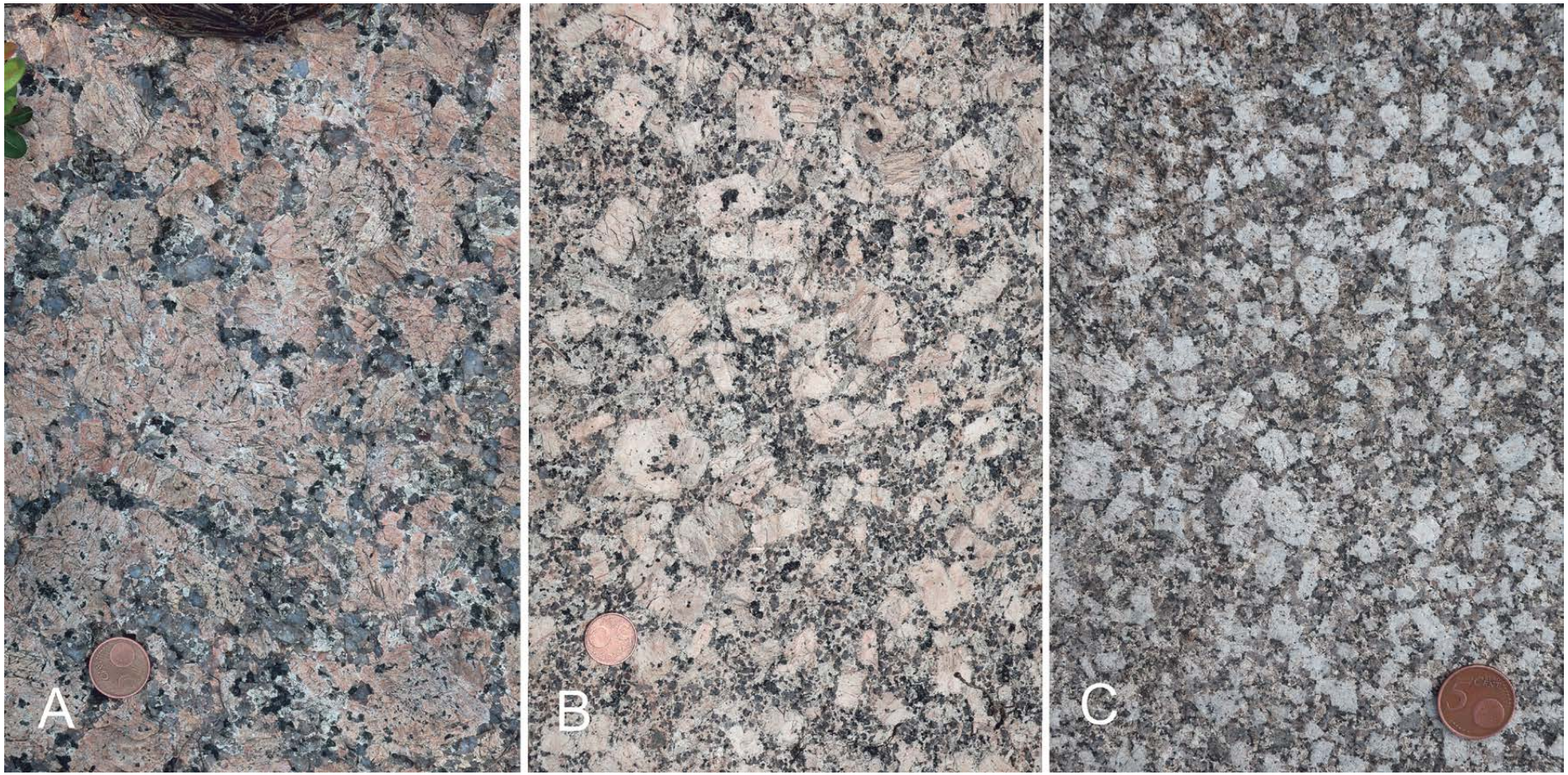

Fig. 20. Three varieties of porphyritic rapakivi granite. A. Typical porphyritic rapakivi granite. Location: Verla, Jaala. (Coordinates: x=6768944, y=478673 EUREF FIN TM35FIN). B. Porphyritic Savitaipale granite. Location: Viuhonpää, Savitaipale. (Coordinates: x=6782130, y=542150 EUREF FIN TM35FIN). C. Porphyritic Sinkko granite. Location: Sinkkola, Lappeenranta. (Coordinates: x=6765668, y=568706 EUREF FIN TM35FIN). The coin is 2 cm in diameter. Photos: Paavo Härmä.

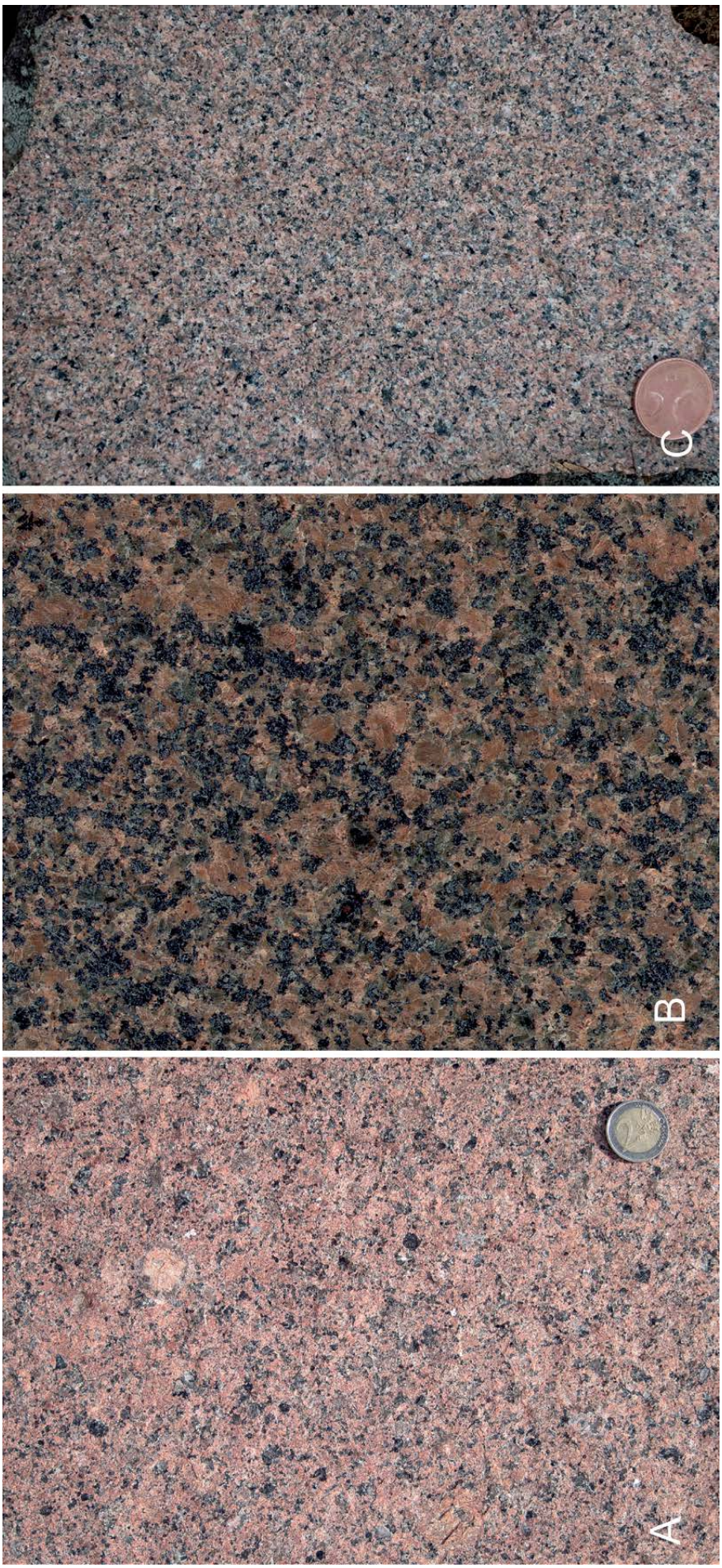

Fig. 21. Three varieties of even-grained rapakivi granite. A. Even-grained biotite rapakivi granite. The coin is 3 cm in diameter. Location: Enäjärvi, Kouvola. (Coordinates: x=6742500, y=508560 EUREF FIN TM35FIN). B. Even-grained hornblende rapakivi granite. Location: Pieni-Laihala, Lappeenranta. (Coordinates: x=6762530, y=576285 EUREF FIN TM35FIN). C. Topaz-bearing even-grained granite. The coin is 2 cm in diameter. Location: Sääksjärvi, Iitti. (Coordinates: x=6743425, y=454600 EUREF FIN TM35FIN). Photos: Paavo Härmä.

5.2.6 Dark rapakivi granites

Dark rapakivi granites comprise a lithological group that consists of rock types with varying texture, but which are similar in mineralogical composition. They can be dark green, dark greenish brown or black. The dark green, even-grained rapakivi variety has been called "tirilite" by Hackman (1934) and Simonen (1987).

The grain size of the dark rapakivi granites varies from fine- to coarse-grained and the texture from vaguely porphyritic to even-grained. The megacrysts in the dark rapakivi granites comprise angular and rounded K-feldspar crysts, as well as K-feldspar ovoids (Fig. 22A). There are also abundant angular, euhedral and dark-coloured (dark grey or even black) plagioclase megacrysts of andesine composition (usually in the range of An_{40-50}) (Fig. 22B). The size of these megacrysts varies from 0.5 to 6 cm in diameter. In addition, fine-grained mafic enclaves (1–10 cm in size) are occasionally present (Fig. 22C). Enclaves of wiborgite (under 30 cm in diameter) have been randomly observed.

The dark rapakivi granites contain quartz, plagioclase and K-feldspar in varying proportions. Hornblende, olivine, biotite and clinopyroxene are the mafic minerals, which together amount to up to 20 vol%. In all of the dark rapakivi granites, fayalitic olivine is present with hornblende and magnetite. Randomly, proportions of magnetite can be several volume percent in places.

The mineralogical composition of the dark rapakivi granites is similar to that of the dark wiborgite, but the dark wiborgite contains more K-feldspar ovoids mantled by plagioclase than the dark rapakivi granite.

The dark rapakivi granites are found often in close contact with even-grained hornblende rapakivi granite and anorthosites in northeastern and eastern part of the batholith (Fig. 3). A typical area is located between the villages of Rumpu and Villala.

5.2.7 Aplitic rapakivi granite

Aplitic rapakivi granite, also known as porphyry aplite (Simonen 1987, Rämö et al. 2014), is often found as small bodies of gradational to even-grained biotite rapakivi granite and usually in contacts between wiborgite and pyterlite (Fig. 3). In addition, subvertical and subhorizontal dykes of variable dimensions (thickness from metres up to a hundred metres) are common in the Wiborg batholith.

The aplitic rapakivi granite contains occasional, often mantled K-feldspar megacrysts in a fine-grained aplitic matrix (Fig. 23).

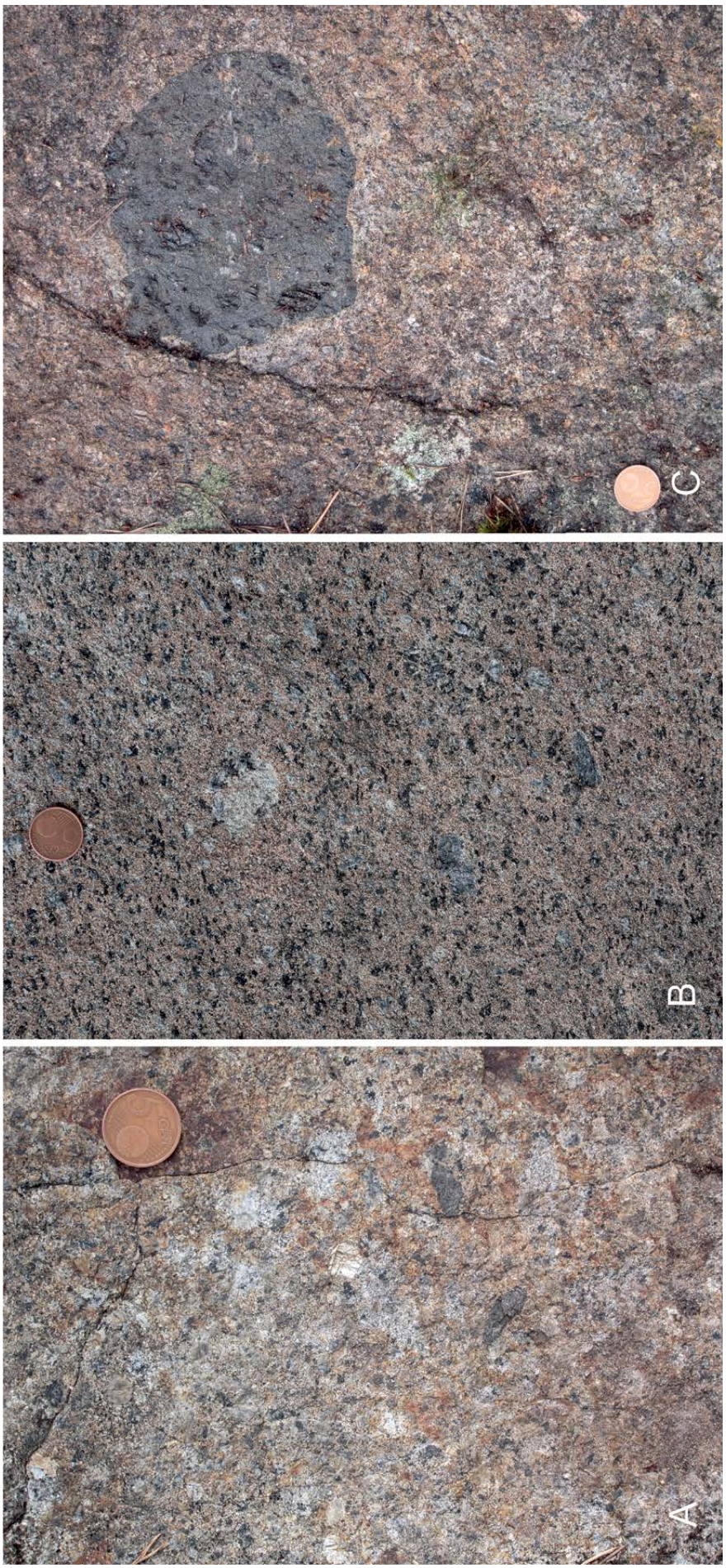

Fig. 22. Three examples of textural variations in dark rapakivi granite. A. Vaguely porphyritic dark rapakivi granite. Location: Melkkola, Lappeenranta. (Coordinates: x=6756350, y=561960 EUREF FIN TM35FIN). B. Angular, dark-coloured plagioclase megacrysts in a dark rapakivi granite. Location: Keskisaari, Lappeenranta. (Coordinates: x=6753035, y=576990 EUREF FIN TM35FIN). C. Fine-grained mafic enclaves in a dark rapakivi granite. Location: Melkkola, Lappeenranta. (Coordinates: x=6756350, y=561960 EUREF FIN TM35FIN). The coin is 2 cm in diameter. Photos: Paavo Härmä.

Fig. 23. Typical aplitic rapakivi granite with random K-feldspar megacrysts (ovoids, 1–2 cm in diameter). The coin in the upper part of the photo is 2 cm in diameter. Location: Inkeroinen, Kouvola. (Coordinates x=6725860, y=495570 EUREF FIN TM35FIN). Photo: Paavo Härmä.

5.2.8 Other rock types

Red or red brown quartz porphyry dykes are found in the southern part of the Wiborg batholith, striking NW–SE (Simonen 1987). They exhibit chilled contacts against the main rapakivi granite varieties. The megacrysts are comprised of K-feldspar and quartz.

Pegmatite and quartz veins cut the rapakivi granites of the Wiborg batholith. They have the same trends as the main fractures in the batholith. Miarolitic cavities are also common in wiborgite and pyterlite in the southern part of the batholith.

Anorthosite is the common name for mantle-derived leucocratic gabbroid cumulates (leucogabbronorite, leucotroctolite and anorthosite) associated with the rapakivi granites in the Wiborg batholith (Simonen 1987, Arponen & Rämö 2005, Arponen et al. 2009, Härmä & Selonen 2017). The rock is coarse-grained, grey, black or bluish black with an ophitic texture. The Wiborg batholith contains six anorthosite areas ranging from 0.1 to 1.5 km^2 (Arponen et al. 2009, Härmä & Selonen 2017) (Fig. 3). Five of them are located at the contact between wiborgite and dark rapakivi granite. The anorthosites are comprehended as large inclusions within the rapakivi batholith. Plagioclase (An_{50-70}) in the anorthosite iridescences strongly in spectral colours, and is hence called spectrolite.

5.3 General observations on fracturing in the Wiborg batholith

A total of 874 subvertical fractures were defined in this study (Table 1) and plotted as rose diagrams (Fig. 24). A prevalent fracture orientation of N30°W is observed in the entire Wiborg batholith (Fig. 24A), but the orientation of the subvertical fractures in the SW–NE direction is ambiguous, showing a cluster of maximum orientations. This divided character of the subvertical fracture pattern in the SW–NE orientation is found in the southeastern part of the batholith, showing two maxima at N55°E and N75°E (Fig. 24B), reflecting a diagonal fracture pattern.

Intensive subhorizontal fracturing (sheeting) (Fig. 25) is prominent in all rapakivi granite types of the batholith based on the field observations. The topography of these sites is usually low and flat over a large area at the top of the outcrop, limited by

long and intense subvertical fractures on the sides. Subvertical fractures are only prevalent in those outcrops where the subhorizontal fractures are scarce or weakly developed (Fig. 26). The subvertical fractures are usually easy to observe and to measure in these outcrops, while one direction is commonly dominant, making the outcrop elongated in that direction. The topography of these sites includes a high and narrow flat area at the top of the outcrop with steep slopes on the sides.

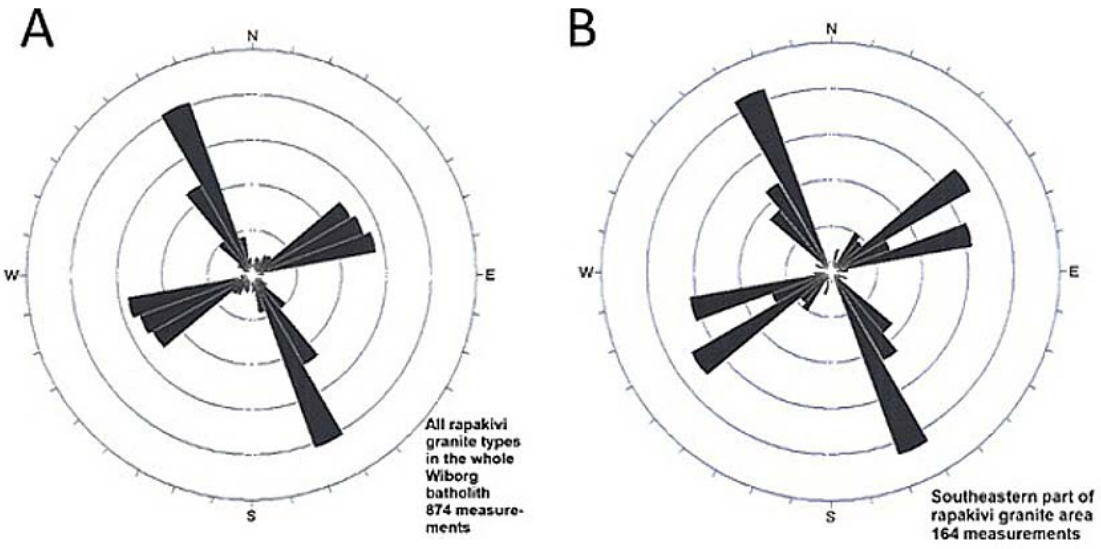

Fig. 24. Fracture orientation data (subvertical fracture planes dipping between 45° and 90°) from the Wiborg batholith. A. From all rapakivi granite types in the whole batholith area, B. From the southeastern part of the batholith in varying rapakivi granite types. A clear peak in the direction N30°W can be observed, but the SW–NE fracture orientations are clustered.

Fig. 25. Prevalent subhorizontal fractures (sheeting) in a wiborgite outcrop. Location: Kannuskoski, Luumäki. (Coordinates: x=6755480, y=514311 EUREF FIN TM35FIN). Photo: Paavo Härmä.

Fig. 26. Subvertical fractures prevail in this wiborgite outcrop. Location: Lapatto, Savitaipale. (Coordinates: x=6774230, y=533320 EUREF FIN TM35FIN). Photo: Paavo Härmä.

The ovoids in wiborgite and pyterlite usually have prominent microfractures that have the same orientation as the main macroscopic subvertical fractures in the batholith (Fig. 27). The microfracturing is particularly distinct parallel to the macroscopic subhorizontal fractures, as observed on the subvertical sections of outcrops.

The subhorizontal fractures are commonly open in the Wiborg batholith. The subvertical fractures in the direction of N30°W are frequently open and can be filled with quartz, pegmatite and aplite. The subvertical fractures in the two other main orientations, N55°E and N70°E, are mainly tight and closed. No filled fractures were observed in the field in these directions.

A number of quartz veins of varying thickness (1–50 cm), occasionally with epidote along the margins, are common in the western and central part of the Wiborg batholith. All of them are in one direction, N30°W, having the same orientation as

one of the main macroscopic subvertical fractures. The subvertical fractures in the directions N55°E and N75°E cut across the quartz veins (Fig. 28). In addition, there are occasional "fire lines"[1] in the orientation of N30°W with a thickness of a few millimetres, usually under 2 mm. Around these fire lines, most often in wiborgite and pyterlite, the rock is red coloured (Fig. 29) instead of the original, real colour of granite.

Fig. 27. Microfractures in the wiborgite ovoids are in the same orientations as the main subvertical fractures of the Wiborg batholith: N30°W and N70°E. The width of the compass in the upper left corner in 5 cm. Location: Inkerilä, Kouvola. (Coordinates: x=6763890, y=502920 EUREF FIN TM35FIN). Photo: Paavo Härmä.

[1] "Fire line" is a term used in the natural stone industry to describe thin veins with red-coloured surroundings, usually filled with a thin film of quartz, epidote and sometimes chlorite, and sporadically even with fluorite.

Fig. 28. A quartz vein over 30 cm thick with epidote in the orientation of N30°W and in contact between aplitic rapakivi granite on the left and wiborgite on the right side. Subvertical fractures (N55°E and N75°E) cut across the quartz vein. The coin is 3 cm in diameter. Location: Suljento, Kotka. (Coordinates: x=6719315, y=489765 EUREF FIN TM35FIN). Photo: Paavo Härmä.

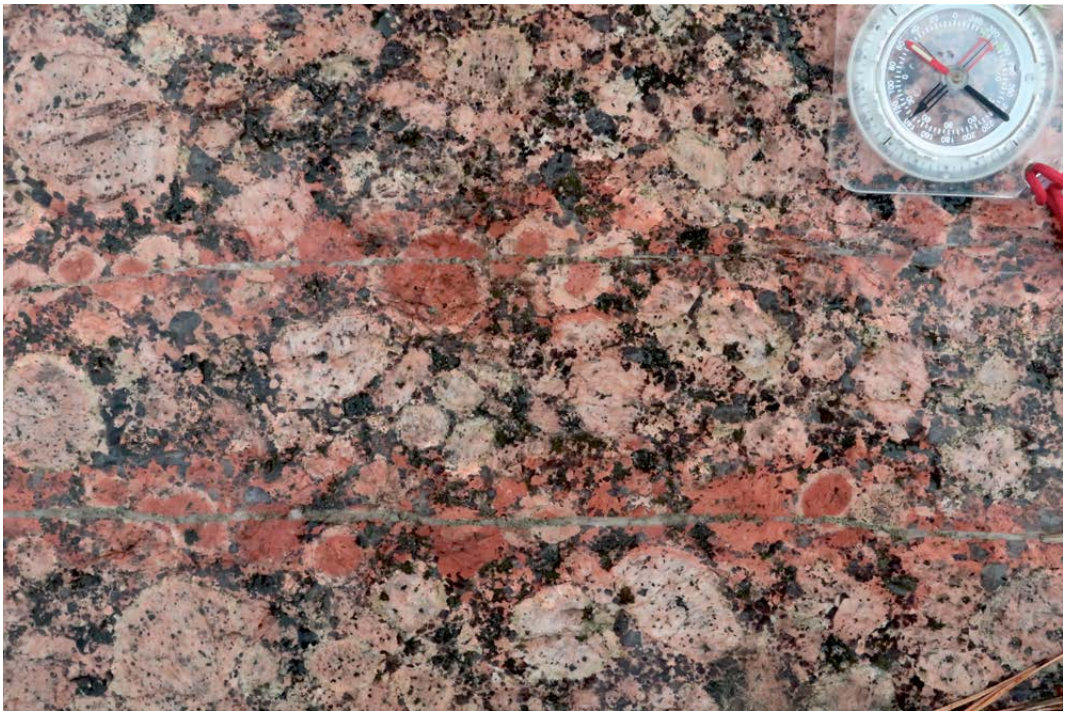

Fig. 29. Fire lines with the orientation of N30°W in wiborgite, the colour of which is red around the fire line. The thin fractures are mainly filled with quartz and epidote. Minor dislocation of an ovoid can be observed along the upper fire line. The width of the compass in the upper right corner in 5 cm. Location: Viuhkola, Luumäki. (Coordinates: x=6773108, y=518890 EUREF FIN TM35FIN). Photo: Paavo Härmä.

5.4 Fracturing in the rock types

5.4.1 Wiborgite

The macroscopic fracture pattern in the wiborgite is dominantly orthogonal with both open and closed fractures. The main fractures that cut across the outcrops are often open and in the orientation of N30°W (Fig. 30A). Other main fractures are in the orientation of N75°E. The subvertical fractures in the orientation of N55°E are not well developed in wiborgite, but the rock shows a weak diagonal fracture pattern besides the orthogonal pattern.

The outcrop fracturing of the wiborgite is sparse, and the spacing of the subvertical fractures is 3–6 m on average, but can in places be up 20 m (Fig. 31). The average spacing of the subhorizontal fractures is 2–4 m.

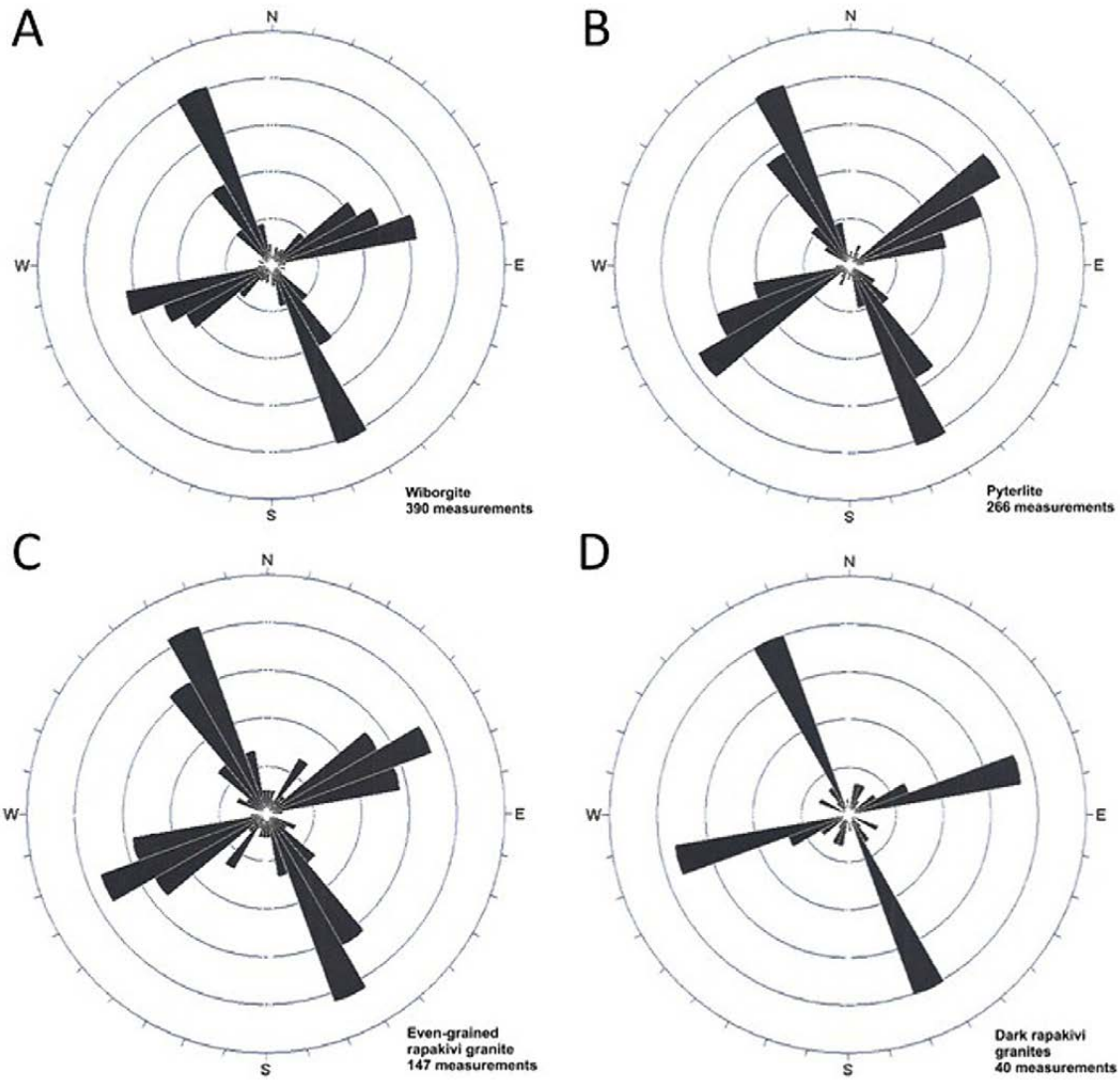

Fig. 30. Fracture orientation data (subvertical fracture planes dipping between 45° and 90°) measured in the entire Wiborg batholith area. A. Wiborgite, B. Pyterlite, C. Even-grained rapakivi granites, and D. Dark rapakivi granites. A clear peak in the direction N30°W can be observed in all rock types. The maximum peak of the orientations in the SW–NE direction varies according to the rock type.

Fig. 31. Sparse fracturing in wiborgite with spacing of the subvertical fractures of 15–20 m. Location: Myllykylä, Pyhtää. (Coordinates: x=6711760, y=481030 EUREF FIN TM35FIN). Photo: Paavo Härmä.

5.4.2 Dark wiborgite

The fracture pattern in dark wiborgite is orthogonal with open and closed fractures. The spacing of the subvertical fractures is 3–4 m on average, and the spacing of the subhorizontal fractures varies between 2 and 3 m.

5.4.3 Pyterlite

The fracture pattern of pyterlite is orthogonal with open and closed fractures. The main subvertical fractures are often open, at least in the direction of N30°W. The prevalent fracture orientation is N30°W, but fractures in the orientation of N55°E (Fig. 30B) are observed. The subvertical fractures in the orientation of N75°E are less developed in the pyterlite than in the wiborgite, showing a weak diagonal fracture pattern besides the orthogonal pattern. Random diagonal fractures are also found in the direction of N20°E (Fig. 30B).

On average, the fracturing in the pyterlite is sparse, with the spacing of the subvertical fractures being 3–5 m and that of the subhorizontal fractures 2–4 m. In some cases, the spacing between parallel subvertical fractures can be 10–15 m (Fig. 32).

5.4.4 Porphyritic rapakivi granites

The fracture pattern in the porphyritic rapakivi granites is orthogonal with open and closed fractures. The main fractures are generally open and the average spacing of the subvertical fractures is up to 4 m, while that of the subhorizontal fractures is 2–3 m. Sheeting is well developed and dense in the Sinkko-type porphyritic rapakivi granite.

5.4.5 Even-grained rapakivi granites

The fracture pattern in the even-grained biotite and hornblende granites is mainly orthogonal, but diagonal patterns are also present. The spacing of the subvertical fractures varies up to 3 m. The spacing of the subhorizontal fractures ranges from 0.5–2 m, but is 1–2 m on average.

An intense fracture orientation can be observed in the N30°W direction, as in the wiborgite and the pyterlite, as well as the fracture orientation of N70°E (Fig. 30C). An interesting feature is the fractures in the direction N30°E, which has not been observed in other rock types. These fractures are sparse but rather distinct. Another interesting fracture direction is N70°W, which is rare, but fractures

Fig. 32. Sparse fracturing in pyterlite with the spacing of the subvertical fractures being ca. 15 m. Location: Ala-Pihlaja, Virolahti. (Coordinates: x=6712620, y=535220 EUREF FIN TM35FIN). Photo: Paavo Härmä.

are continuous as they cut across the outcrops. This fracture orientation is sporadic but prominent.

5.4.6 Dark rapakivi granites

The fracture pattern in the dark rapakivi granites is mainly orthogonal. The subhorizontal fractures dominate over the subvertical ones. The spacing of the subvertical fractures varies between 1 and 3 m, and that of the subhorizontal fractures between 0.5 and 2 m.

An intensive fracture orientation of N30°W, as in the other rapakivi granite types, can be discerned (Fig. 30D), as well as a dominant and distinct fracture direction of N75°E (Fig. 30D), which is also observed in wiborgite.

5.5 Local variation in fracturing, a case study

The spacing and orientation of the subvertical fractures were examined in detail in two natural stone quarries in the southeastern part of the batholith (Fig. 33). The distance between these quarries is ca. 3 km. Subvertical fractures were measured from a selected bench in the quarries. The rock type in both quarries is wiborgite.

In Quarry A, a strong fracture orientation of N30°W is distinct (common in wiborgite) (Fig. 34A). In addition, a fracture orientation of N75°E (Fig. 34A) is also prevalent. Interesting fracture planes occur in the direction of N70°W. As in the even-grained rapakivi granites, they are long and continuous fractures that cut across the whole quarry.

Fractures in Quarry B show prevalent orientations of N35°E, N50°E and N75°E (Fig. 34B). The fracture direction N40°E (Fig. 34B) is less intensive than in Quarry A, while the fractures trending N75°E are as dominant as in Quarry A. Many fracture planes are in the directions of N30°E and N50°E, which are not observed in Quarry A.

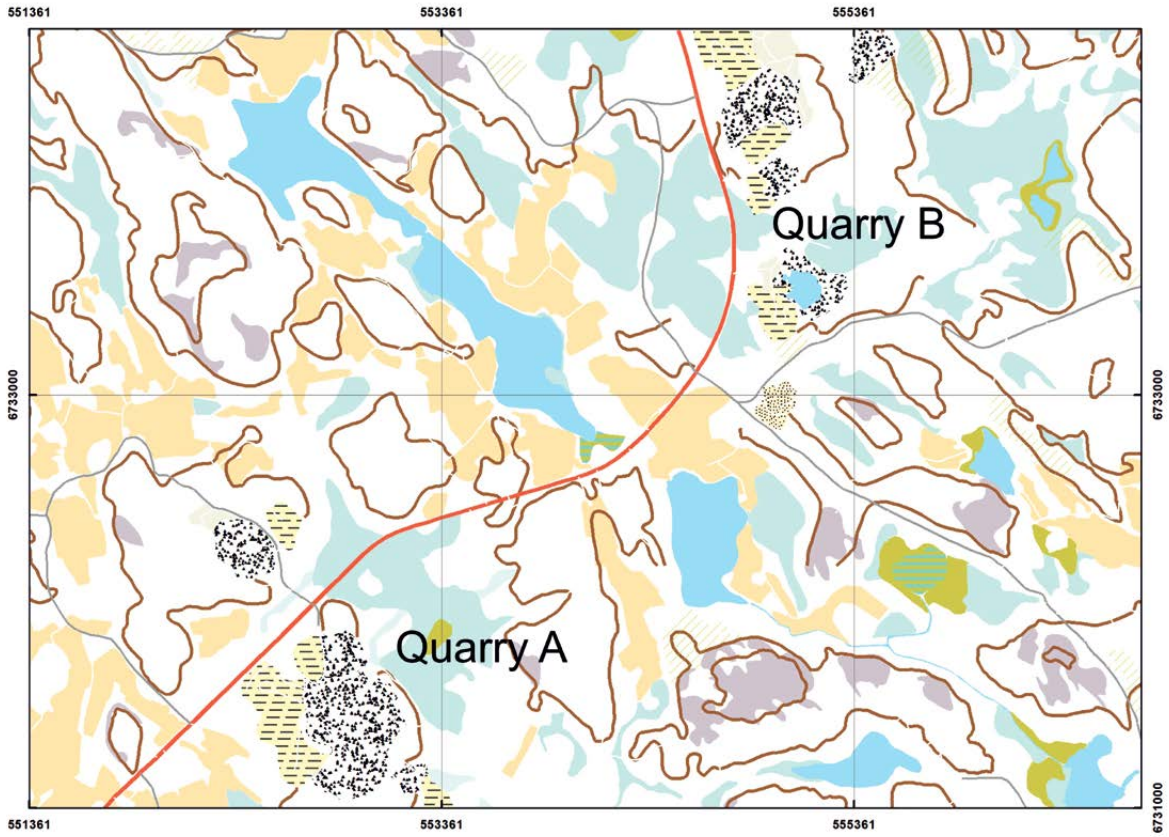

Fig. 33. Location of Quarry A and Quarry B in the southeastern part of the Wiborg batholith. The distance between the wiborgite quarries is ca. 3 km. Base maps: © National Land Survey of Finland.

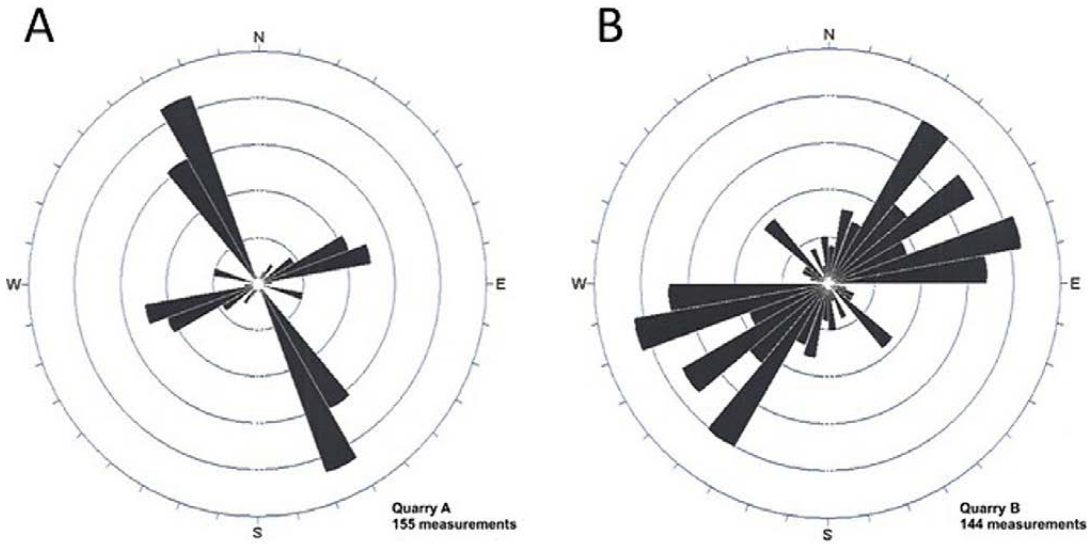

Fig. 34. Fracture orientation data (subvertical fracture planes dipping between 45° and 90°) measured in wiborgite from a selected bench in Quarry A (A) and in Quarry B (B). A clear peak in the direction N30°W can be seen in Quarry A. Several maximum peaks are observed in Quarry B in the direction of SW–NE, namely N35°E, N55°E and N75°E, and a small peak in the direction of N40°W.

5.6 Main observations regarding rock types and fracturing

- The Wiborg batholith comprises seven main rapakivi granite types: wiborgite, dark wiborgite, pyterlite, porphyritic rapakivi granite, even-grained rapakivi granite, dark rapakivi granite and aplitic rapakivi granite. The contacts between the granite bodies are commonly in a subhorizontal position.

- Areas with a distinct and homogeneous colour and texture are found inside the different rapakivi granite types, e.g. inside wiborgite and pyterlite.

- The fracture pattern in the rapakivi granites in the Wiborg batholith is mainly orthogonal, with two subvertical fracture directions perpendicular to each other accompanied by well-developed sheeting. A diagonal fracture pattern in the southeastern part of the batholith is found.

- The main fracture orientations in the Wiborg batholith are N30°W (dominant), N55°E and N75°E. Rare but strong fracturing is also discerned in the directions of N30°E and N70°W.

- Subhorizontal fractures are dominant in all rapakivi granite types; subvertical fractures only occasionally prevail. The orientations of fractures can vary significantly between closely located areas.

PART III RAPAKIVI WEATHERING

6 WEATHERING OF RAPAKIVI GRANITES

6.1 Introduction to weathering features

The weathering of rocks comprises the weakening and breaking down of rocks and minerals. Three types of weathering can be discerned: physical/mechanical weathering, chemical weathering and biological weathering (e.g. Goldich 1938, Vuorinen et al. 1981, Uusinoka 1983, Ollier 1984, Carroll 2012). In physical or mechanical weathering, rocks break into pieces, whereas chemical weathering results from the interaction of water and temperature. Oxidation is a type of chemical weathering in which the iron in rocks reacts with oxygen and water, leading to rust. Biological weathering is a result of plant, animal and even microbial influence.

According to Goldich (1938), igneous silicate minerals that form at higher temperatures and pressures are less stable and more likely to weather than minerals formed at lower temperatures and pressures. Thus, the first crystallized minerals also weather first. Olivine weathers more easily than mica and quartz, and Ca-rich plagioclase easier than the sodium-rich varieties. Two main types of chemical weathering exist: some minerals alter to other minerals or some others dissolve completely, and their components go into solution. For example, feldspar is altered by hydrolysis to clay minerals (Earle 2015). Chemical weathering reactions happen with cations that bind the silica tetrahedral units together. Hence, quartz is most stable, as it is completely formed of interlocking silica tetrahedra units with no lattice-modifying cations.

The surficial weathering of rapakivi granite has been known in Finland for over a hundred years. It has been studied since the late 19th century, and a variety of explanations for the special type of weathering have been presented. Rapakivi granite weathers to crumbly rock or to sharp-edged grit. This type of weathering is known as "grusification" and it comprises both mechanical and physical processes (Kejonen 1985 and references therein). In his rock aggregate studies, Vallius (1995) observed surface weathering of rapakivi granites and its influence on rock sampling.

The first theories implied that the chemical weathering of oligoclase in granite could cause disintegration. Sederholm (1891) noted that the typical rapakivi texture is more prone to the breakdown of mineral grains than, for instance, an even-grained texture. Eskola (1930) suggested that the main reason for weathering is the "simple" texture with smooth and straight contacts between the mineral grains. He also argued that micro-sheeting loosened the texture, after which chemical weathering decomposes Fe-rich minerals. He pointed out that only the coarse-grained rapakivi varieties and the rapakivi types containing rather large amounts of dark Fe-rich minerals were weathered. Furthermore, the most complete weathering could be found in outcrops on southward slopes, which are most exposed to sunlight. According to Nyström & Selonen (2004), during the weathering of dark wiborgite, the mobilized elements include CaO, Co, Mo, Sr, Th, U, Y, Zn, lanthanides ± F, Hf, Sc, MgO and P2O5.

According to Kejonen (1985), two main types of rapakivi weathering can be defined. The most common type is the disintegration of matrix surrounding the K-feldspar ovoids, where the ovoids themselves remain less weathered. The other types are triggered by micro-sheeting that randomly intersects all minerals and which develops subconformably to the rock surface or to the primary subhorizontal fractures. The weathering is also most intense along fractures, and the spatial variation of the weathering is connected to the structure and texture of the granitic rocks (Kejonen 1985).

Kejonen (1985) summarized the results of earlier studies on surficial rapakivi weathering as follows. "Grusification", i.e. rapakivi weathering, mostly

affects the coarse-grained rapakivi granite types, in particular wiborgite. Dark varieties of rapakivi with a higher content of amphibole and mica have a higher tendency to weather than light varieties. Strongly weathered horizontal or vertical zones can be found within intact zones. Usually, the weathering is caused by tectonic movements affecting the texture of the granite.

In addition, it should also be noted that weathering is a slow process, and the primary stages of weathering often date back to pre-glacial times.

6.2 Study area and methods

Studies on the surficial weathering of the rapakivi granite outcrops were carried out as field mapping covering the entire Wiborg batholith and as site investigations on selected outcrops. The study was focused on the uppermost parts of the outcropping granites, and on the early stages of the weathering phenomena. Usually, the weathering was rather easily recognised on the outcrop, but the identification occasionally needed more investigation and subvertical sections of outcrops. More attention was paid to wiborgite and pyterlite in the field, as they are the most weathered rapakivi varieties.

During the field mapping, the weathering stage of outcrops was defined visually together with the rock type, colour, texture, appearance, homogeneity and soundness of the rapakivi granites. Samples were taken from the surface of rock using a hand-held diamond saw to study the weathering stage of the different rocks types. From some of the samples, thin sections were prepared in order to examine the weathering phenomena at the microscopic scale.

Site investigations were executed on outcrops without soil cover or along cleaned investigation traverses on selected outcrops (Fig. 35). The selection of outcrops was based on the representativeness of the weathering phenomena. The spacing of the macroscopic fractures was measured along the traverses. The general colour, the colour variations and texture of the rapakivi granite were visually observed. Furthermore, diamond core drilling (cores of approx. 40 mm in diameter) was carried out on selected traverses (Fig. 35). The soundness and the variations in appearance and colour were logged in detail from the drill cores, paying special attention to the upper part of the drill cores.

The samples for resin-impregnated preparations were selected from the 136 samples collected with a hand-held diamond saw during the field mapping and the site investigations (Fig. 36). The resin-impregnated preparations were made in order to verify the weathering phenomena observed macroscopically on outcrops. The resin contained fluorescent, UV-light-reflecting powder for the study of microfractures and cracks (cf. Nishiyama & Kusuda 1996). Besides the impregnated preparations, thin sections were prepared from the specimens.

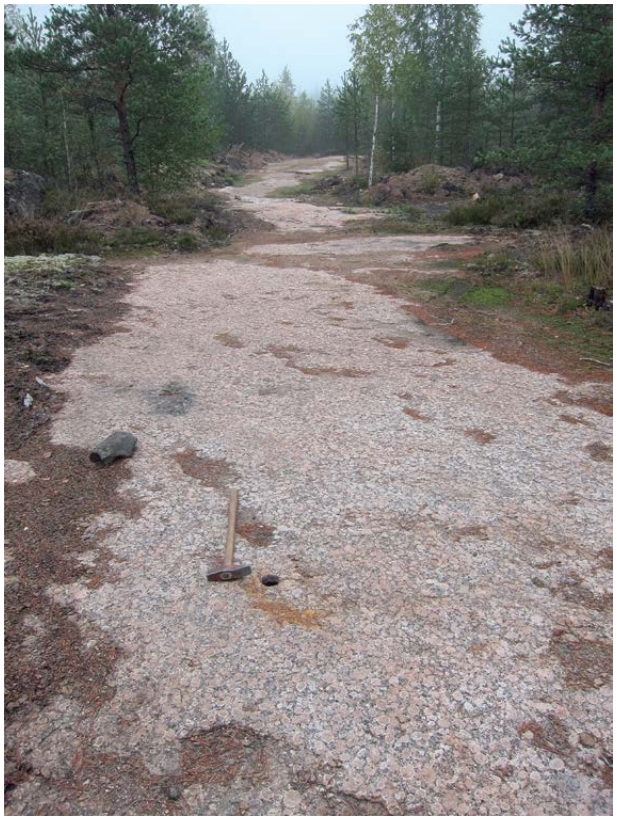

Fig. 35. Site investigations with core drilling (in front, near a hammer) were carried out along cleaned investigation traverses on selected outcrops during weathering studies. The length of the hammer handle is 70 cm. Location: Ala-Pihlaja, Virolahti. (Coordinates: x=6712460, y=536070 EUREF FIN TM35FIN). Photo: Paavo Härmä.

Fig. 36. Sampling was carried out with a hand-held diamond saw, producing specimens of ca. 8 cm in height and 20 cm in length. The long side of this sample is in the direction N60°W. The section of a resin-impregnated rapakivi granite specimen presented in Fig. 40A was made from this sample. The length of the compass is 12 cm. Location: Sippola, Kouvola. (Coordinates: x=6737508, y=495686 EUREF FIN TM35FIN). Photo: Paavo Härmä.

6.3 Weathering as observed on outcrops

6.3.1 Wiborgite

The surficial weathering of the wiborgite varies in intensity from weakly weathered (change of colour) (Fig. 37) to the total disintegration of the rock. The upper parts of wiborgite are weathered down to an average depth of 1–2 m. The dark varieties of wiborgite weather more easily than the light ones. In places, the wiborgite is weathered on a single outcrop with nearly intact and weathered parts mixed randomly together. Weathering was also observed along subhorizontal and subvertical fractures and zones deeper down in wiborgite (Fig. 38). The colour of the rock on the outcrop often corresponds to the colour of weathered rock, having paler and sometimes rustier tints than the true colour of the fresh rock.

Fig. 37. Weathered outcrop of wiborgite. The real colour of the wiborgite cannot be reliably determined from the outcrop. The coin in the lower left corner is 3 cm in diameter. Location: Ravijärvi, Virolahti. (Coordinates: x=6720940, y=525715 EUREF FIN TM35FIN). Photo: Paavo Härmä.

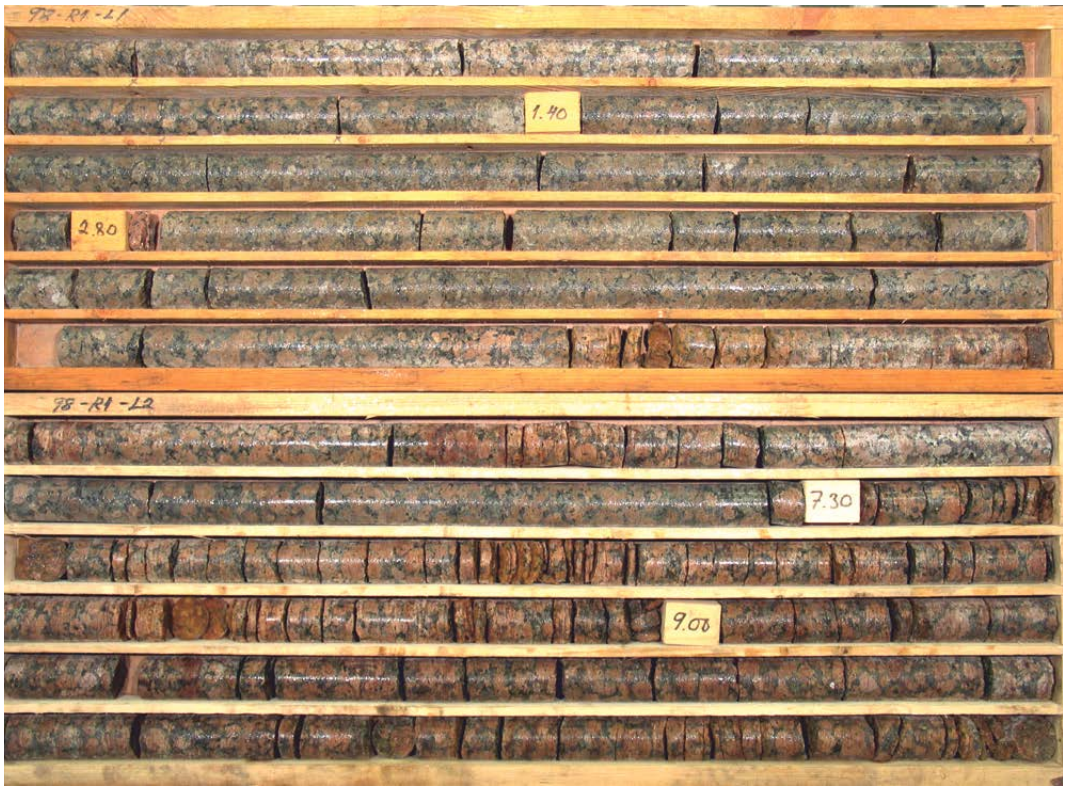

Fig. 38. Drill core of wiborgite. The wiborgite from the depth of 7.30 to 11.50 m is strongly weathered, showing dense subhorizontal fracturing. Location: Ylijärvi, Lappeenranta. (Coordinates: x=6736000, y=548000 EUREF FIN TM35FIN). Photo: Paavo Härmä.

6.3.2 Dark wiborgite

The surficial weathering in the dark wiborgite varies in intensity according to the colour of the rock, where the darker variations are more weathered than the lighter ones. The upper parts of dark wiborgite are commonly weathered. Weathering along subhorizontal and subvertical fractures deeper in rock was also observed. The colour of the weathered dark wiborgite on the outcrop is lighter than the real colour of the rock. Sometimes, the rock can even be grey or rust-coloured.

6.3.3 Pyterlite

The upper parts of the pyterlite are weathered down to 1–2 m depth with variation in intensity. The outcrops can in places appear to be intact on the horizontal surface, but the vertical section of the same outcrop reveals that the rock is totally weathered down to a couple of metres depth (Fig. 39). The colour of the pyterlite on the outcrop is often altered and represents the colour of weathered rock, with pale and rusty colours.

6.3.4 Porphyritic rapakivi granite

The upper parts of the porphyritic rapakivi granites are typically weathered down to 1–2 m depth on average. The colour of the rock on the outcrop usually represents the colour of weathered rock, with light colours.

6.3.5 Even-grained rapakivi granites

The surficial parts of the even-grained rapakivi granites are usually slightly weathered down to 1 m depth or appear almost unweathered. The dark-coloured varieties are more weathered than the light-coloured ones.

6.3.6 Dark rapakivi granites

The upper parts of the dark rapakivi granites are weathered down to 1–2 m depth, with variation in intensity depending on the grain size. Medium and coarse-grained varieties are more weathered than the fine-grained ones. The colour of the dark rapakivi granites on the outcrop is often altered and represents the colour of weathered rock, with pale and greyish colours.

6.3.7 Other rocks

Outcrops of the other rock types in the Wiborg batholith, such as the aplitic rapakivi granite and anorthosite, as well as the pegmatite and quartz veins, seem to be unweathered; only the surface of the rocks can be weathered down to a depth of 1 cm.

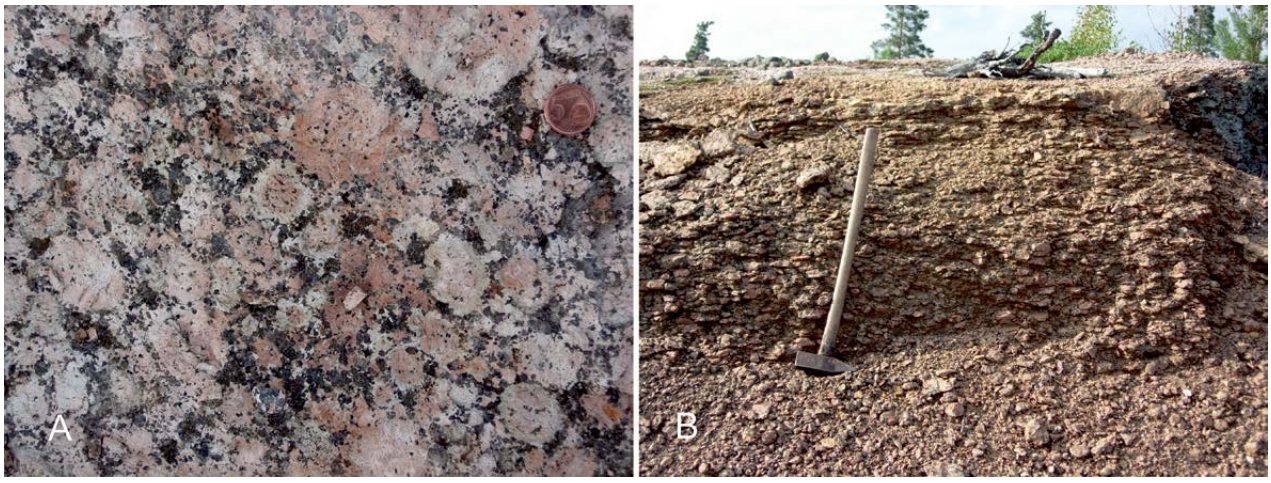

Fig. 39. On the left (A) is a subhorizontal surface of a pyterlite outcrop. The coin in upper right corner is 2 cm in diameter. The subvertical section of the same pyterlite outcrop shows that the rock is totally grusified (B). Length of the hammer handle is 70 cm. Location: Ala-Pihlaja, Virolahti. (Coordinates: x=6713200, y=535100 EUREF FIN TM35FIN). Photos: Paavo Härmä.

6.4 Hand sample and microscopic observations

Weathering and fracturing can be observed in the resin-impregnated samples and in the thin sections (Figs. 40 and 41). At least three generations of microfractures can be discerned.

Two subvertical fracture directions were observed (J1 and J2) (Fig. 41). J1 fractures are associated with K-feldspar alteration, whereas no alteration is observed along the J2 fractures. Microfractures with the same subvertical orientations as J1 and J2 in K-feldspar ovoids were also recognized in the field on the same outcrop from where the resin-impregnated sample and thin section were collected. It was observed that the J2 orientation is more dominant than J1. According to field observations, no noticeable alteration can be found in the fractures in the dominant J2 direction, whereas the fractures of the weaker direction (J1) are filled with alteration products, corresponding to the microscopic observations.

In the rock samples and thin sections, the predominant feature is subhorizontal microfracturing (J3 in Fig. 41), which does not follow any boundaries of mineral grains or ovoids, but cuts straight through the texture of rock along the whole length of the sample. The subhorizontal microfractures penetrate the K-feldspar ovoids almost straightforwardly, and only small dislocations can be seen when transecting subvertical microfractures or the cleavage plane of K-feldspar (Fig. 41, red lines with mark J3). No alteration products have been found in the subhorizontal microfractures in these samples.

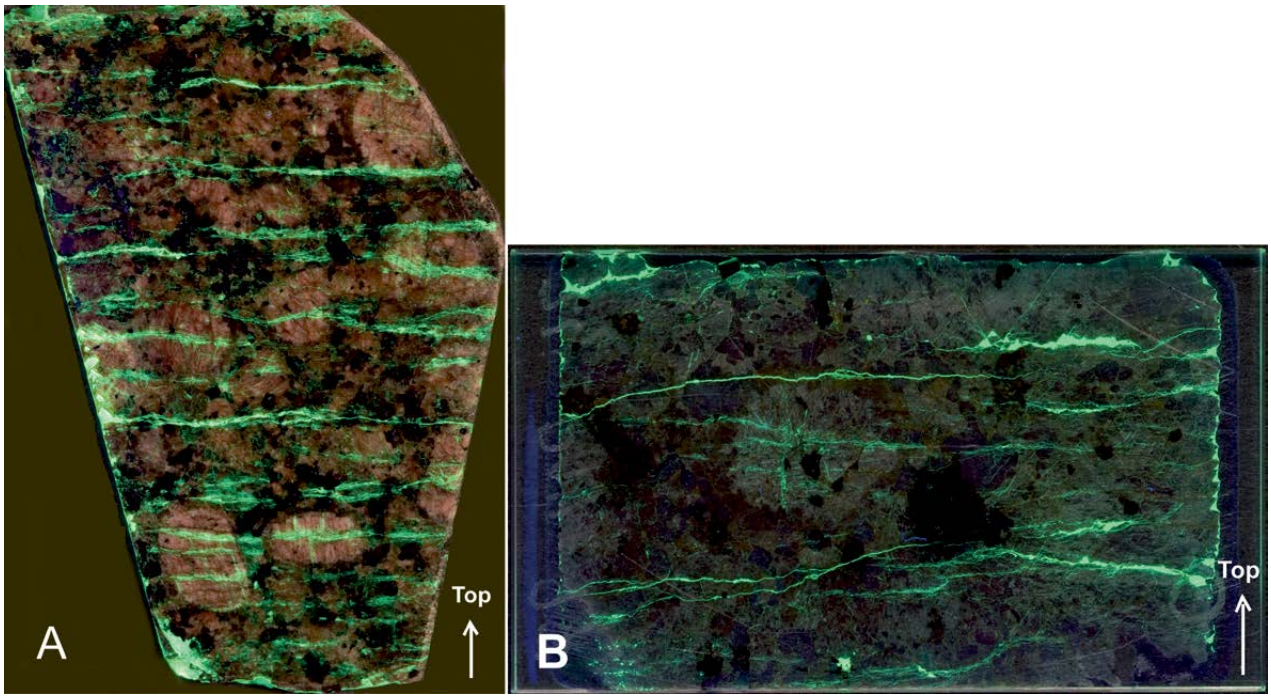

Fig. 40. A. Subvertical section of a resin-impregnated rapakivi granite specimen, which was taken using a hand-held diamond saw, as shown in Fig. 36. The specimen was taken vertically from the surface of the outcrop and the height of sample is 8 cm. B. A thin section from the same rock specimen as in 40A. The length of the thin section is 3 cm. The pale stripes are fluorescent resin along the subhorizontal microfractures. The photos were taken under UV light by Jari Väätäinen.

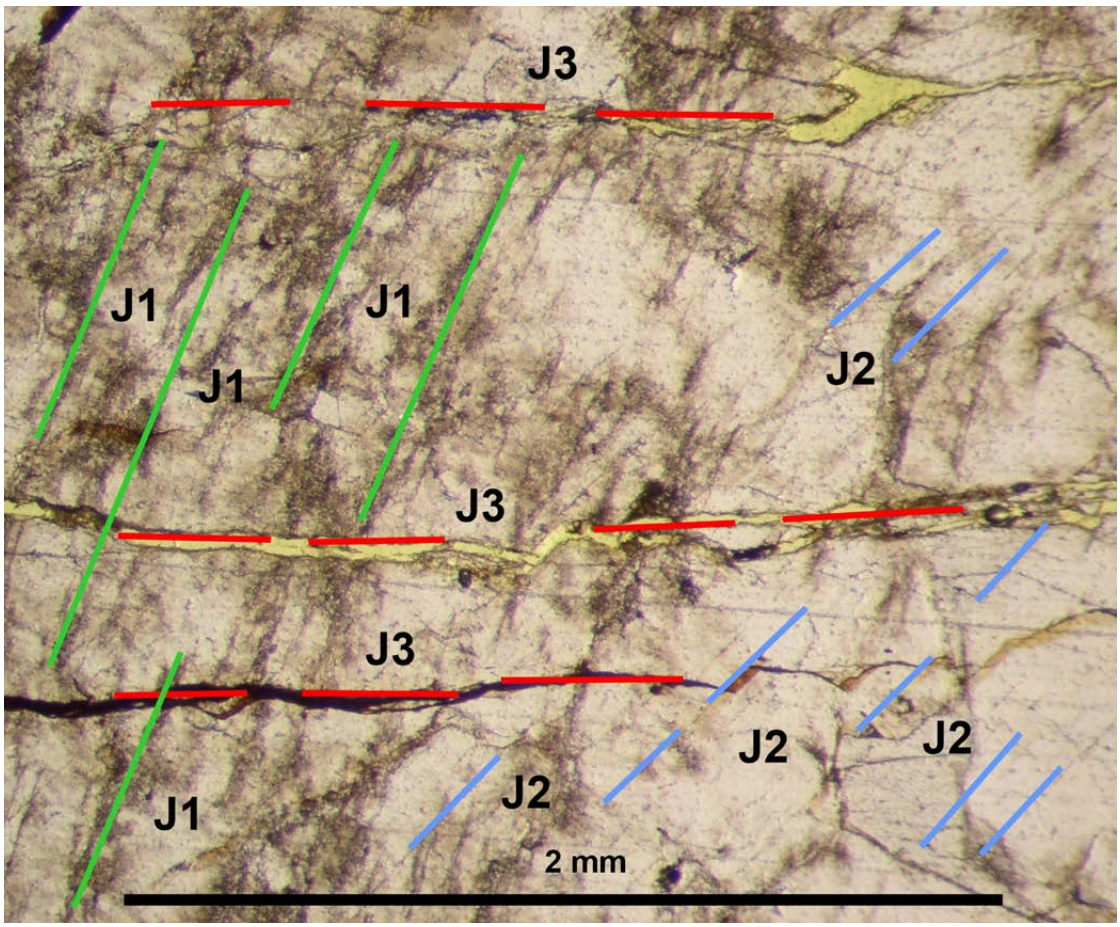

Fig. 41. A view of one K-feldspar ovoid in the thin section of Fig. 40B. The pale stripes are fluorescent resin in subhorizontal microfractures (red lines marked with J3). The dark stripes from the top of the photo towards the lower left corner are subvertical microfractures (green lines marked with J1). The thin stripes in the right-hand corner of the photo are other subvertical or inclined microfractures (blue lines marked with J2). The thin section was prepared from the sample shown in Figs. 36 and 40A. The section is in a subvertical position and the plane of view is in the orientation N20°E. Photo: Paavo Härmä.

6.5 Main observations on weathering

- The upper parts of the wiborgite, dark wiborgite, pyterlite, porphyritic rapakivi and coarse-grained dark rapakivi granite are affected by weathering of varying intensity. The weathering can reach from the surface down to a depth of 1–2 metres.
- Weathering may also appear as random subhorizontal and subvertical zones deeper in the rock.
- Weathering changes the colour, texture and soundness of rapakivi granite.
- Subhorizontal microfractures have a central role in the development of surficial weathering.

PART IV GEOPHYSICIAL AND MORPHOLOGICAL DATA

7 GEOPHYSICAL AND MORPHOLOGICAL DATA: ROLE IN EXPLORATION

Geophysical and morphological methods can be used in exploration for natural stone during the desk stage and in the detailed examination of a prospect. The main purpose of the methods during the detailed studies is to estimate the soundness of the prospect.

Low-altitude aeromagnetic data show the distribution of magnetic minerals in the bedrock. These data are well suited to structural and lithological mapping, regardless of the scale of the study area, and are often used in the desk stage. Positive magnetic anomalies in airborne geophysical maps are commonly caused by mafic rocks, whereas granites generally show only weak magnetism (Airo & Säävuori 2013). In cases, there appears to be a correlation between the soundness of the rock and its magnetivity: the soundest and the most magnetic parts correlate with each other (Vartiainen 2017). The airborne geophysical data sets have also been utilized to predict the prevalent fracture directions in bedrock through trend analysis of aeromagnetic high-resolution data (e.g. Airo et al. 2008, Airo & Wennerström 2010). Furthermore, airborne frequency domain electromagnetic data sets and airborne radiometric data sets can be useful when visually outlining and characterizing geological units and when defining lithological boundaries (Härmä et al. 2013).

The rapakivi granites of the Wiborg batholith usually have low magnetic anomalies (Aeromagnetic Anomaly Map of Finland). Some large positive anomalies coincide with anorthosite inclusions or dark rapakivi granites (Arponen et al. 2009, Härmä et al. 2013, Härmä & Selonen 2017). With the aeromagnetic low-altitude data, the outlines and form of individual, previously "unknown" intrusions or intrusion phases have been defined in the batholith (Karell 2006, Härmä et al. 2013). New intrusion phases and their distribution in covered areas can be identified more precisely than in ordinary geological mapping. The potentially interesting areas for natural stone prospects will thus increase in number.

Geophysical ground survey methods have been applied in natural stone exploration in order to gain a more detailed view of the lithological boundaries and fractures, because airborne low-altitude geophysical data are too rough in most cases to characterise details such as fractures and weakness zones on outcrops. Electromagnetic (VLFR and EM31) and seismic ground survey methods have been tested for exploring the soundness of rock (Carvalho et al. 2008, Vartiainen 2017). The results of these methods have been uncertain in soundness assessment in deposit-scale studies (Vartiainen 2017).

Ground-penetrating radar (GPR) is a well-known, widely used geophysical ground survey method in natural stone exploration (Luodes 2015 and references therein). Being rapid and easy to use, it is well suited to studying the overall soundness of a prospect, particularly in granitic rocks. Furthermore, the results can be seen immediately during a survey. Subhorizontal fractures and weakness zones clearly appear in radargrams down to 20 m below the outcrop, especially when the fractures are water-filled. Subvertical fractures are more challenging to define; if they are tight and dry, without water or weathering products, the reflection of the radar pulse can be weak. GPR has also been tested in assessing the soundness of rapakivi granite at the quarry and deposit scales (Heikkinen et al. 2012, Tahvanainen et al. 2013).

Diamond core drilling is a valid method to confirm the soundness of the prospect, but is also the most expensive one and only reflects the properties of the prospect at the drilling point. Geophysical ground measurements could be an alternative to drilling, as these methods yield data from a larger area and are less expensive.

7.1 Study area

7.1.1 Target selection

The study area of the geophysical ground measurements was located in the village of Ravijärvi in the southern part of the Wiborg batholith (Fig. 3). The idea was to implement the geophysical measurements at a site where the bedrock is assumedly homogeneous so that the variations in the bedrock would not affect the measurements themselves. The bedrock in the study area is entirely composed of wiborgite (Simonen 1973, 1987), the most common rock type in the batholith. Indications of the surficial weathering of the rock were also found during the preliminary investigation (Fig. 37). Hence, the location was an ideal site to test the feasibility of the geophysical methods.

7.1.2 Practical procedures in the study area

Before undertaking the geophysical ground measurements, nine investigation traverses were implemented in the study area (Fig. 42). The traverses were placed so that they would cover the study area as widely as possible, especially the assumed weathered parts, and in order to best represent the possible starting points for quarrying. The traverses were exposed by an excavator, washed, cleaned and positioned with the VRS GPS equipment. During the mapping of the traverses, the colour, texture and fracturing of the wiborgite were defined. Samples for aesthetic evaluation and laboratory tests were also taken and the most potential areas for exploitation were determined.

The detailed mapping revealed that the wiborgite is intruded by a number of thin (2–15 cm) dykes of aplitic rapakivi granite. Furthermore, inclusions of even-grained rapakivi granite with an irregular form and a size of ca. 1 m were found in the wiborgite.

The detailed studies also included a GPR survey that was carried out on the mapped traverses to determine the subhorizontal fractures in the site. The depth penetration of the GPR with antennae of 200 MHz was ca. 15 m. After the GPR measurements, a diamond core drilling project was implemented in ten locations to especially investigate the surface weathering and to verify the existence of the fractures defined in the GPR survey. In addition, the colour and texture variations of the rock were logged.

A description of the GPR survey and core drilling is not given here, as they are commonly used methods in natural stone exploration (e.g. Leinonen 2005, Luodes 2015). At the study site, GPR gave good reflections from open water-saturated subhorizontal fractures (see Huotari et al. 2018), and with the core drilling, the weathered surface parts of the wiborgite were confirmed (see, e.g. Fig. 53).

7.2 Methods

The geophysical and morphological methods applied in this study included electrical resistivity tomography (ERT), induced polarization (IP), ground magnetic intensity measurements, and the use of LiDAR data. Furthermore, measurements of geophysical properties in drill holes were performed.

ERT and IP surveys were selected for the study because they have given good results in urban geology investigations carried out by GTK in order to locate weakness zones and fractures in bedrock (Huotari & Wennerström 2017). These methods have not been used in natural stone exploration or in the study of weathering in Finland. Ground magnetic intensity measurements had not previously been applied to rapakivi granite in Finland in natural stone exploration, although this is a well-known geophysical ground measurement method in other types of exploration (e.g. Vartiainen 2017). The LiDAR data reveal changes in the topography of an area. In addition, possible fracture or weakness zones in the bedrock can be observed if no soil cover exists on the bedrock. LiDAR data have not previously been utilised in natural stone exploration. The measurement of geophysical properties in drill holes with new probes was a method that had not previously been used in natural stone exploration. The method was in the development stage, and it was applied in the study area to test its suitability for natural stone exploration. Data on the petrophysical properties of rock are crucial in the interpretation of drill hole measurements, and petrophysical measurements were therefore also carried out on drill core samples at the petrophysical laboratory of GTK.

The main aim of the selected geophysical ground survey methods was to explore the soundness of the

wiborgite with special reference to the weathering of the surficial parts of the rock, and the presence of subvertical and subhorizontal open fractures.

7.2.1 Electrical resistivity tomography (ERT) and induced polarization (IP)

Electrical resistivity tomography (ERT) is an electrical method that models the structure of the subsurface by measuring resistivities (Huotari & Wennerström 2017). In practice, rocks should be insulating, as the minerals of rocks are mainly silicates. However, rocks have pores and fractures that usually contain fluids, which are more or less conductive, and the rocks behave as ionic conductors with variable resistivity. ERT is used to reconstruct the subsurface electrical resistivity distribution through the measurement of electrical potentials. This is usually carried out by using linear arrays of electrodes that are connected to a resistivity meter via multi-core cables. By using multiple receiver channels, a number of potentials can be measured at the same time, considerably reducing the measurement time. A subsurface resistivity model is then calculated through an inverse process (Huotari & Wennerström 2017, Uhlemann et al. 2018). ERT is seldom used in the exploration of bedrock properties (e.g. Stan & Stan-Kłeczek 2014), while the main applications can be found in engineering (e.g. Chambers et al. 2006, Ungureanu et al. 2017) and in agricultural (e.g. Garré et al. 2012) and hydrogeological (Jodry et al. 2019) studies. However, it has been applied in locating weakness and fracture zones in bedrock (e.g. Huotari & Wennerström 2017), as well as in mapping bedrock topography (Sibul et al. 2017). The method has also been used as a non-invasive tool to obtain information on stone properties, e.g. weathering, karstification and fracturing, at a marble quarry prior to extraction (Uhlemann et al. 2018).

Induced polarization (IP) is a polarization effect in the ground caused by an electric current transmitted into the subsurface through electrodes. If the electric current supply to the ground is interrupted, the voltage between the potential electrodes does not immediately drop to zero, but with a certain delay (several seconds or even minutes). This effect is called induced polarization (IP) and it is typical for ground with conductive minerals (Airo & Kiuru 2012, Uhlemann et al. 2018). If IP is measured, ERT is also obtained. ERT is measured when the electric current is on and IP when it is switched off. The IP method is commonly used in base metal mineral exploration to locate low-grade ore deposits, e.g. disseminated sulphides (e.g. Vanhala & Peltoniemi 1992). It has other applications in hydrogeophysical surveys (e.g. Azwan et al. 2015), environmental investigations (e.g. Vanhala 1997, Slater & Lesmes 2002) and geotechnical engineering projects (e.g. Aristodemou & Thomas-Betts 2000). The IP method makes it possible to remotely estimate the chargeability distribution of the subsurface by using surface electromagnetic data (e.g. Haldar 2018, Zhdanov 2018).

In the study area, ERT and IP were measured along four traverses (3, 5, 6 and 7) (Fig. 42). In addition, ERT was measured further along three traverses (1, 8 and 9) (Fig. 42).

The electrode spacing was 1 m in traverse 9 and 0.5 m in the other measured traverses. Thus, the depth extent in interpretation profile 9 was ca. 13 m in the middle of the profile, and in the other profiles it was ca. 7 m in the middle of the profiles. The measurements were carried out with a dense electrode spacing so that it would be possible to detect small features (e.g. weathering) near the surface, mostly within the first 5 m below the outcrop surface.

In total, the measurement length was 80 m in traverse 9 and 40 m in the other traverses. The profiles followed the topography of the ground surface, and the topography was afterwards compiled from LiDAR data.

The equipment used in the ERT and IP surveys was an ABEM Terrameter SAS4000 with a Lund Imaging cable system. The electrode system was a multiple gradient array that was a combination of Schlumberger and Pole-Dipole arrays.

7.2.2 Magnetic ground measurements

In magnetic surveys, the magnetic properties of rocks are detected (Stevens 2010). Variations in the magnetic properties of the ground reflect the distribution of magnetic minerals in the bedrock and cause local magnetic anomalies to the measurement results (Huotari & Wennerström 2017). Magnetic susceptibility is related to the varying amount of minor accessory minerals present in all rocks that contain iron, such as magnetite, pyrrhotite and hematite. Magnetite is the most important magnetic mineral, because it has relatively high

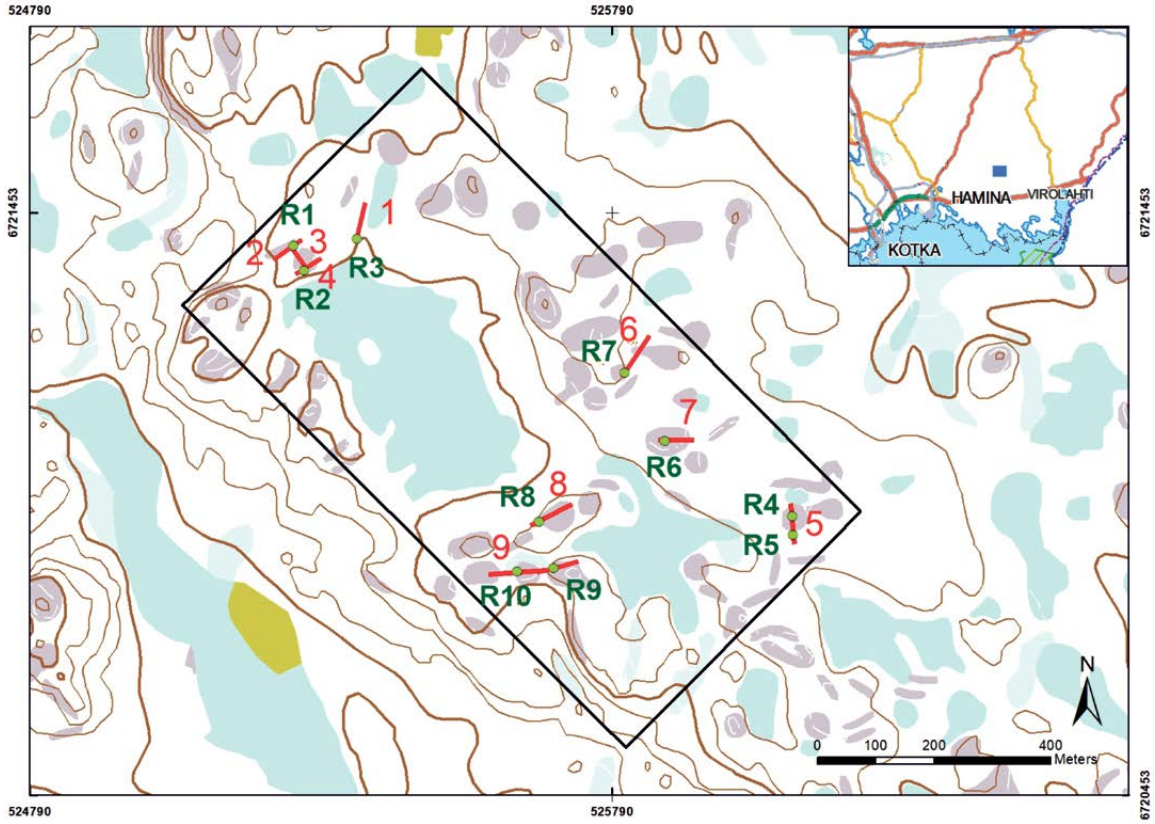

Fig. 42. The study area (black rectangle) with nine investigation traverses (red lines) in the village of Ravijärvi in southeastern Finland (blue rectangle in the insert). Electrical resistivity tomography (ERT) and induced polarization (IP) were measured along four traverses: 3, 5, 6 and 7, and ERT further along three traverses: 1, 8 and 9. Diamond core drilling was carried out at locations R1–R10. Base maps: © National Land Survey of Finland.

magnetic susceptibility. A magnetic survey can map changes in the amount of magnetic minerals, as well as associated rock types. Thus, a magnetic map can help to locate mineral deposits by identifying specific rock types and geological features (Stevens 2010). The anomalies can be interpreted to determine the location, extent, depth, position and strength of the magnetization. During the interpretation, the relationships between rock types are determined. In addition, the measurements can give information on the geological structures, such as fracture zones (Huotari & Wennerström 2017). Magnetic ground surveys are commonly applied in ore exploration to detect variations in the magnetic properties of minerals (e.g. Muravyev et al. 2019) and have also been used in localizing tectonic details in solid bedrock (Vartiainen 2017).

In the study area, a total of 53 magnetic Overhauser lines were measured, covering the whole area (Fig. 43). The length of each line was ca. 540 m, depending on the topography. The direction of the lines was SW–NE. The line spacing in the total field ground magnetic measurements was the commonly used 20 m.

7.2.3 LiDAR data

LiDAR (light detection and ranging) is an optical remote-sensing technique that uses laser light to monitor the surface of the earth and produces highly accurate 3D measurements (LiDAR UK 2019). Laser pulses emitted from a LiDAR system reflect from objects both on and above the ground surface. A single emitted laser pulse can return to the LiDAR sensor as one or several returns, where the last return is usually from the ground surface.

The LiDAR maps presented in this study are based on LiDAR pulse data reflected from the ground surface. A hillshaded elevation model of the study area was compiled by using LiDAR data from the National Land Survey of Finland (Fig. 44).

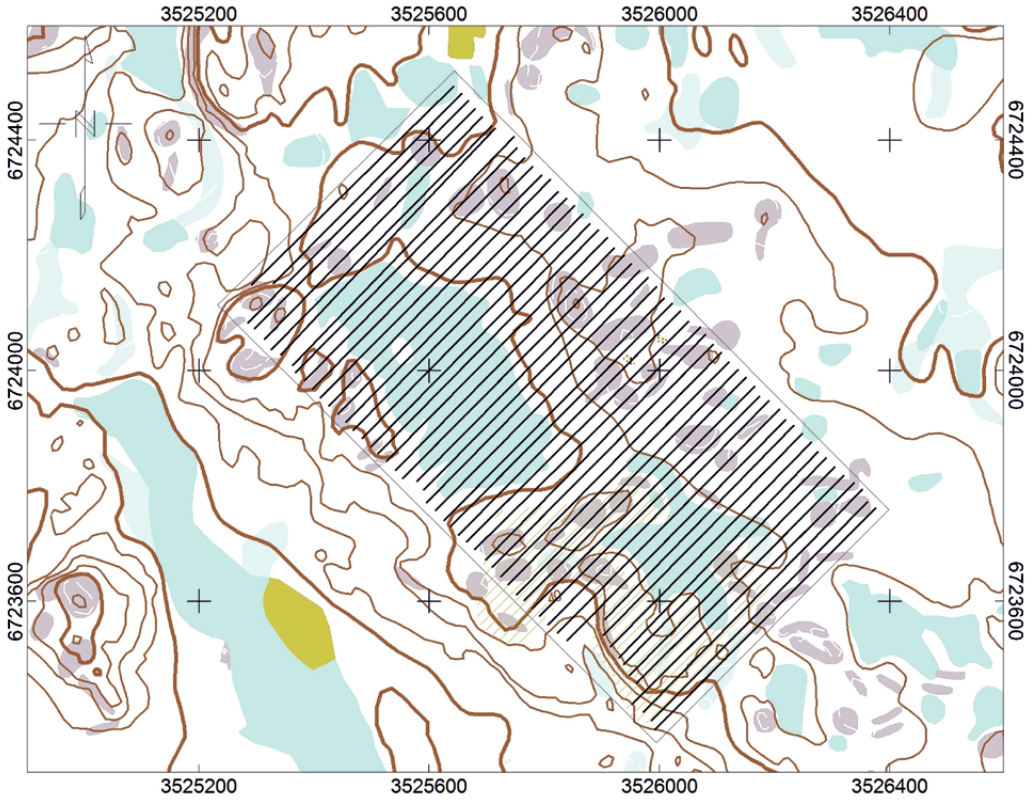

Fig. 43. Total magnetic field ground measurement lines in the study area are shown as thin black lines. Base maps: © National Land Survey of Finland.

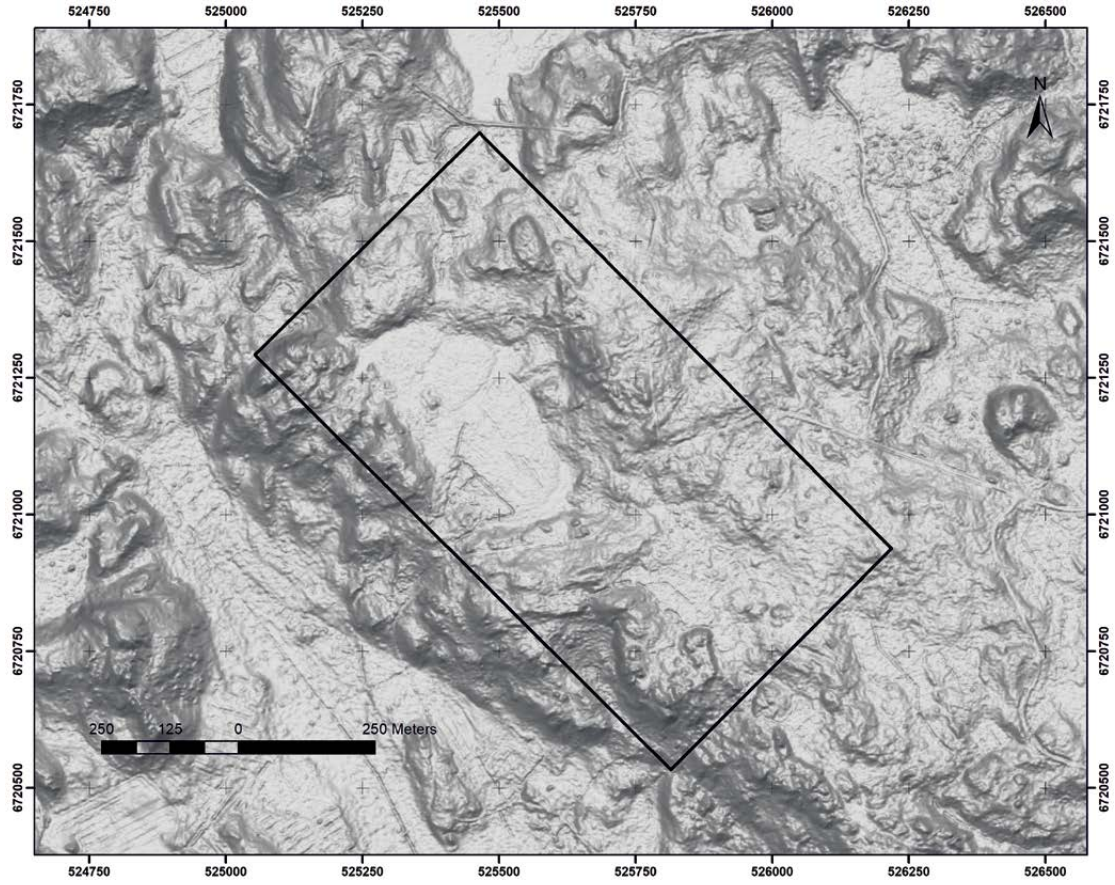

Fig. 44. Hillshaded elevation map of the study area (black rectangle) produced with LiDAR data. Contains 2014 data from the Topographic Database of the National Land Survey of Finland © NLS, HALTIK and LiDAR 2013.

7.2.4 *In situ* geophysical measurements in drill hole

All the drill holes (R1–R10 in Fig. 42) were scanned with new geophysical drill-hole probes (Fig. 45) designed by Vatjus-Micro Oy. The measurement system includes four separate probes that measure magnetic susceptibility, resistivity, density and natural gamma radiation in the drill hole *in situ*. The distance between the measurement point and the probe end varied for the separate measurements as follows: 10 cm for susceptibility, 8 cm for natural gamma, 6 cm for gamma density (from radiation source connection) and 52 cm for resistivity.

The density measurement system is based on radiation, the source of which is Cs137 that scatters from the surrounding bedrock, causing secondary radiation to be detected with a scintillation counter. The natural gamma measurement system is equivalent to the density measurement system, excluding the radiation source.

The system records the data while the probe is moved down (in) and up (out) the drill hole. A travelling wheel was used during the measurement to quantify the distance of the probe from the ground surface (Fig. 45).

Fig. 45. The set-up of the *in situ* geophysical measurements in a drill hole. Photo: Paavo Härmä.

7.2.5 Petrophysical measurements from drill core samples

For the calibration of the data from drill hole measurements, data on the petrophysical properties of the drill core samples are always needed in the case of susceptibility and density data.

Petrophysical properties (porosity, susceptibility and density) were defined for 117 core samples chosen from the ten drill cores from locations representing changes in the texture and density of wiborgite. Samples were also chosen from locations with detected changes in values or peaks of values in the drill hole measurements. In addition, eleven samples were collected from magnetic minima and maxima locations to provide a reference for magnetic interpretation. The sampling depth of the eleven samples was ca. 15–20 cm from the ground surface. Finally, petrophysical properties were measured from ten randomly selected samples from drill cores R1–R10.

Sampling from the most interesting parts of the drill cores, such as the fractured parts, was

Table 2. Susceptibility and dry calculated bulk density of eight randomly selected drill core samples at given depths.

Drill hole id	Susceptibility (10^{-6} SI)	Bulk density (kg/m^3)	Depth (m) (from the rock surface)
R1	755	2669	14.7
R2	423	2648	9.5
R3	1476	2708	12.2
R5	541	2671	6.3
R6	1109	2665	3.4
R8	1071	2695	8.2
R9	701	2666	1.0
R10	799	2693	6.3

challenging due to the lack of solid rock in these parts, and due to fact that the minimum length of a solid rock sample should be at least 5 cm for petrophysical measurements. Drill holes R1–R10 with measured sample depths, susceptibilities and bulk densities of the randomly selected samples are presented in Table 2.

7.2.6 Resistivity and radiation

Resistivity data were recorded with the Wenner configuration in the drill holes as an *in situ* measurement. The petrophysical measurements were carried out for water-saturated samples. The resistivity data from the drill hole measurements were not calibrated with temperature or water due to the lack of data. The difference in scale of the samples also had an influence on the data; the drill hole data were measured from a larger area than the petrophysical properties measured from the drill core samples. In addition, the water level in the bedrock had a significant effect on the drill hole *in situ* measurements. The bedrock was not water saturated near the surface. Therefore, the resistivity values in drill holes were higher than those obtained in the petrophysical measurements, because the latter were carried out from water-saturated samples. Natural gamma radiation was measured from drill hole R6 when the probe was pulled out of the drill hole.

7.3 Results

7.3.1 ERT and IP measurements

The data from the ERT and IP surveys were interpreted using Res2DInv inversion software (Loke & Barker 1996, Geotomo software 2014) regarding the topography changes in the profiles and without giving a weight coefficient to any direction of the geological structures. By doing this, the interpretation did not exaggerate geological structures or faults in any particular direction.

The interpretations were also checked in the field for ground truth. Hence, the interpretation of profile 6 (Figs. 46 and 48) and profile 7 (Figs. 47 and 49) includes field observations made on outcrops. The outcome of the surveys along traverses 6 and 7 is presented here as an example of the ERT and IP interpretation (Figs. 46, 47, 48, and 49), because in these traverses, both ERT and IP were measured, providing a good response to the measurements.

The resistivities (ERT) in the study area are high due to the solid bedrock. However, some variation in the resistivity could be detected. The resistivity of wiborgite is lower below the outcrop along a 0.5–1-m-thick sheet (Figs. 46 and 47), corresponding to the weathered surface part of the wiborgite. The same feature was identified in all of the profiles. More conductive subvertical features could also be detected in the middle of profile 6 (Fig. 46) and profile 7 (Fig. 47), as well as in couple of other profiles.

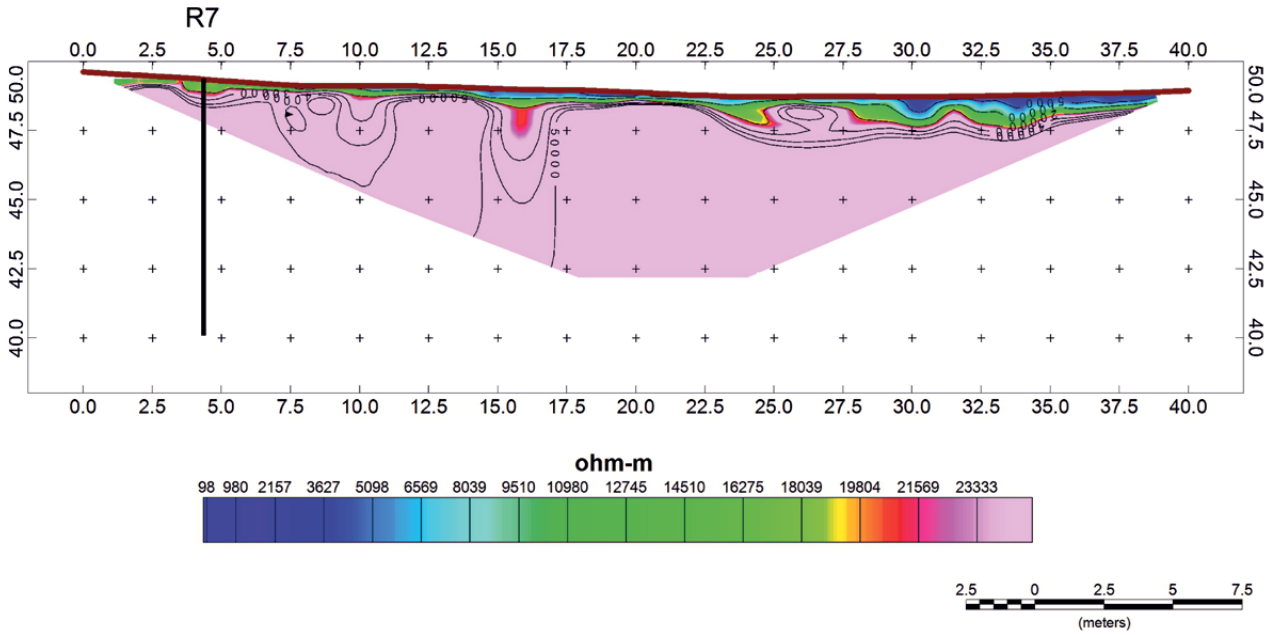

Fig. 46. Profile of resistivity (ERT) along traverse 6. The location of drill hole R7 is shown in the left part of the profile. The resistivity of the wiborgite is lower below the surface along a 0.5–1-m-thick zone. Equipment: ABEM Terrameter SAS4000 with Lund Imaging cable system.

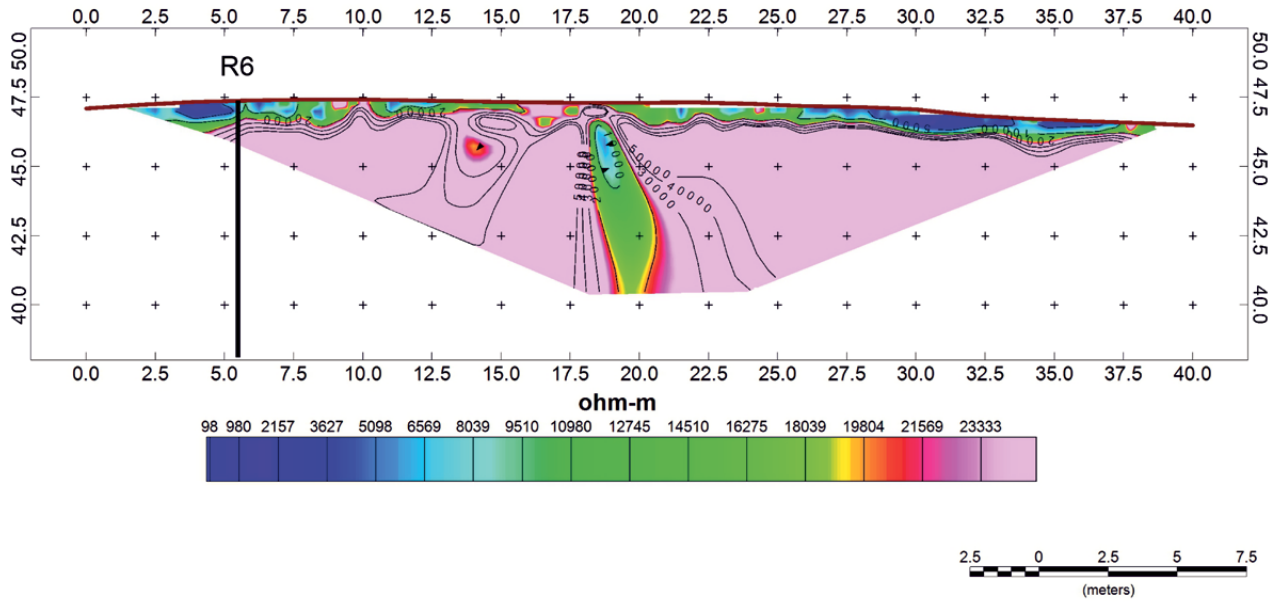

Fig. 47. Profile of resistivity (ERT) along traverse 7. The location of drill hole R6 is shown in the left part of the profile. A 0.5–1-m-thick zone of low resistivity can be observed directly below the rock surface. More conductive subvertical features can be detected in the middle of the profile. Equipment: ABEM Terrameter SAS4000 with Lund Imaging cable system.

The IP survey revealed anomalies with higher IP values in profile 6 (Fig. 48) and profile 7 (Fig. 49) below the rock surface. In both profiles, the higher IP values at the surface correlate with the weathered surface zone, especially in places where the conductivity is higher and the resistivity is lower. This result is a consequence of the fact that when wiborgite is water-saturated at deeper levels, the IP values are not as high as at levels where the rock pores only include moisture, and the weathered zone is thin (only 0.5–1 m thick). However, higher IP values were also recorded in deeper parts of wiborgite in profile 7 (Fig. 49), which remained unresolved due to the lack of appropriate data (data on the drill core samples).

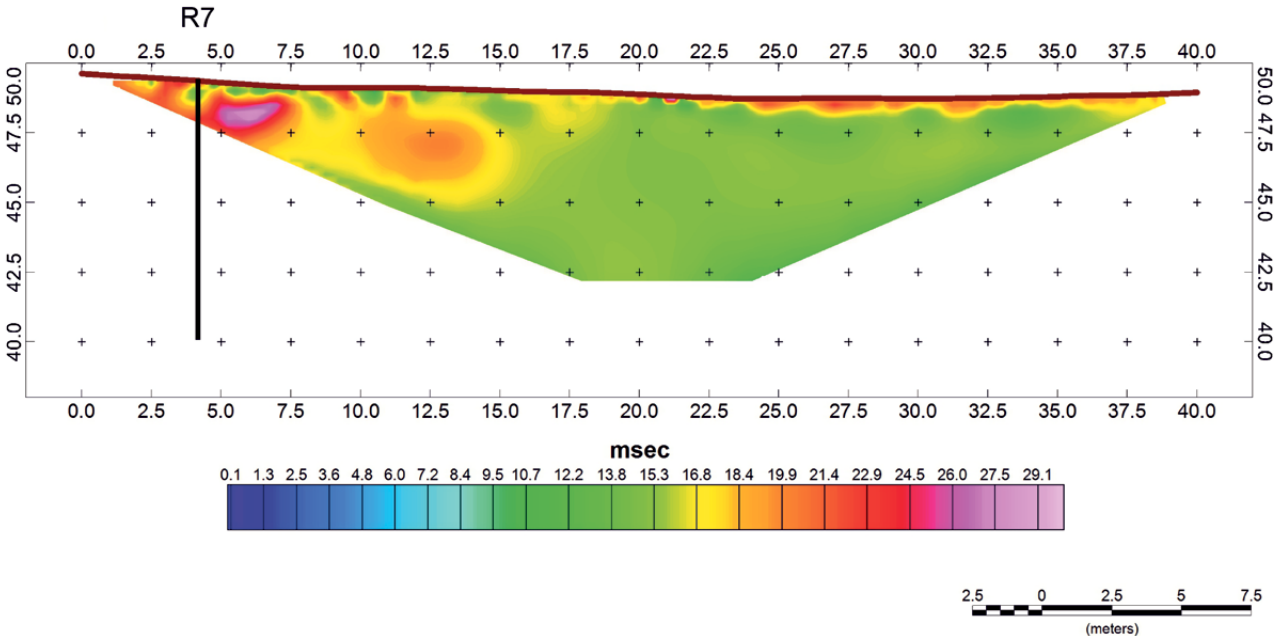

Fig. 48. Profile of induced polarization (IP) along traverse 6. The location of drill hole R7 is shown in the left part of the profile. The IP values in the wiborgite are higher near the upper surface along a 0.5–1-m-thick zone. Equipment: ABEM Terrameter SAS4000 with Lund Imaging cable system.

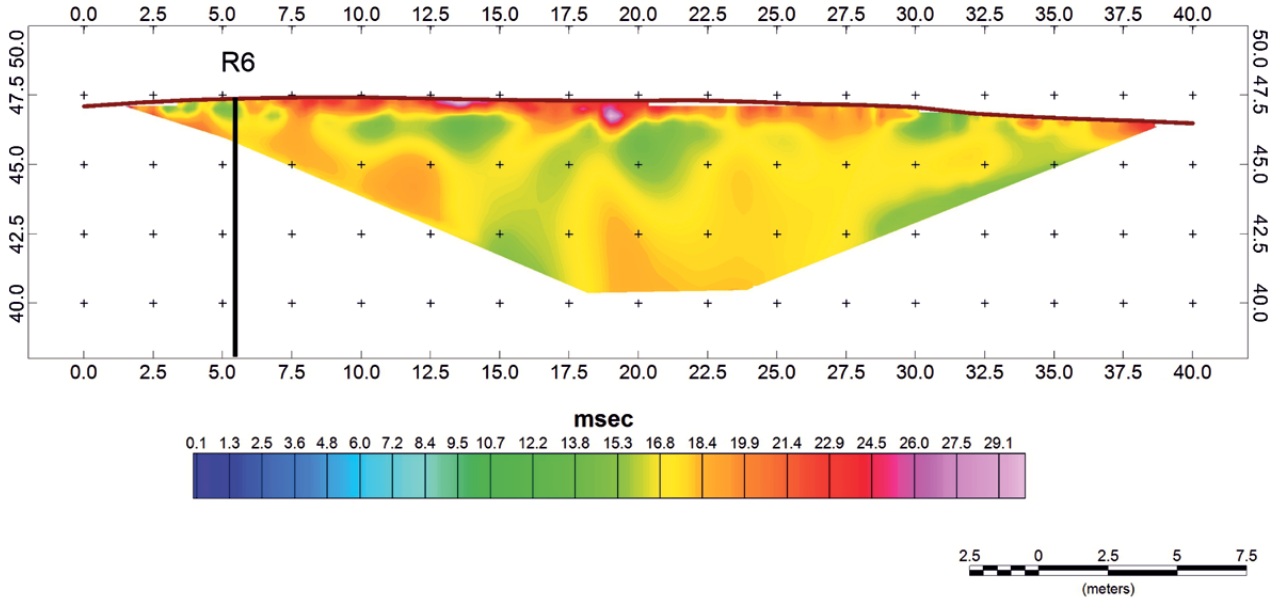

Fig. 49. Profile of induced polarization (IP) along traverse 7. The location of drill hole R6 is shown in the left part of the profile. A 0.5–1-m-thick zone with high IP values in the wiborgite below the outcrop can be observed. Higher IP values can also be seen in deeper parts of the wiborgite. Equipment: ABEM Terrameter SAS4000 with Lund Imaging cable system.

7.3.2 Magnetic ground measurements

The bedrock composed of wiborgite was expected to be magnetically homogeneous, as shown in the high-resolution airborne magnetic data of GTK (Aeromagnetic Anomaly Map of Finland). The magnetic data with continuous measurement and a dense line spacing revealed some anomalies in the total field magnetic intensity (Fig. 50). Some variations in the magnetic intensity can be explained by the varying thickness of the soil cover. Most of the area had only a thin soil cover or the bedrock was exposed. In the exposed parts, the magnetic anomalies are commonly higher than in the parts with a thicker soil cover (cf. Vartiainen 2017).

An interesting feature in the total field magnetic intensity (TMI) map is an almost E–W-oriented worm-like anomaly in the middle of the measured area near the beginning point of traverse 6 (marked with black arrows in Fig. 51), which has the highest nT values (52110 nT) of the whole area. The anomaly could be explained by a weakness zone or a change in the magnetic mineral composition of the wiborgite. There could also be a narrow, unexposed aplitic dyke in the wiborgite, containing more magnetic minerals than the wiborgite. However, no interpretive features for this anomaly could be verified on the outcrop.

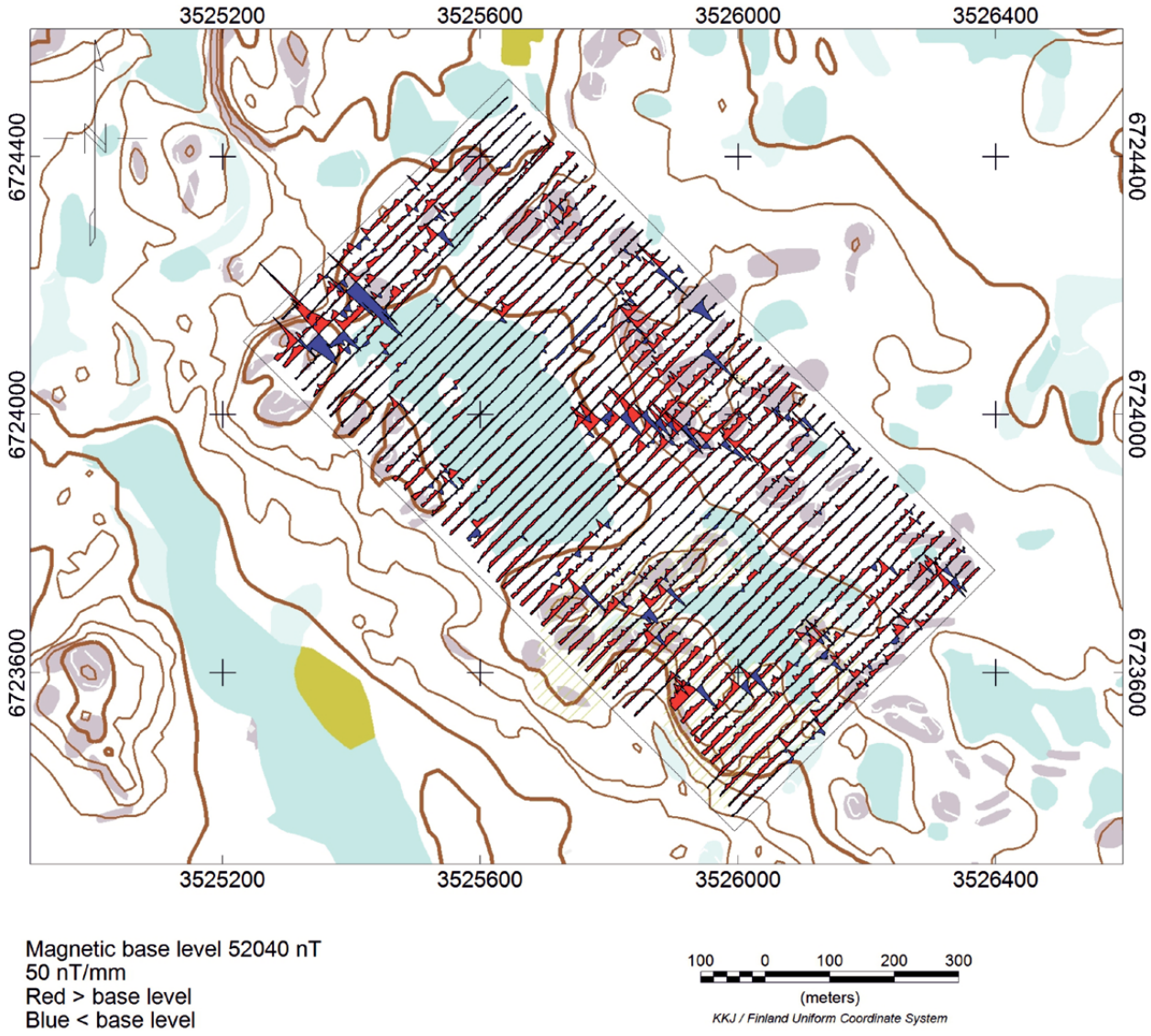

Fig. 50. Total field magnetic profile map of the study area measured using an Overhauser magnetometer. The red peaks reflect the magnetic total intensity over the base level in the area, while the blue peaks mirror the intensity under the base level. Contains 2014 data from the Topographic Database of the National Land Survey of Finland © NLS and HALTIK.

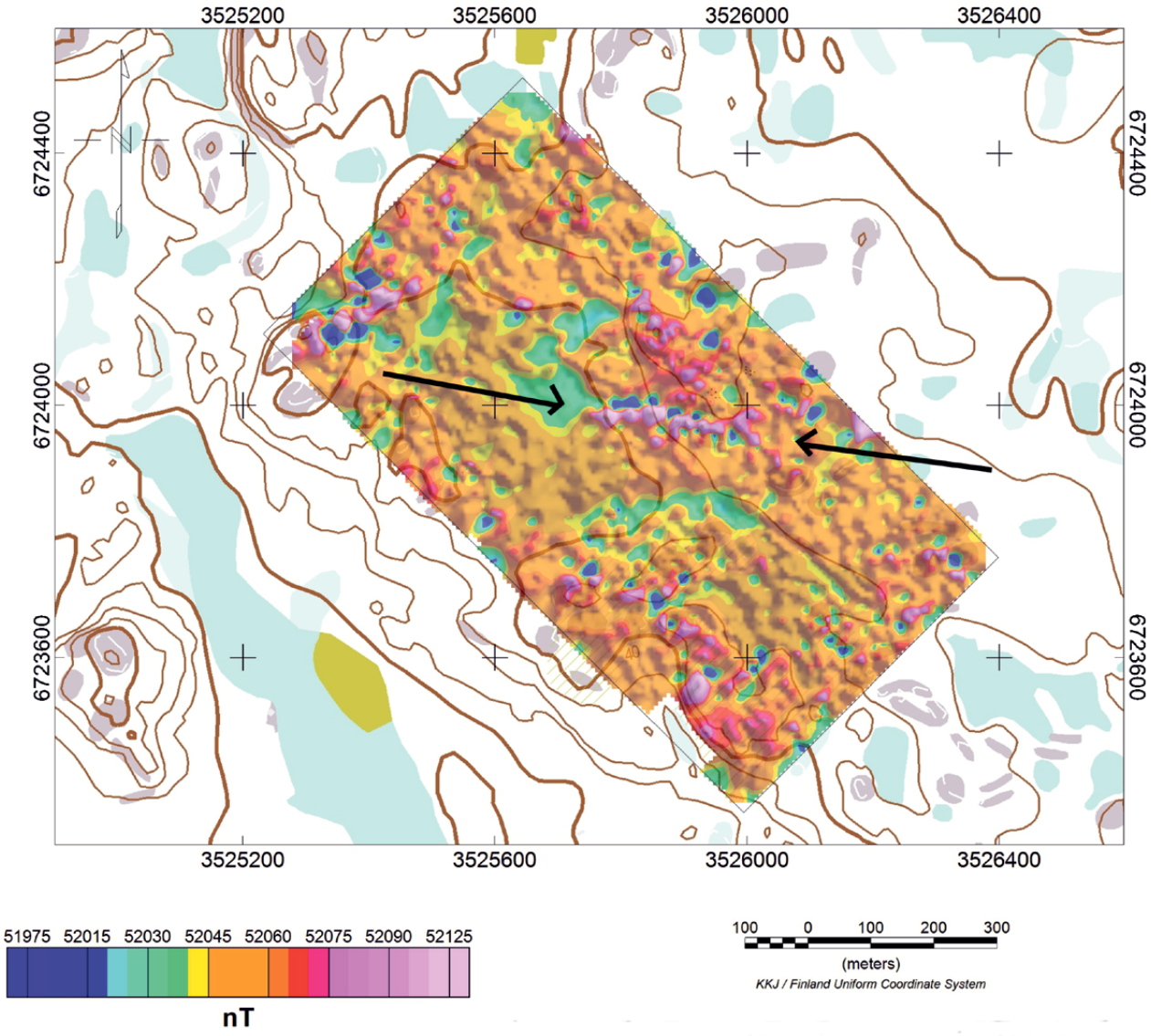

Fig. 51. Total field magnetic intensity (TMI) map of the study area measured using an Overhauser magnetometer. The black arrows indicate an almost E–W-oriented anomaly. See the text for an explanation. Contains 2014 data from the Topographic Database of the National Land Survey of Finland © NLS and HALTIK.

7.3.3 LiDAR data

The topographically low areas in the LiDAR data usually coincide with magnetic minima (small blue-coloured points in Fig. 52). The topographical lows could be interpreted to represent subvertical fracture zones in the bedrock (marked with black arrows in Fig. 52). The interpretation here was based on the visual impression from the LiDAR data combined with magnetic anomalies and magnetic minima points, but the features could not be observed in the fieldwork. The soil cover on the bedrock and weathering could cause minor errors in the interpretation.

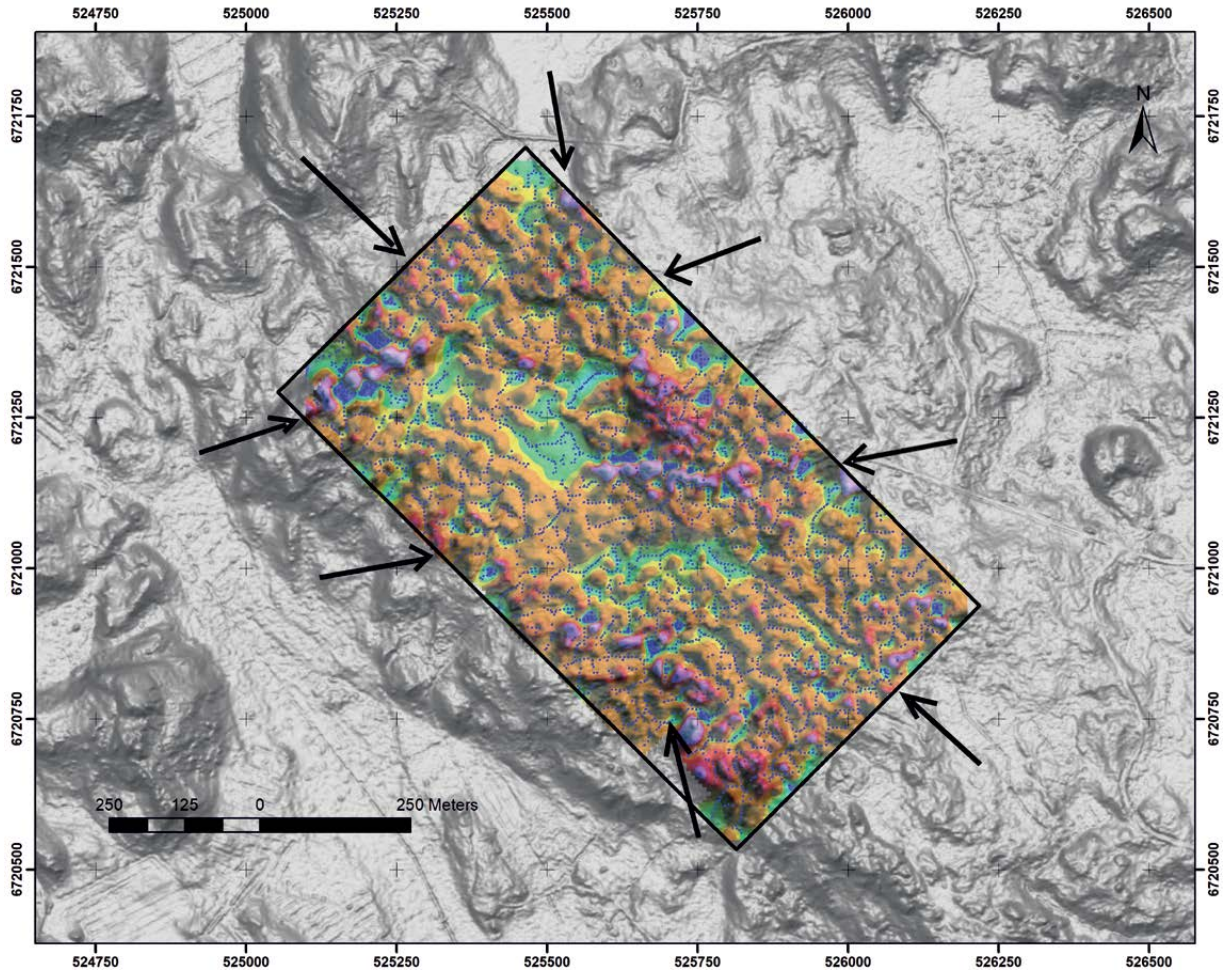

Fig. 52. LiDAR data with a magnetic map (see colour scale in Fig. 50). Black arrows point to structures that could be interpreted to be subvertical fracture zones in the bedrock (however, they could not be localised on outcrops). Contains 2014 data from the Topographic Database of the National Land Survey of Finland © NLS, HALTIK and LiDAR 2013.

7.3.4 Measurements in drill holes compared to petrophysical measurements

The data on petrophysical properties and the drill hole *in situ* measurements, compared to logging data from drill cores are illustrated with the case of drill core R6, because it was the most representative of the drill cores, giving the best response to the measurements.

Susceptibility measurements from the petrophysical samples and the drill hole *in situ* are compared with the logging data from drill core R6 in Fig. 53. The susceptibility value is much lower at the depth of 5.5–6 m than in other parts of the drill hole (Fig. 53). There is a change in the rock type at that point in the drill core, where the wiborgite comprises an at least 40-cm-thick inclusion of even-grained rapakivi granite with a smaller grain size and an equigranular texture.

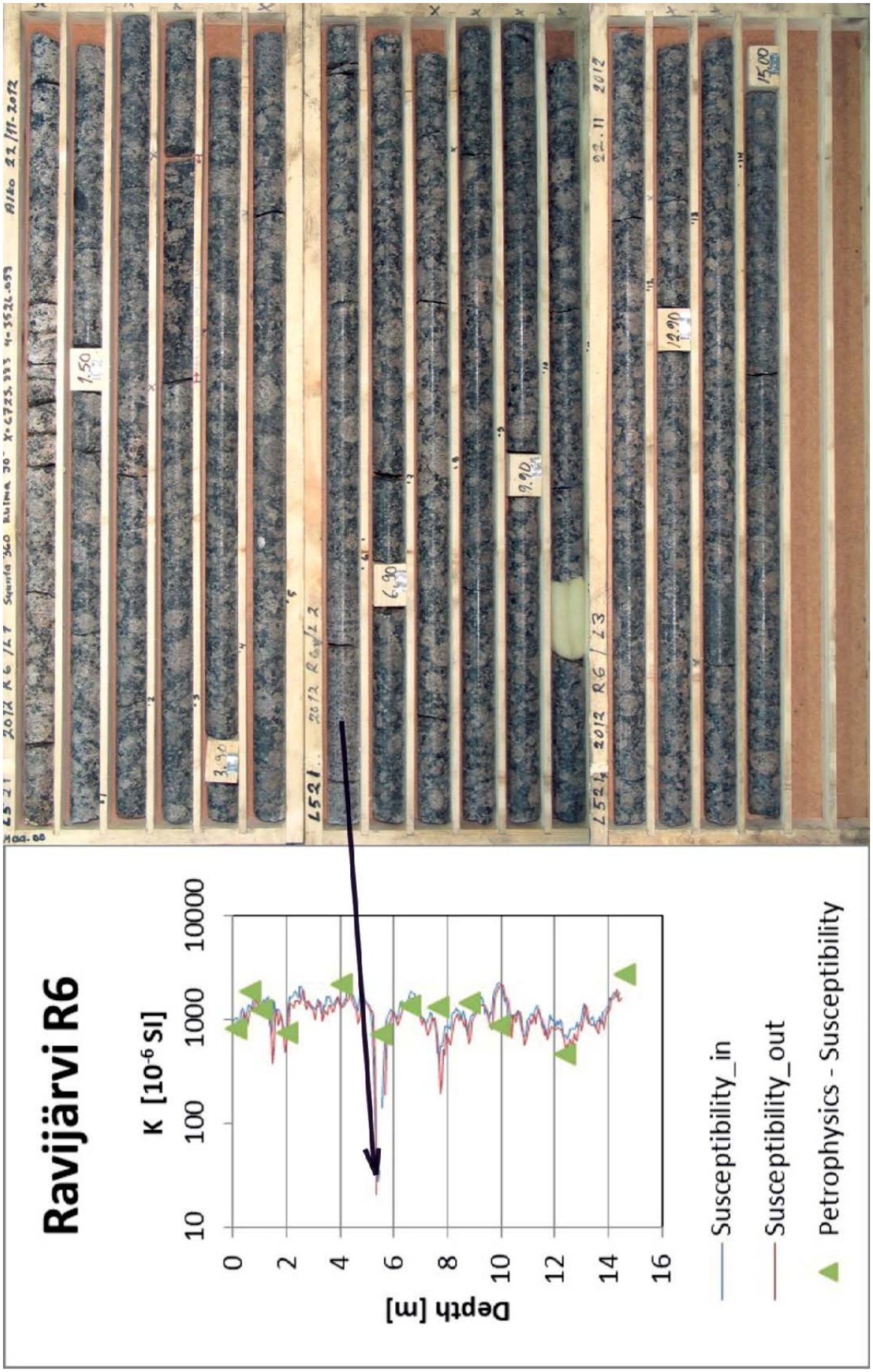

Fig. 53. Calibrated susceptibilities from the drill hole measurement (thin lines), together with susceptibilities measured from the drill core samples (green triangles), are presented on the left side and a photo of the drill core on the right side. There is a distinct anomaly in the susceptibility at the depth of 5.5–6 m, marking a change from wiborgite to even-grained rapakivi granite inclusion.

The density data measured from drill hole R6 were calibrated with the petrophysical data (Fig. 54). There is a clear anomaly that has a low density value at 1 m depth (Fig. 54). At this depth, a subhorizontal, open fracture in the wiborgite is observed in the logging data of the drill core.

The petrophysical results indicate that the resistivities of the wiborgite samples near the surface are lower than in the deeper parts (Fig. 55). This corresponds to the higher porosity of the weathered wiborgite below the surface. The pores in the wiborgite are water-saturated, reducing resistivity. The water level is approximately at the depth of 4 m from the surface. This is possible to interpret from the drill hole measurement data, in which the values approach the same level as the resistivities of petrophysical samples at the same depth (Fig. 55).

The resistivities in the drill core samples were measured with three different frequencies (Fig. 55), which would reveal the induced polarization (IP) effect, even if the results for different frequencies differ from each other. In the deeper parts, there are more differences in the resistivity values. The calculated IP estimate has the highest value for the deepest sample in the drill hole. This was the highest value obtained from all the drill core samples in the study area. The values of resistivities measured with three frequencies showed a distinct level change at 2 m depth. Wiborgite is no longer weathered below that depth, as also shown by the logging data from the drill core (Fig. 55).

In the results from the natural gamma radiation measurements, only natural variation in the values was observed. The radiation levels of the inclusion of even-grained rapakivi granite were equal to those of the wiborgite (Fig. 56): the wiborgite and the even-grained rapakivi granite could not be distinguished by means of radiation.

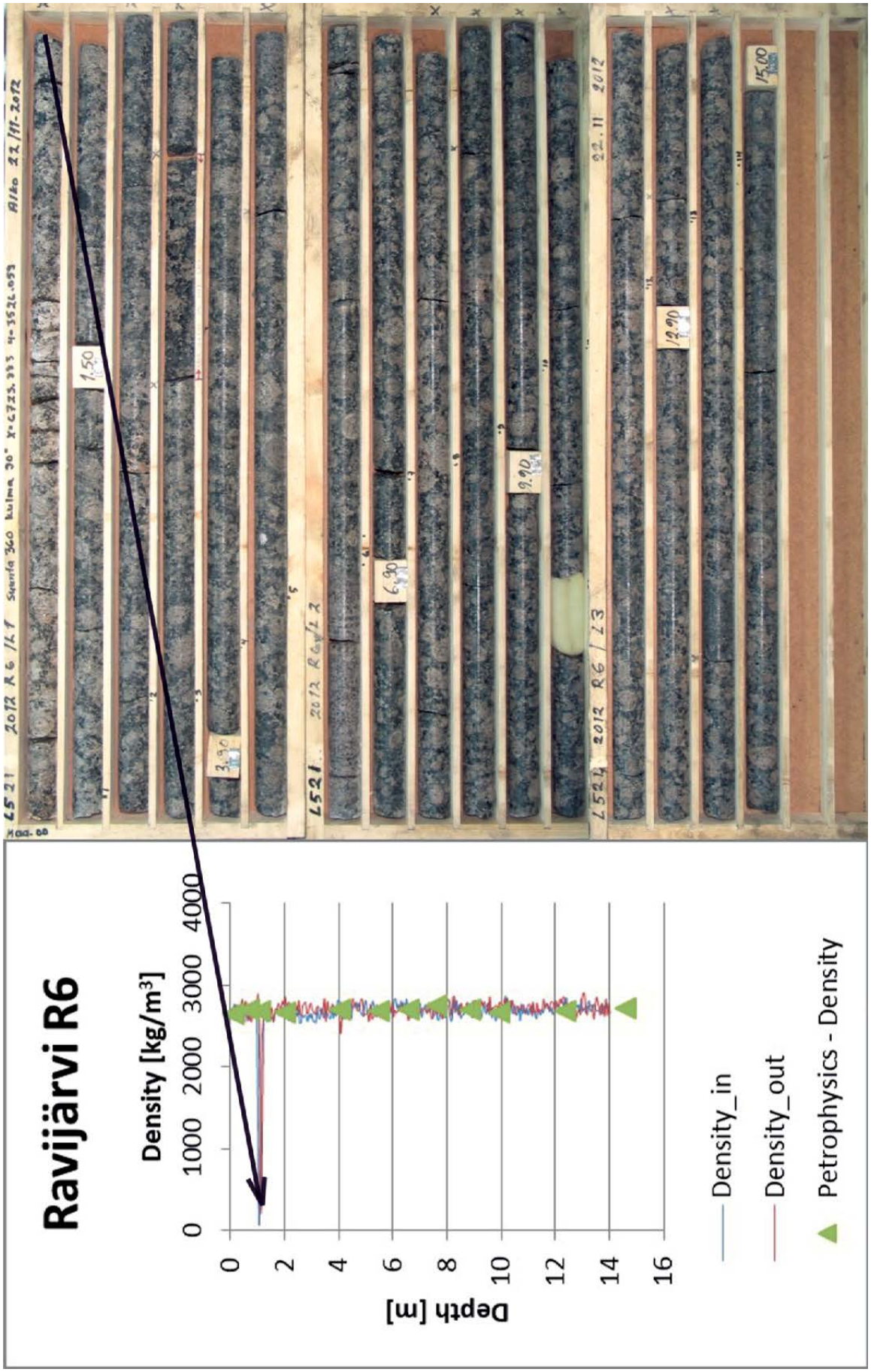

Fig. 54. Calibrated densities from drill hole measurement (thin lines), together with densities measured from the drill core samples (green triangles), are presented on the left and a photo of the drill core on the right. A distinct change in the measured density at the depth of 1 m can be observed, corresponding to an open fracture in the drill core.

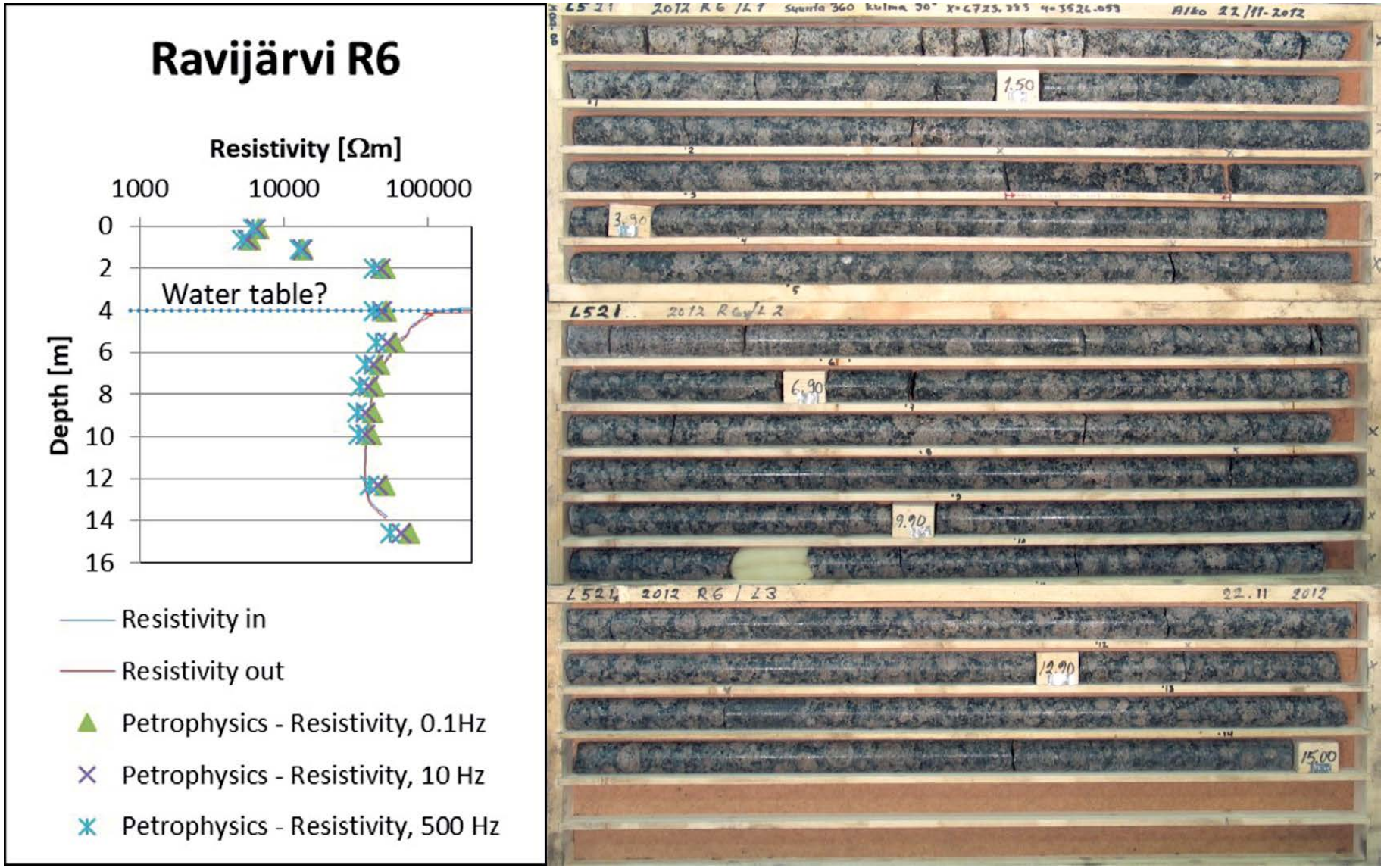

Fig. 55. Resistivities from the drill core samples measured with three different frequencies (green, violet and blue symbols), together with resistivities measured from the drill hole (thin lines), are presented on the left and a photo of the drill core on the right. The values of resistivities show a distinct level change at 2 m depth, implying that the quality of wiborgite improves at that depth, i.e. wiborgite is no longer weathered.

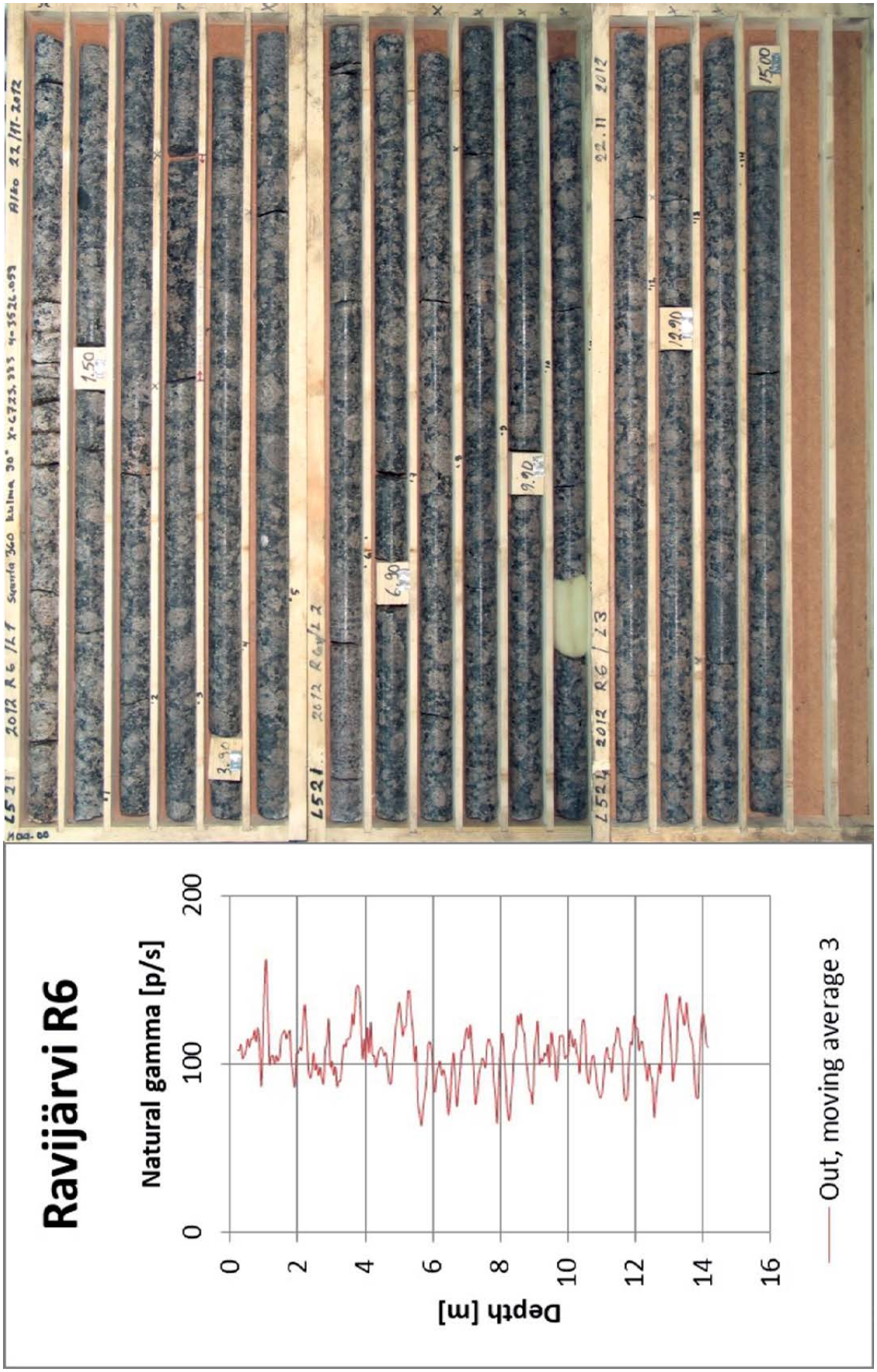

Fig. 56. Natural gamma radiation data from the drill hole measurement when moving the probe from the drill hole (only out with the moving average) is presented on the left side and a photo of the drill core on the right. There appears to be no significant change in the natural gamma data, only natural variation. The radiation levels in the inclusion of the even-grained rapakivi granite at the depth of 5.5–6 m are equal to those of the wiborgite.

7.4 Main observations regarding the geophysical methods

- ERT and IP surveys exposed the 0.5–1-m-thick weathered zone of wiborgite below the outcrops. Indications of open subvertical fracture zones were detected with these two methods.

- The high-resolution ground magnetic data could not reliably detect structural details of the bedrock. The soil cover on outcrops can disturb the interpretations.

- The usefulness of LiDAR data in the detection of subvertical fracture zones was restricted. The soil cover on outcrops can cause errors in the interpretations. The drill hole measurements provided good supplementary data (e.g. susceptibility and resistivity) on the bedrock quality, but data on the petrophysical properties are needed to calibrate the measurement data.

PART V DISCUSSION AND CONCLUSIONS

8 RESULTS AND DISCUSSION

The use of rapakivi granites as natural stone is based on the unique visual expression regarding the rapakivi texture and homogeneity, which should be constant in an area large enough for production. A homogeneous colour and texture, as well as adequate soundness, are among the most important criteria for good quality natural stone, and the precise determination of these parameters is essential in the evaluation of natural stone (e.g. Shadmon 1996, Selonen 1998, Selonen et al. 2000, Lorenz & Gwosdz 2003, Bradley et al. 2004, Romu 2014, Luodes 2015).

During the standard exploration process (e.g. Luodes et al. 2000, Selonen et al. 2000, Selonen & Heldal 2003, Ashmole & Motloung 2008, Carvalho et al. 2008, Luodes 2015, Härmä et al. 2017), colour variations and the soundness of different rock types are visually evaluated on outcrops, and the decision on further assessment or even production could be based on this surficial evaluation. In typical cases, this could be justified. However, with the rapakivi granites of the Wiborg batholith, the explorer cannot solely rely upon observations made on outcrops, as the surficial weathering masks the properties of the fresh rock. Therefore, an exploration approach especially developed for the rapakivi granites of the Wiborg batholith is needed.

In this chapter, I shall present the key findings of my study and discuss their implications.

8.1 Boundary conditions from lithology and fracturing

8.1.1 Rock types

Seven main rapakivi granite types were defined in this study in the Wiborg batholith: wiborgite, dark wiborgite, pyterlite, porphyritic rapakivi granite, even-grained rapakivi granite, dark rapakivi granite and aplitic rapakivi granite. Wiborgite has the widest areal distribution, ca. 75% of the batholith, and pyterlite, even-grained granites and dark rapakivi granites are next most abundant, with equal areal coverages of ca. 6%. The porphyritic granites occupy 3% and the other rock types 4% of the area.

According to Simonen (1987), the main rapakivi types of the Wiborg batholith are wiborgite, dark wiborgite, pyterlite, porphyritic rapakivi granite, even-grained rapakivi granite and aplitic rapakivi granite. The geological classification in this study is in accordance with Simonen (1987) regarding the wiborgite, dark wiborgite and pyterlite. Based on appearance and mineralogical composition, the group of porphyritic rapakivi granites is defined more precisely than in Simonen (1987) by the determination of three different types of porphyritic rapakivi granites. A new type, the porphyritic Savitaipale granite, is also identified.

The classification in this study also differs from that of Simonen (1987) regarding the even-grained rapakivi granites. Simonen (1987) combined all the dark rapakivi granites into the dark even-grained granite group, while the grain size of these rocks actually varies from fine to coarse-grained and the texture from vaguely porphyritic to even-grained. Abundant K-feldspar ovoids, angular K-feldspar megacrysts and euhedral plagioclase megacrysts of andesine composition are found in the porphyritic types. In addition, fine-grained mafic enclaves are occasionally present. In this work, these granites are named as dark rapakivi granites, including the dark even-grained types. The mineral composition of the dark rapakivi granites is exceptional compared to the other rapakivi granites in the batholith. All types of them include several percent of fayalitic olivine together with hornblende, magnetite and clinopyroxene. The new classification of the

dark rapakivi granites in this work comprises three main types of even-grained rapakivi granites: biotite granite, hornblende granite and topaz-bearing even-grained granite.

In the field, the dark rapakivi granites are often found in close contact with even-grained hornblende rapakivi granites and anorthosites, indicating a genetic relationship between these rocks. According to Rämö et al. (2014) and Heinonen et al. (2017), these dark rapakivi granites can be interpreted to be a mixture of mafic and felsic magmas in the bimodal magmatism of rapakivi granites. The observed transitions between the different granite types are mostly found in a subvertical direction in the field, indicating sheet-like intrusions of the granite bodies, which confirms previous interpretations (e.g. Suominen 1980, Suominen 1981, Luosto et al. 1990, Elo & Korja 1993, Front et al. 1999).

Within the areas of the individual granite types, with detailed mapping, I have been able to identify distinct areas of rock with a uniform colour and texture. These include the light brown and dark green varieties of wiborgite, brown, green and red varieties of pyterlite (Fig. 19A, B) and the black varieties of dark wiborgite. Distinct textural areas with, for instance, equal-sized ovoids, can be identified in both wiborgite and pyterlite. These types of areas, having a different appearance compared to the "normal" rock, have not been described before in the Wiborg batholith. All the areas mentioned above are large and homogeneous enough to be considered as potentially interesting for natural stone.

The detailed mapping in this work provided a more accurate picture of the lithological features of the Wiborg batholith, which, regarding natural stone, has traditionally been considered to consist of only "unexciting" and "monotonous" wiborgite. The more precise geological classification together with the definition of the "new" rock areas has increased the possibilities for finding new natural stone qualities in the Wiborg batholith, as shown in Chapter 8.4.

Good knowledge of rock types and their appearances in the target area is an essential factor for successful exploration. In conventional bedrock mapping, small differences in the appearance of rock (cf. Chapter 2.1.1) are easily overlooked, as they might not have a direct bearing on, for example, compiling a bedrock map of an area. Bedrock maps should only be considered as a basis for more detailed exploration mapping. It can be concluded that natural stone mapping is a refinement of geological bedrock mapping. Geological observation procedures are systematically used in both processes, but in natural stone exploration, particular emphasis is placed on observing the homogeneity, colour, texture and soundness of the rock, which are not often observed in ordinary bedrock mapping. However, successful natural stone mapping requires good knowledge of the criteria for feasible natural stone.

8.1.2 Fracture orientations and patterns

Fracturing in rock is usually explained to be a result of the prevalent rock stress field, and fractures are formed in rock at oblique angles perpendicular to the dominant stress (e.g. Blenkinsop 2008, Zang & Stephansson 2010, Deliormanli & Maerz 2016). The tension and stress fields in the rapakivi granites generate subvertical and subhorizontal fractures regionally and locally, and the development of these fractures is connected to the overall tectonic deformation of the bedrock. The general assumption has been that, in the Wiborg batholith, the fractures are a result of intrusion mechanics or brittle deformation after the intrusion, and no larger faults exist. No faults were observed along the subvertical fractures in the fieldwork of this study. Dislocation of only a few millimetres along the filled fractures (fire lines) in the direction of N30°W was observed (Fig. 29).

The fracture orientation of N30°W is dominant in all rapakivi granite types. These fractures are commonly filled with quartz and other minerals, forming quartz veins and fire lines, indicating that the open fractures formed in an extensional stress field. Elo & Korja (1993) have described areal extension in the SW–NE direction in the interpretation of seismic and gravity data from the Wiborg batholith.

My field observations indicate that the subvertical fractures with the orientation of SW–NE have at least two maxima: N55°E and N75°E. This feature is clearly observed in the southeastern part of the batholith (Fig. 24B) and also weakly seen in the rose diagrams of wiborgite and pyterlite (Figs. 30A and 30B). No filled fractures, quartz veins or fire lines have been observed in these directions (N55°E and N75°E), as the fractures are commonly tight and closed. As interpreted from the fracturing patterns, the fractures in the direction of N30°W are older than those in the directions of N55°E and N75°E, as they are filled fractures and they are cut by the tight and closed fractures. In addition, interesting rare

fracture directions of N30°E and N70°W occur, but the fractures are continuous and prominent, as they cut across the outcrops. My observations here differ from those presented previously. For example, Simonen (1987) demonstrated only one maximum peak in the SW–NE direction (N60°E). Parkkinen & Huomo (1978) identified at least two directions of lineaments in the NW–SE direction based on their interpretation of remote sensing. A lineament and fracturing pattern was connected to the early, syn and late phases of intrusion of the Wiborg batholith, but the model was never substantiated in the field.

The orientation of the dominant fractures can be predicted from the prominent microfractures in the ovoids in the wiborgite and pyterlite. Commonly, the two microfracture directions observed in the ovoids are parallel to the regional main subvertical fractures of the area. Occasionally, only one direction is seen in the ovoids, while the other direction is weakly developed. If observations are made from subvertical outcrops, the microfractures (microcracks) are parallel to the subhorizontal fractures (e.g. in Fig. 40A). This fracture geometry at different scales has also been implied by Pirhonen (1990), who demonstrated that the rectangular symmetry of the subvertical fractures and the fracture zones can be observed in satellite pictures, maps, aerial photographs, outcrops and even at the microscopic scale.

The fracture pattern in the rapakivi granites of the Wiborg batholith is mainly orthogonal, with two subvertical fracture directions perpendicular to each other accompanied by well-developed sheeting. A diagonal pattern is found in the southeastern parts of the batholith. The coarse-grained granites are more sparsely fractured than the fine-grained ones. The subhorizontal fractures are dominant in the batholith, often cutting the rapakivi granites into thin sheets in upper part of rock exposures (cf. Suominen 1980, Okko et al. 2003). Intensive subhorizontal fracturing can be observed, even at the depth of 10 m. The feature is frequent and dominant in all rapakivi granites, but especially in wiborgite, pyterlite and dark rapakivi granites, and can be found throughout the batholith. Sporadically, the subvertical fractures have been observed to be dominant instead of the subhorizontal ones.

Locally, the fracture pattern can vary significantly. The fracture pattern can differ between sites rather close to each other, as shown in the case study (Chapter 5.5). The differences in fracture patterns between these quarries can be due to their location in separate blocks of wiborgite divided by a weakness zone in the direction N30°W, as marked by an elongated band of small lakes (Fig. 33). The blocks might have different rock stress fields that could explain the difference in the fracture pattern. Another reason for the varying fracture systems could be that the quarries belong to different intrusion phases of wiborgite. The randomly selected benches in the quarries and their relative orientation could also have had an effect on the measurements. Variations in the local fracture pattern and in the related local stress fields in the eastern part of the Wiborg batholith have also been discussed by Meriluoto (2008).

Besides the appearance of rock, the soundness of the deposit is an essential precondition for feasible natural stone. Hence, the definition of fractures during exploration is of utmost importance. The directions and the spacing of fractures define the block size and form and are important in the planning of extraction (e.g. the correct direction of the back line). The case study (Chapter 5.5) of this doctoral thesis indicates that the orientations of fractures can vary significantly in closely located areas due to variations in rock stress in the bedrock, even in seemingly homogeneous rapakivi granite areas. This calls for care in the mapping of fracturing in the target area during exploration. Besides the orientation of the fractures, the type and mode of the fractures (open, closed, filled) are important aspects to be observed. Careful mapping of the fractures can also enable us to estimate the palaeo- and prevalent stress fields in the target area (e.g. Meriluoto 2008, Shekov 2015). These data can be utilised, for example, in quarry planning. For the mapping and interpretation of fracturing, a simple analysis of the deformational features of the exploration area should already be carried out in the desk study, because it would be beneficial for understanding the overall tectonics of the area.

8.2 Significance of weathering

Weathering of rocks is an essential subject in geology, and it has been a target of research for a long time (e.g. Goldich 1938). Nowadays, the weathering of stone is also of interest in the natural stone branch, and the study of weathering (durability) of memorial stones and gravestones has recently increased (e.g. Přikryl & Smith 2007). Rapakivi weathering is a special case of weathering and has attracted interest in Finland since the late 19th century (e.g. Sederholm 1891, Eskola 1930). However, no scientific research has been published on these issues in Finland since Kejonen (1985).

My observations indicate that the weathering in the Wiborg batholith mostly affects the coarse-grained rapakivi varieties: wiborgite, dark wiborgite, pyterlite, porphyritic rapakivi granite and dark rapakivi granite. The surficial parts of the outcropping bodies of these granites are affected by weathering of varying intensity. The weathering can reach from the surface down to 1–2 m depth, which is in accordance with estimates of <3 m by Kejonen (1985) and 0.5–1.5 m by Vallius (1995). The weathering is found as a surficial phenomenon on the outcrops, and randomly along subhorizontal and subvertical fractures. Usually, the weathering proceeds along subhorizontal fractures, making the rock look like sheets, as in Fig. 7. In particular regions of the study area, ca. 75–80% of the outcrops with the coarse-grained rapakivi types can be weathered. As seen in the samples and thin sections (Figs. 40 and 41), the structure of the rock is loosened along the weathered zones. In the weathered upper parts of the outcropping granites, the colour of the rock is altered and the soundness of the rock is diminished. The colour varies, for instance in the wiborgite, where it can change randomly from brown to reddish brown on outcrop. Most of the colour variations in the surficial parts of the rock exposures can be attributed to weathering.

Studies with impregnated rapakivi granite specimens and thin sections have demonstrated that the principal feature connected to weathering is the penetrative subhorizontal microfracturing, cutting through mineral grains and ovoids (cf. Eskola 1930). The subhorizontal fractures appear to break down the surficial parts of the rapakivi granite, and this is the essential factor at the beginning of the grusification process of the rock exposures. The weathering and grusification of rapakivi granites begins mechanically along subhorizontal and subvertical fractures. The older fractures have had a longer time to affect the minerals, and the alteration of minerals thus develops earlier in their directions (along the J1 fracture direction in Fig. 41). After this mechanical impact, the rapakivi granites begin to weather chemically, with the alteration of minerals towards the weathering processes, which could be both mechanical and chemical. The endogene alteration of K-feldspar is the early stage of weathering, followed by exogene weathering processes. This is the first step towards the weathering of rapakivi granites, but it does not explain the random grusification of rapakivi granites observed on outcrops.

In the course of the fieldwork in the Wiborg batholith, the real rock colour on outcrops was difficult to define because of the surficial weathering and staining. The colour of the rapakivi granite on outcrops almost invariably represents the colour of the weathered rock. Weathering did not usually influence the determination of the texture of the rock. Nevertheless, depending on the intensity of weathering, the texture of the rock can be masked, and the result of long-term weathering is sharp-edged gravel. However, in some cases, weathering enhanced the visibility of texture in the rapakivi granite.

The definition of macroscopic soundness was not a major challenge in the fieldwork because of the generally wide-spaced fracturing of the rapakivi granite in the study area. In contrast, microscopic soundness was heavily influenced by the surficial weathering of the granites. Even if the macroscopic fracturing was sparse enough for production, I could not be sure, based on outcrop observation alone, that the rock would also be sound on the microscopic scale. The observation that most of the outcrops with coarse-grained rapakivi types are weathered has a significant impact on the exploration for and assessment of natural stone. This stresses the need to use subsurface evaluation methods, especially in heavily weathered areas. Due to the strong surface weathering in the Wiborg batholith, diamond core drilling is an essential method to assist in the determination of the colour, but is also the most costly method. Hence, economical and easy-to-use sampling equipment for shallow core drilling should be utilised. Furthermore, alternative methods (e.g. geophysical) for studying weathering in rock are needed.

8.3 Novel application of geophysical and morphological data

8.3.1 Methodological aspects

I have used shallow sampling with a mini-drill or a hand-held saw, GPR and diamond core drilling as subsurface methods for investigating the rock properties beneath the outcrops.

These methods are commonly used in natural stone evaluation, and with these methods, the quality of rock can be adequately assessed. However, in the study area, shallow sampling was not a successful method for determining the subsurface properties. Neither the real colour of the rock nor its soundness could be determined, because the effects of weathering extend below the 5–10 cm depth of sampling obtained with the hand-held diamond saw. The mini-drill can be used for taking 15–25-cm-long cores with a diameter of 2.5–4.0 cm. This depth of vertical penetration is sufficient in most cases to obtain unweathered samples, but as shown by this study, it is not enough in the Wiborg batholith.

Diamond core drilling was invaluable in defining both the colour and the soundness of the rapakivi granites. With core drilling, the weathered surface zone could be penetrated and the depth of weathering exactly defined. While core drilling produces actual rock samples in which the colour and the soundness can be studied, and is a very useful method in natural stone investigations, it is also the most expensive one. A challenge with core drilling is also that a natural stone prospect or a deposit cannot be drilled as densely as, for instance, an ore body, because the drill holes can spoil otherwise good-quality stone. As a natural stone prospect cannot be extensively drilled, alternative and non-invasive methods for studying the weathering of rock are required.

Subsurface fracturing is commonly investigated with GPR. The measurements are performed along cleaned investigation traverses directly on the bare rock surface, often using antennae of 200 MHz. Distinct subsurface horizontal or subhorizontal fractures can be defined with GPR. In general, GPR is suitable for studying the overall soundness of rapakivi granites, because they have a homogeneous structure with no ductile deformation, and the major subhorizontal fractures are consequently easily detectable (Luodes 2007a, 2007b, 2015). However, the resolution of GPR with the commonly used 200 MHz antennae is not sufficient to detect the loosened and weathered surface of rapakivi granite. Many properties in the weathered portions can disturb the interpretation of the results of a GPR survey, comprising uneven contours of the weathered parts, gradual lower contact to the fresh rock, and uneven moisture conditions in the weathered rock. These can cause scattering of energy and attenuation of the GPR pulse, and the radargram received from the measurement can be ambiguous. The depth penetration of a GPR survey depends on the frequency of the antennae. With low frequencies, the signal can penetrate deeper, but the detection of small targets is insufficient. With higher frequencies, the detection of smaller details is better, but the penetration is shallow, although it can be enough for the study of surficial weathering. Thus, with high-frequency antennae of, for example, 400–1000 MHz, it might be possible to detect the weathered upper zone. In this case, however, the success of GPR heavily depends on favourable dielectric properties of the rock (cf. Markovaara-Koivisto et al. 2014).

Besides GPR, in the natural stone projects at GTK in which I have been involved, some other geophysical methods have been tested in the evaluation of natural stone prospects, including magnetic, electromagnetic VLF-R and EM31, seismic and microgravimetric methods (Elo 2006, Lanne 2007, Vartiainen 2017). It seems that while some of the geophysical methods could be applied in assessing the macroscopic fracturing of rock (especially in defining fracture zones), the evaluation of microfracturing and weathering was a more challenging task.

With the microgravimetric method, the thickness of the weathered surface part of the rock can be determined (Härmä & Selonen 2008). A microgravimetric study includes accurate gravity measurements along traverses, calculation of the standard Bouguer anomaly, calculation of regional terrain correction, modelling of the local features of the measurement site and analysis of the measurements (Elo 2006). The site should be free from soil cover. Furthermore, accurate GPS equipment capable of determining the vertical and horizontal coordinates within ±0.02 m should be used. The measured residual gravity minimum coincided relatively well with the mapped surficial weathering on outcrops, indicating the usefulness of the method. The results can still be improved, for instance with

more detailed modelling of the local characteristics of the measurement site (e.g. topographical features) and more precise knowledge of the density contrast between the weathered and unweathered rock (Elo 2006).

8.3.2 Application

In this study, the tested geophysical methods included electrical resistivity tomography (ERT), induced polarization (IP) and magnetic ground measurements. ERT measurements are not often applied in exploration, whereas the IP method is a frequent tool in ore prospecting (e.g. Vanhala & Peltoniemi 1992). ERT has, however, given good results when localizing fractures and fracture zones in bedrock (Huotari & Wennerström 2017), as well as in topographical studies (Sibul et al. 2017). In a marble quarry environment, ERT has been applied to detect properties such as fracturing, karstification and weathering (Uhlemann et al. 2018).

Electrical resistivity tomography (ERT) was carried out together with the measurement of *induced polarization (IP)* along four investigation traverses, and ERT alone along three traverses in the study area. ERT can be used alone (e.g. as in Uhlemann et al. 2018) to define the tectonic features in an area. In this study, the ERT method was, however, combined with IP, because I wanted to also test IP and to examine the combined effect of the methods. As shown by Azwan et al. (2015), for example, possible fractured areas can be identified more precisely with the combination of ERT and IP data. Methodologically, when IP is measured, ERT results can also be obtained during the same procedure. In all of the interpretation profiles, low ERT and high IP values were clearly observed along a 0.5–1-m-thick horizontal zone directly below the wiborgite outcrop. This refers to the higher porosity of the rock near the surface, where the pores are water-saturated. The ERT and IP values at the surface thus correlate well with the weathered zone in the upper parts of the rock. As the phenomenon was constantly observed in all of the interpreted profiles (examples shown in Figs. 46–49), the result can be regarded as reliable. It seems that the weathered surface zone could be slightly more distinguishable in the IP profiles. In the ERT profiles, a few highly conductive subvertical features could also be observed (examples given in the middle of the profiles in Figs. 46 and 47). Some indications of the same features could be detected in the IP profiles (Fig. 49). According to Azwan et al. (2015), if the subvertical fractures are open and not filled, for example with clay minerals, the IP might give a weaker response. These anomalies were investigated in the field, but due to the local thick soil cover, the exact location was not possible to identify. Being so distinct in the ERT profiles, these features are highly likely to be reflections of subvertical open fracture zones in the bedrock; an interpretation corresponding to that of Uhlemann et al. (2018). The results of the ERT and IP surveys indicate their good applicability for exposing the weathered surface of the rapakivi granite.

The electrode spacing for ERT and IP measurements in this study was 0.5 m or 1 m, depending on the investigation traverse, giving a depth extent of ca. 7–13 m in the middle of interpretation profiles. With denser electrode spacing, some depth penetration can be lost, but it is possible to detect small features (e.g. weathering) in the subsurface, mostly within the first 5 m below the outcrop surface. The possible minimum spacing between the electrodes could be 10–20 cm. The optimal distance between electrodes should be further tested in order to determine whether even closer electrode spacing would give a clearer picture of the upper parts of the rock. Better results could surely be achieved if the electrodes were bolted directly into the rock instead of into the loose soil, but this would be a very laborious and time-consuming process. A balance between the time used for the carrying out the measurements and the accuracy of the results should be found.

A high-resolution magnetic ground survey was conducted over the whole study area. The survey indicated homogeneous and low values, as expected for a felsic rapakivi granite with no specific magnetic sources. However, the measurement revealed a worm-shaped anomaly (Fig. 51). This could be interpreted as a structural feature, e.g. fractures or fracture zones, but no indications of this could be found on outcrop. A possible cause for the anomaly could be located below the surface, e.g. a dyke rock with higher magnetic properties than the wiborgite. The soil cover appears to be important, because its variable thickness can reduce the intensity of the magnetic anomalies and disturb the interpretation of the magnetic ground measurement. According to Vartiainen (2017), magnetic field fluctuations can often be connected to soil cover, so that covered small topographical lows on an outcrop can produce local minima in the general level of the magnetic

field. As the wiborgite of this study is not highly magnetic, the observed magnetic field variations here could also be caused by soil cover, not by the rock properties. Small changes in the total magnetic intensity in wiborgite can also complicate the interpretation.

No indication of the weathered surface of wiborgite was found in the high-resolution magnetic ground survey. Measurements indicated that it is only possible to detect some structural details of the bedrock with a high-resolution magnetic ground survey if the soil cover is thin or absent. The results indicate that the resolution of the method is not sufficient for assessing the soundness of the homogeneous wiborgite. In areas with several rock types of varying magnetic properties, the method could be more useful, for instance, in identifying the lithological contacts of certain rock types, such as diabase or soapstone (see, e.g., Selonen & Heldal 2003, Pirinen et al. 2018). If the distance between the measurement lines was smaller (e.g. 5 or 10 m) than the normally used 20-m spacing, it would improve the resolution, and a high-resolution magnetic ground survey might also give better results with homogeneous rock.

LiDAR data have been applied in geomorphology, but not often in mineral exploration (e.g. Meiser 2019). In this study, the LiDAR topography provided a few indications of features that could be interpreted as subvertical fractures or weakness zones in the bedrock (Fig. 52). However, these structures could not be observed on outcrops. The soil cover (or the weathering) can effectively disguise the topographical forms of the bedrock, and cause errors in the interpretation of LiDAR data. Hence, the method is more reliable in areas where the soil cover is thin or absent. In cases, LiDAR data integrated with, for example, geophysical magnetic ground measurement can increase the options to obtain a better interpretation of weakness zones or fracturing.

The results of the LiDAR measurement demonstrate that the resolution of the method was not sufficient for assessing the soundness of the wiborgite. The method is more appropriate for studying the topographical features on a larger scale than on prospects, and can be used earlier in the exploration process, such as while selecting targets for field mapping during the desk stage (cf. Selonen et al. 2014, Palmu & Nenonen 2015). Selonen et al. (2014) presented the relationships between topography, sheeting, fracture zones and the general soundness of rock in southern and central Finland. They concluded that these aspects could be utilized as guidelines for exploration in making prognoses on areas suitable for natural stone. LiDAR data could be well suited to this type of analysis.

Magnetic susceptibility, resistivity, density and natural gamma radiation were measured *in the drill hole in situ* in this study. In addition, the petrophysical properties of rock regarding porosity, susceptibility and density were defined from selected drill core samples. Anomalies in susceptibility and resistivity, as well as in density in the drill hole measurements correlated well with changes in the rock types and water saturation levels observed in the drill cores. The petrophysical results revealed that the resistivities of the drill core samples in the upper parts of the core are much lower than in the deeper parts of the core, confirming the results of the ERT survey. The petrophysical data from the deeper parts of drill cores provided a good estimate of the quality of the rock, with values indicating unweathered wiborgite, whereas the samples from wiborgite outcrops were all affected by weathering, further verifying the observations of surficial weathering obtained with other methods.

Even if the drill hole measurements corresponded well with the logging data from the drill cores, the usefulness of the measurements in natural stone exploration can be debated. Information on the petrophysical properties of drill core samples is always needed for the calibration of data from drill hole measurements, at least for susceptibility and density data, while petrophysical data act as reference for the interpretation of drill hole measurements. This is a complicated procedure in exploration, while the quality of rock can be observed in the actual drill core without drill hole measurements. If the measurements could be carried out in drill holes without calibration, the method would be more suitable for exploration. Drill hole measurements can be useful if the drill holes are so close to each other that information on the quality properties of the rock types measured from drill core samples can be extrapolated to the surroundings of the drill core. Another example could be when, for some reason, drill cores are not continuous. In this case, drill hole data could reveal the properties of the missing parts. However, further development should be carried out on the processing of the data from drill hole measurement in the future. The applicability of a drill hole survey in drill holes produced by percussion drilling instead of diamond core drilling should also be assessed.

I find the subsurface methods commonly used in natural stone evaluation insufficient for the weathered rapakivi granites in the Wiborg batholith. Diamond core drilling gives good results, but it is costly, with a total cost of ca. 300 euros per metre, including all work operations. For example, to study weathering in a prospect area such as that described in Chapter 7 with ten 10-m drill holes, the cost would be 30 000 euros.

Of the non-invasive geophysical methods, ERT, IP and microgravimetric methods are applicable for defining the dimension of the weathered surface. With ERT and IP, open subvertical fracture zones can be detected. The ERT and IP methods are more economical, with approximated costs of 2500 euros per working day, compared to core drilling. The total cost for the study area described in Chapter 7 would be approximately 5000 euros. ERT and IP are easier to use than the microgravimetric method, and are thus to be preferred.

The other tested, non-invasive geophysical and morphological methods, high-resolution magnetic ground survey and LiDAR, did not give sufficient results in assessing the soundness of the rock, and thus cannot be recommended for use in the evaluation of natural stone.

8.4 Natural stone potential of the Wiborg batholith

The Wiborg batholith has been an important resource for natural stone in Finland through time. The utilization of granite in the batholith dates back to Medieval times, when local granites were used in the construction of churches. The end of the 18th century marked the most important phase in the history of stone quarrying on the batholith, when vast amounts of rapakivi granite were used in the construction of the city of St Petersburg, Russia (Bulakh et al. 2010). In the 1970s, there was a significant increase in production when the full potential of the brown wiborgite (*Baltic Brown*) in the municipality of Ylämaa was discovered (Puntanen & Talka 1999). Nowadays, the demand for the current stone qualities is constant, and new stone qualities are always sought after by the natural stone market.

The observations of this study (Chapter 5) demonstrate that wiborgite and pyterlite have good future potential as natural stone, and the other main rock types at least moderate potential (Table 3). The reserves for both the current stone qualities and new stone qualities were determined in the detailed mapping of this study (see Chapter 8.1.1). This study emphasizes the significance of rapakivi granites of the Wiborg batholith as an important resource for natural stones in Finland and also in the global market.

8.4.1 Wiborgite

The main rapakivi granite type, wiborgite, is a well-known rock type in the natural stone market, having a typical rapakivi texture with large ovoids (diameter over 2 cm) (Fig. 17A). Wiborgite typically has a low frequency of fractures, and sites with fracturing sparse enough for extraction can easily be identified. Wiborgite has an intensive dark brown colour in large relatively uniform areas. Other potential colours include brown, light brown and green. Occasional shades of reddish or greenish brown can be found. The textural appearance of wiborgite can vary, but homogeneous areas with uniform texture can be found, creating preconditions for specifying new stone qualities. Sporadic pegmatite and aplite dykes, as well as quartz veins, are found. The potentiality of the wiborgite for future quarrying is good.

8.4.2 Dark wiborgite

Dark wiborgite is the variety of wiborgite with K-feldspar ovoids occasionally mantled with plagioclase and angular, dark-coloured plagioclase megacrysts (1–5 cm in diameter) in a dark-coloured matrix (Fig. 18). Dark wiborgite has a low frequency of fractures. The colour and the texture of the rock can vary, but homogeneous areas for production can be found. The potential colours comprise dark brown and black. Occasional shades of dark greenish brown are found. Sporadic quartz veins and aplite and pegmatite dykes can be observed. The dark wiborgite does not yet exist in the stone market, but has a good future potential for natural stone.

8.4.3 Pyterlite

Pyterlite is a well-known rock type in the natural stone market with a texture of rounded, densely dispersed K-feldspar ovoids lacking the rim of plagioclase (Fig 19). The density of fractures is typically low, allowing extraction. The potential colours of the pyterlite include red, brown and green. Sporadic variations in colour, including pale red and

brownish red, are found. The rapakivi texture is rather homogenous, with a slightly varying size of ovoids in the different intrusions. Areas of different uniform colours in pyterlite imply possible new stone qualities. Sporadically, aplite and pegmatite dykes, as well as quartz veins, can be observed. The pyterlite has a good future potential for natural stone.

8.4.4 Porphyritic rapakivi granites

Three main types of porphyritic rapakivi granites are found in the Wiborg batholith (Fig 20). The porphyritic rapakivi granites have a moderate potential for natural stone due to the limited distribution of the individual granite types (mainly in the northern part of the batholith). The density of fractures is generally acceptable, but the appearance of the granites is not yet well known in the stone market. The typical porphyritic rapakivi granites have an interesting colour combination, with bluish quartz and red K-feldspar. The sound Savitaipale granite has a beige colour (sometimes pale red), while the main colour of the Sinkko granite is grey (occasionally pale red). In the latter, subhorizontal fractures are, however, rather frequent. Occasional aplite dykes and quartz veins, as well as a red colour around some fractures, can be found in all varieties of the porphyritic rapakivi granites.

8.4.5 Even-grained rapakivi granites

Three main types of even-grained rapakivi granites are found as small separate intrusions in the Wiborg batholith. The red-coloured, even-grained biotite rapakivi granite is the most exploited, e.g. *New Balmoral* and *Kymen Red* (Fig. 16). The brown even-grained hornblende Lappee granite and the grey even-grained topaz-bearing Sääksjärvi granite have been locally extracted in the past. The potentiality of the even-grained rapakivi granites for natural stone is moderate, challenged by the relatively dense fracturing.

8.4.6 Dark rapakivi granites

Dark rapakivi granites consist of rock types with varying texture but with a similar mineralogical composition (Fig. 22). The dark rapakivi granites have a moderate potential for natural stone due to varying texture and colour, and the relatively dense subhorizontal fracturing. The texture of the rocks varies from vaguely porphyritic to even-grained, and the grain size from fine to coarse-grained. Potential colours include dark green, dark greenish brown and black. Occasional shades of dark grey are observed. Homogeneous areas can be found inside the area of dark rapakivi granite with an even-grained texture, while the vaguely porphyritic dark rapakivi granites are challenged by the heterogeneity of the material. The dark rapakivi granites have not yet appeared on the stone market, but they could have potential as black granites on the gravestone market.

8.4.7 Aplitic rapakivi granite

The density of fractures in aplitic rapakivi granite is too high for the rock to be used in the production of natural stone.

8.4.8 Anorthosite

Anorthosite has a good potential for manufacturing gemstones, but only a moderate potential for natural stone production. This is because of the close spacing of fractures and the heterogeneity of the material.

Table 3. The properties of the main rock types of the Wiborg batholith in their assessment for natural stone suitability. Criteria according to the description in Chapter 2.1.

Granite type	Fracturing	Potential colours	Remarks	Potentiality
Wiborgite	Orthogonal fracture pattern, diagonal fractures in places. Spacing of the subvertical fractures 3–6 m and of the subhorizontal fractures 2–4 m on average	Brown Light brown Dark brown Dark green	Aplite and pegmatite dykes, quartz veins occasionally	Good
Dark wiborgite	Orthogonal fracture pattern. Spacing of the subvertical fractures 3–4 m and of the subhorizontal fractures 2–3 m on average	Dark brown Black	Occasional aplite and pegmatite dykes, quartz veins	Good (not yet on the stone market)
Pyterlite	Orthogonal fracture pattern, diagonal fractures in places. Spacing of subvertical fractures 3–5 m and of subhorizontal fractures 2–4 m on average	Red Brown Dark green	Sporadically aplite and pegmatite dykes quartz veins	Good
Porphyritic rapakivi granites	Orthogonal fracture pattern. Spacing of the subvertical fractures up to 4 m and of the subhorizontal fractures 2–3 m on average	Red Bluish red Beige Grey	Occasional aplite dykes and quartz veins. Red colourization around some fractures	Moderate
Even-grained rapakivi granites	Orthogonal fracture pattern and diagonal fracturing in places. Spacing of subvertical fractures up to 3 m and of subhorizontal fractures 1–2 m on average	Red Brown Grey	Red colour around some fractures. Variations in colour	Moderate
Dark rapakivi granites	Orthogonal fracture pattern and diagonal fracturing in places. Spacing of subvertical fractures 1–3 m and of subhorizontal fractures 1–2 m on average	Dark green Dark greenish brown Black	Variations in colour	Moderate (not yet on the stone market). Feasible on the gravestone market
Aplitic rapakivi granite	Diagonal and dense fracturing (1–2 m spacing)	Red		No
Anorthosite	Diagonal fracture pattern. Spacing of fractures 1–3 m	Black and variations of dark grey	White coloured plagioclase crystals	Moderate. Good as gemstones

8.5 Exploration process for natural stone in the Wiborg batholith

The common exploration process for natural stone presented in Fig. 8 (e.g. Luodes et al. 2000, Selonen et al. 2000, Selonen & Heldal 2003, Ashmole & Motloung 2008, Carvalho et al. 2008, Luodes 2015, Härmä et al. 2017), involving field mapping and shallow sampling, is not well suited to the rapakivi granites of the Wiborg batholith, because of the intensive surficial weathering documented in the previous chapters. Hence, the exploration process should be modified to be more suitable for the Wiborg batholith. A new, revised natural stone exploration process has been compiled and is presented in Fig. 57, comprising the individual steps of desk study, field mapping and detailed target studies.

In the suggested model, the exploration process starts with a reconnaissance phase, a desk study during which geological and geophysical data are combined with topographical data and compared with restrictions posed by the infrastructure and the environment using GIS software, or as a desk study utilising applicable maps. As a result of the desk study, a checklist of target areas for regional mapping is produced.

In the next phase, the selected target areas are mapped in the field, focusing on visual observations of the characteristics of the rock, such as colour, texture, soundness, fracturing and homogeneity. Because surficial weathering changes both the colour and the soundness of rapakivi granite, light core drilling with a depth penetration of 5–10 m is used to verify the thickness of the weathered zone, as well as the real colour and texture of the rock under the weathered surface of the most promising targets. The lateral width of surficial weathering, defined by light core drilling, can be extrapolated to the surrounding areas with subsurface ERT and IP methods. The electrical surveys should be positioned so that the drill holes are in the middle of the electrical traverses, as the depth extent is better in the middle. No cleaned investigation traverses are required, as the ERT and IP methods need a thin cover of soil on the outcrops. The process can be repeated in the several selected, potential target areas during regional mapping.

Sites for the detailed target studies can now be selected on the basis of the field mapping and the associated confirmation carried out with light core drilling and with ERT and IP. The selection by an experienced geologist is based on the colour, texture and soundness of the rock.

During detailed target studies, investigation traverses are prepared and mapped in ample detail to quantify and qualify the fractures of different dimensions and to elaborate the colour, texture and homogeneity of the rock. The subsurface properties of the prospect are investigated with combinations of GPR, ERT and IP, and diamond core drilling methods. It is recommendable to carry out the non-invasive geophysical exploration methods prior to diamond core drilling.

The most suitable geophysical method for defining the spacing between subhorizontal fractures during detailed target studies is GPR. ERT and IP methods are better suited to specifying the dimension of the weathered zone and the open subvertical fracture zones. The combined application of ERT and IP is suggested, as together they give more information on the bedrock than when used individually. When all the above-mentioned methods are applied in the study area, ERT and IP should be performed before cleaning the investigation traverses. These methods require a thin cover of soil on the outcrop, while GPR gives the best results when executed on a bare bedrock surface. In this way, ERT and IP profiles can also be placed at the same location as a GPR survey, and at the point where the soil is removed for mapping of the bedrock.

The depth extent of the most homogeneous and soundest parts of rocks defined by detailed mapping, light core drilling and geophysical methods should be verified by diamond core drilling down to the depth of 10–15 m. Inclined drill holes (e.g. 60°) are to be favoured in order the obtain more lateral information. Drill hole measurements can be carried out, as they are easy to execute in drill holes when the core drilling has already been completed. Larger block samples are extracted by drilling and wedging to evaluate the homogeneity of the rock, for aesthetic evaluation, and for laboratory tests (cf. Chapter 2.2.3).

The detailed target studies can be accompanied by test quarrying, during which, for example, 1000 m^3 of rock is extracted for test slabs. During quarrying, the drillability, and during processing, the sawability, flaming ability, honability and polishing ability are determined with special reference to possible weathering effects. The technical

properties of the rocks are defined using the latest EN standards.

If the criteria for good natural stone are satisfied, the prospect is ready for production. This can be launched when there is demand for the stone in question on the natural stone market, and once permits for extraction have been acquired.

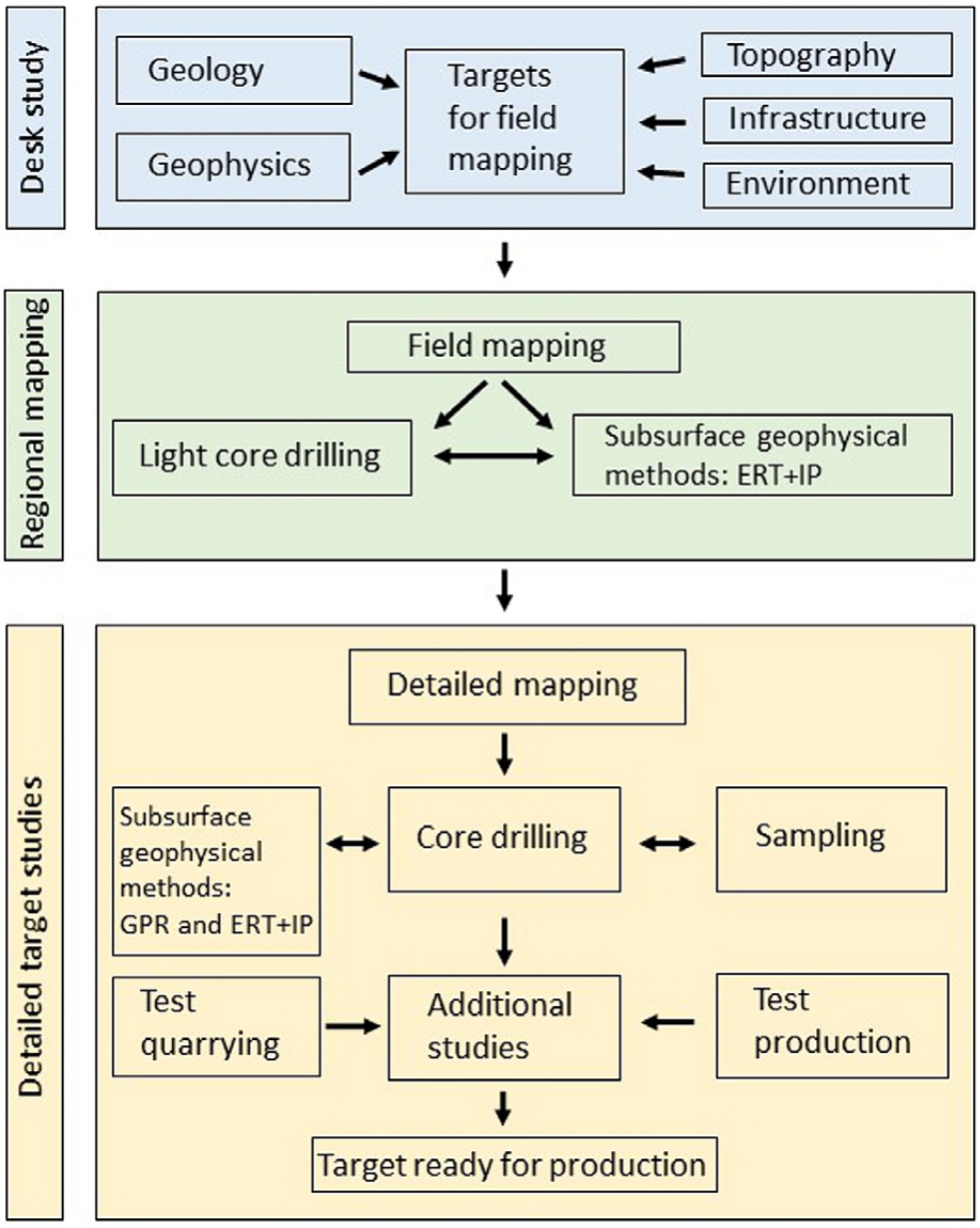

Fig. 57. A revised exploration process for natural stone, especially applied to the rapakivi granites of the Wiborg batholith. ERT = Electrical resistivity tomography, IP = induced polarization, GPR = ground penetrating radar. Environmental aspects are omitted. Modified from Luodes (2015).

9 CONCLUSIONS

The results presented in this doctoral thesis lead to the following conclusions:

1. Seven main rapakivi granite types have been defined in the Wiborg batholith: wiborgite, dark wiborgite, pyterlite, porphyritic rapakivi granite, even-grained rapakivi granite, dark rapakivi granite and aplitic rapakivi granite. The granite bodies are commonly found in a subhorizontal position.
2. Through detailed mapping, a more accurate picture of the lithology of the Wiborg batholith has been obtained, showing a variety of rocks with varying colour and appearance. Consequently, the number of potentially interesting areas for natural stone has increased.
3. The fracture orientation of N30°W is dominant in all rapakivi granite types. Two maxima in the SW–NE direction can be observed: N55°E and N75°E. The fracture orientations can vary due to the local rock stress field, even between nearby areas. This highlights the need for care while mapping the fractures during natural stone exploration, even in seemingly homogeneous granite areas.
4. Major parts (75–80%) of the outcrops of wiborgite, dark wiborgite, pyterlite and porphyritic rapakivi granite are weathered with varying intensity, from the surficial parts of outcropping granites to a depth of 1–2 m. Weathering changes both the colour and the soundness of the rapakivi granite.
5. The dimensions of surficial weathering should always be investigated in rapakivi granite areas. Electrical resistivity tomography (ERT) and induced polarization (IP) are the most applicable geophysical ground measurements in characterising the thickness of the weathered surface zone in the rapakivi granite. These methods are also suitable for characterising open subvertical fracture zones.
6. The thickness of the upper weathered zone, as well as the colour and soundness of rapakivi granite, can be reliably confirmed by diamond core drilling, but this is a costly method. More affordable light drilling equipment for shallow core sampling should be utilised. The depth penetration of the light core drill should be 5–10 m.
7. Based on the results of this study, a revised exploration process for natural stone was compiled to be applied especially to the weathered rapakivi granites in the Wiborg batholith. The process includes the individual steps of desk study, regional mapping and detailed target studies.
8. This study demonstrated that the natural stone potential for future quarrying in the Wiborg batholith is good. Prospects can especially be identified in areas dominated by wiborgite and pyterlite, but the commercially less known rapakivi varieties are also prospective.

ACKNOWLEDGEMENTS

I warmly thank my supervisors, Docent Olavi Selonen, Åbo Akademi University, and Professor O. Tapani Rämö, University of Helsinki, for their valuable comments and precious encouragement over the life span of the manuscript. The pre-examiners, Dr Vitali Shekov, Deputy Director of the Institute of Geology of the Karelian Research Center, Russian Academy of Sciences, and Docent Pekka Vallius, Geopex Oy, are commended for their thorough and critical comments on the manuscript, which considerably improved the text. I am also grateful to Professor Emeritus Ragnar Törnroos (University of Helsinki), who supervised this work at the beginning. Ms Taija Huotari, Geological Survey of Finland (GTK), is warmly thanked for sharing her expertise in geophysical surveys and for profound discussions on the development of the geophysical methods. Mr Heikki Sutinen (GTK) is acknowledged for giving insights into the GPR surveys. Mr Seppo Elo, Mr Heikki Forss, Mr Kai Nyman and Ms Tuire Valjus (all from GTK) contributed to the geophysical surveys, which is highly appreciated.

Ms Kirsti Keskisaari, Ms Mirjam Ajlani, Ms Riitta Turunen and Mr Fredrik Karell (all from GTK) are thanked for drawing maps, and Mr Jari Väätäinen (GTK) for taking the UV photos of the rock slabs. I also acknowledge my colleagues at GTK: Mr Timo Ahtola, Mr Pekka Karimerto, Mr Heikki Nurmi,

Mr Tuure Nyholm, Mr Heikki Pirinen, Mr Markku Putkinen, Mr Reino Räsänen, Dr Pekka Sipilä, Mr Pentti Toivonen, Mr Markus Torssonen, Mr Tuomo Turunen and Mr Jouko Vuokko, for their assistance in the fieldwork. The memorial stone company Vikmanin Kivi Ky is thanked for the preparation of the rock slabs, and Palin Granit Oy for access to the Ravijärvi site. Ms Päivi Kuikka-Niemi (GTK) provided valuable help with the final layout of this doctoral thesis. Dr Roy Siddall is thanked for the language revision.

This work was carried out in connection with various projects on natural stone exploration at GTK, which were partly supported by different funding programmes: the European Regional Development Fund (ERDF), the South-East Finland – Russia ENPI CBC Programme 2007–2013, and the European Agricultural Fund for Rural Development (EAFRD). Finally, I am grateful to my employer, the Geological Survey of Finland, for making it possible to accomplish this work.

10 REFERENCES

Aeromagnetic anomaly map of Finland. [Referred 14.6.2019]. Available at: https://hakku.gtk.fi/en/locations/search

Airo, M.-L. & Kiuru, R. 2012. Petrofysiikan perusteet. (Basics in petrophysics). Report Series in Geophysics No. 68. University of Helsinki, Division of geophysics and astronomy. 140 p.

Airo, M.-L. & Säävuori, H. 2013. Petrophysical characteristics of Finnish bedrock – Concise handbook on the physical parameters of bedrock. Geological Survey of Finland, Report of Investigation 205. 33 p. [Accessed 24.10.2019]. Available at: http://tupa.gtk.fi/julkaisu/tutkimusraportti/tr_205.pdf

Airo, M.-L. & Wennerström, M. 2010. Application of regional aeromagnetic data in targeting detailed fracture zones. Journal of Applied Geophysics 71 (2–3), 62–70.

Airo, M.-L., Elminen, T., Mertanen, S., Niemelä, R., Pajunen, M., Wasenius, P. & Wennerström, M. 2008. Aerogeophysical approach to ductile and brittle structures in the densely populated urban Helsinki area, southern Finland. In: Pajunen, M. (ed.) Tectonic evolution of the Svecofennian crust in southern Finland - a basis for characterizing bedrock technical properties. Geological Survey of Finland, Special Paper 47, 283–308. [Accessed 24.10.2019]. Available at: http://tupa.gtk.fi/julkaisu/specialpaper/sp_047_pages_283_308.pdf

Al-Ani, T. 2015. REE-bearing minerals in the Rapakivi Granite, Southern Finland. Open Geosciences 7, 646–662.

Al-Ani, T., Ahtola, T., Kuusela, J. & Al-Ansari, N. 2018. Mineralogical and Petrographic Characteristics of Indium and REE-Bearing Accessory Phases in the Kymi Granite Stock, Southern Finland. Natural Resources 9, 23–41.

Aristodemou, E. & Thomas-Betts, A. 2000. DC resistivity and induced polarisation investigations at a waste disposal site and its environments. Journal of Applied Geophysics 44, 275–302.

Arponen, E. & Rämö, T. 2005. Ylämaalta löytynyt uudentyyppinen seoskivi. (New hybrid rock identified in Ylämaa). Kivi 4, 6–7. (in Finnish)

Arponen, E., Härmä, P., Selonen, O., Luodes, H. & Pokki J. 2009. Anorthosite and spectrolite in the Wiborg rapakivi granite batholith and the lithological control of spectrolite deposits. Geological Survey of Finland, Report of Investigation 178. 41 p. (in Finnish with English summary). [Accessed 13.5.2019]. Available at: http://tupa.gtk.fi/julkaisu/tutkimusraportti/tr_178.pdf

Ashmole, I. & Motloung, M. 2008. Dimension stone: the latest trends in exploration and production technology. In: The International Conference on Surface Mining 2008 – Challenges, technology, systems and solutions – Papers. Johannesburg, Republic of South Africa: The Southern African Institute of Mining and Metallurgy, 35–70.

Azwan, M., Zawawi, M., Mat Toridi, N. & Wayayok, A. 2015. Detection of fractured aquifer using combination of resistivity and induced polarization analysis. Jurnal Teknologi (Sciences & Engineering) 76 (15), 119–124.

Bedrock aggregate. [Accessed 22.10.2019]. Available at: https://hakku.gtk.fi/en/locations/search

Berni, G. V., Wagner, T., Fusswinkel, T. & Wenzel, T. 2017. Magmatic-hydrothermal evolution of the Kymi topaz granite stock, SE Finland: Mineral chemistry evidence for episodic fluid exsolution. Lithos 292–293, 401–423.

Blenkinsop, T. G. 2008. Relationships between faults, extension fractures and veins, and stress. Journal of Structural Geology 30, 622–632.

Bradley, F., Founti, M. & Kontodimos, K. 2004. Commercial characteristics. In: Founti, M. (ed.) Stone for construction and architecture from extraction to the final product. OSNET Editions Volume 10. Athens: NTUA. 17–26.

Bulakh, A. & Abakumova, N. 2014. Stone Town Guide St Petersburg No. 1–5. ENPI Report. [Accessed 18.12.2019]. Available at: http://projects.gtk.fi/ENPI/results/history/city_guides.html

Bulakh, A. G., Abakumova, N. B. & Romanovsky, J. V. 2010. St. Petersburg – A History in Stone. St Petersburg: University Press. 173 p.

Calzia, J. P. & Rämö, O. T. 2005. Miocene rapakivi granites in the southern Death Valley region, California, USA. Earth-Science Reviews 73 (1), 221–243.

Carroll, D. 2012. Rock Weathering. Monographs in Geoscience. Springer Science & Business Media. 204 p.

Carvalho, J. F., Henriques, P., Falé, P. & Luís, G. 2008. Decision criteria for the exploration of ornamental-stone deposits: Application to the marbles of the Portuguese Estremoz Anticline. Int. J. Rock Mech. & Mining Sci. 45, 1306–1319.

Chambers, J. E., Kuras, O., Meldrum, P. I., Ogilvy, R. D. & Hollands, J. 2006. Electrical resistivity tomography applied to geologic, hydrogeologic, and engineering investigations at a former waste-disposal site. Geophysics 71, B231–B239.

Cook, N. J., Sundblad, K., Valkama, M., Nygård, R., Ciobanu, C. & Danyushevsky, L. 2011. Indium mineralisation in A-type granites in southeastern Finland: insights into mineralogy and partitioning between coexisting minerals. Chemical Geology 284, 62–73.

Deliormanli, A. H. & Maerz, N. H. 2016. Stress Related Fracturing in Dimension Stone Quarries. IOP Conf. Series: Earth and Environmental Science 44, 1–6.

Dempster, T. J., Hutton, D. H. W., Harrison, T. N., Brown, P. E. & Jenkin, G. R. T. 1991. Textural evolution of the rapakivi granites, south Greenland – Sr, O and H isotopic investigations. Contributions to Mineralogy and Petrology 107, 459–471.

Dempster, T. J., Jenkin, G. R. T. & Rogers, G. 1994. The origin of rapakivi texture. Journal of Petrology 35, 963–981.

Earle, S. 2015. Physical Geology. Victoria, B.C.: BCcampus. [Accessed 29.11.2019]. Available at: https://opentextbc.ca/geology/

Eklund, O. 1993. Coeval contrasting magmatism and magma mixing in Proterozoic post- and anorogenic granites, Åland, SW Finland. Academic dissertation, Åbo Akademi University, Department of geology and mineralogy. 57 p.

Eklund, O. & Shebanov, A. D. 1999. The origin of rapakivi texture by sub-isothermal decompression. Precambrian Research 95, 129–146.

Elliott, B. A. 2001. Crystallization conditions of the Wiborg rapakivi batholith, SE Finland: an evaluation of amphibole and biotite mineral chemistry. Mineralogy and Petrology 72, 305–324.

Elo, S. 2006. Progress and problems in near surface gravity [Electronic resource]. In: Near Surface 2006: 12th European Meeting of Environmental and Engineering Geophysics, 4-6 September 2006, Helsinki, Finland: extended abstracts & exhibitors' catalogue. Houten: EAGE. Optical disc (CD-ROM). 5 p.

Elo, S. & Korja, A. 1993. Geophysical interpretation of the crustal and upper mantle structure in the Wiborg rapakivi granite area, southeastern Finland. Precambrian Research 64, 273–288.

EN 12670:2019. Natural stone – Terminology. European Standard. European Committee for Standardization.

Enqvist, J. 2007. Virolahti. Osa II. Historiallisen ajan muinaisjäännösten inventointi 3.–28.9.2007. (Inventory of historic relicts). Helsinki: Museovirasto, rakennushistorian ja arkeologian osastot. 118 p. (in Finnish)

Enqvist, J. & Suhonen, V.-P. 2004. Loviisan maalinnoituksen inventointi vuonna 2004. (Inventory of Loviisa fortress). Helsinki: Museovirasto, rakennushistorian osaston arkisto. 26 p. (in Finnish)

Eskola, P. 1930. On the disintegration of rapakivi. Bulletin de la Commission géologique de Finlande 92 (8), 96–105.

Front, K., Paulamäki, S., Ahokas, H. & Anttila, P. 1999. Lithological and structural bedrock model of the Hästholmen study site, Loviisa, SE Finland. Posiva Oy, Posiva Report 99-31. 100 p.

Garré, S., Günther, T., Diels, J. & Vanderborght, J. 2012. Evaluating Experimental Design of ERT for Soil Moisture Monitoring in Contour hedgerow Intercropping Systems. Vadose Zone Journal 11, No. 4, 1–14.

Geotomo Software 2014. Lecture notes on 2D & 3D electrical imaging surveys. Tutorial: 2-D and 3-D electrical imaging surveys, Geotomo Software, Malaysia, February 2014. [Accessed 28.08.2019]. Available at: http://www.geoelectrical.com/

Goldich, S. S. 1938. A Study in Rock-Weathering. The Journal of Geology 46 (1), 17–58.

Haapala, I. 1974. Some petrological and geochemical characteristics of rapakivi granite varieties associated with greisen-type Sn, Be, and W mineralization in the Eurajoki and Kymi areas, southern Finland. In: Stemprok, M. (ed.) Metallization Associated with Acid Magmatism (MAWAM). Prague: Ústredniústavgeologický, 159–169.

Haapala, I. 1995. Metallogeny of Rapakivi granites. Mineralogy and Petrology 54, 149–160.

Haapala, I. & Lukkari, S. 2005. Petrological and geochemical evolution of the Kymi stock, a topaz granite cupola within the Wiborg rapakivi batholith, Finland. Lithos 80, 347–362.

Haapala, I. & Rämö, O. T. 1992. Tectonic setting and origin of the Proterozoic rapakivi granites of southeastern Fennoscandia. Transactions of the Royal Society of Edinburgh. Earth Sciences 83, 165–171.

Hackman, V. 1934. Das Rapakiwirandgebiet der Gegend von Lappeenranta (Willmanstrand). (The rapakivi area of Lappeenranta region). Bulletin de la Commission géologique de Finlande 106. 82 p.

Haldar, S. K. 2018. Mineral Exploration. Principles and Applications. 2nd edition. Elsevier. 378 p.

Harju, S., Rämö, O. T., Mänttäri, I. & Luttinen, A. V. 2010. The Taalikkala megaxenolith. In: Heinonen, A., Lukkari, S. & Rämö, O. T. (Compilers) Guide to the IGCP-510 (A-type Granites and Related Rocks through Time) Field Trip, Southeastern Finland, August 14–18, 2010. Department of Geosciences and Geography, University of Helsinki, C3, 22–25.

Härmä, P. & Selonen, O. 2008. Surface weathering of rapakivi granite outcrops – implications for natural stone exploration and quality evaluation. Estonian Journal of Earth Sciences 57 (3), 135–148.

Härmä, P. & Selonen, O. 2017. Spectrolite – a unique natural stone from Finland. Geotechnical report 4. Helsinki, Finland: The Finnish Natural Stone Association. 33 p. [Accessed 20.12.2019]. Available at: https://kivi.info/wp/wp-content/uploads/2019/10/Spectrolite_a-unique-natural-stone-from-Finland.pdf

Härmä, P. & Selonen, O. 2018. Natural stone production in the Wiborg rapakivi granite batholith in southeastern Finland. Geotechnical report 10. Helsinki: The Finnish Natural Stone Association. 34 p. [Accessed 25.12.2019]. Available at: https://kivi.info/wp/wp-content/uploads/2019/10/Natural-stone-production-in-the-Wiborg-rapakivi-granite-batholith-in-southeastern-Finland.pdf

Härmä, P., Airo, M.-L. & Selonen, O. 2013. The use of airborne geophysics in exploration for natural stone. Mineral deposits research for a high-tech world. 12th SGA Biennal Meeting 2013. Proceedings. Volume 4, 1796–1798.

Härmä, P., Luodes, H. & Selonen, O. 2005. Regional explorations of natural stone in Finland. In: Problems in the rational use of natural and technogenic raw materials from the Barents region in construction and technical material technology. Proceedings of Second International Conference 12–16 September 2005. Petrozavodsk: Russian Academy of Sciences. Karelian Research Centre. Institute of Geology.

Härmä, P., Luodes, H. & Selonen, O. 2006. Regional exploration projects for natural stone in Finland. 27th Nordic Geological Winter Meeting, January 9–12, 2006. Abstracts.

Härmä, P., Selonen, O. & Luodes, H. 2001. Prospecting of bedrock resources – dimension stones in a rapakivi granite area, a case history. In: Kuula-Väisänen, P. & Uusinoka, R. (eds) Proceedings of Aggregate 2001 – Environment and Economy. Helsinki, Finland 6–8 August 2001. Volume 1. Publication number 50 of Tampere University of Technology. Tampere: Laboratory of engineering geology, 175–179.

Härmä, P., Selonen, O. & Luodes, H. 2015. The Wiborg Granite Batholith – The Main Production Area for Granite in Finland. In: Lollino, G., Manconi, A., Guzzetti, F., Culshaw, M., Bobrowsky, P. T. & Luino, F. (eds) Engineering Geology for Society and Territory 5, 259–262.

Härmä, P., Vartiainen, R. & Selonen, O. 2017. Evaluation process for natural stone – best practices. In: Hölttä, P., Nenonen, K. & Eerola, T. (eds) 3rd Finnish National Colloquium of Geosciences, Espoo, 15-16 March 2017, Abstract Book. Geological Survey of Finland, Guide 63, 30–31. [Accessed 14.6.2019]. Available at: http://tupa.gtk.fi/julkaisu/opas/op_063_pages_030_031.pdf

Heikkinen, E., Saksa, P., Kurkela, S., Vuento, A. & Ruotsalainen, M. 2012. Kallion rikkonaisuuden geofysikaaliset tutkimukset graniittilouhimolla 2011. (Geophysical studies of soundness of rock at granite quarry 2011). Saimaan ammattikorkeakoulu, Etelä-Karjalan kiviklusteri -projekti. 57 p. (in Finnish)

Heinonen, A., Mänttäri, I., Rämö, O. T., Andersen, T. & Larjamo, K. 2016. *A priori* evidence for zircon antecryst entrainment in Proterozoic megacrystic granites. Geology 44, 227–230.

Heinonen, A., Rämö, O. T., Mänttäri, I., Andersen, T. & Larjamo, K. 2017. Zircon as a Proxy for the Magmatic Evolution of Proterozoic Ferroan Granites; the Wiborg Rapakivi Granite Batholith, SE Finland. Journal of Petrology 2017 (58), No. 12, 2493–2517.

Heldal, T. & Arvanitides, N. 2003. Exploration and prospecting – economic target selection. In: Terezopoulos, N. & Paspaliaris, I. (eds) Dimension stone quarrying in Europe and stability of quarrying operations. OSNET Editions Volume 2. Athens: NTUA, 13–23.

Heldal, T. & Lund, B. 1995. A regional study of the dimension-stone potential in labradorite-bearing anorthositic rocks in the Rogaland Igneous Complex. NGU Bulletin 427, 123–126.

Heldal, T. & Selonen, O. 2003. History and heritage. In: Selonen, O. & Suominen, V. (eds) Nordic Stone. Geological Science series. Paris: UNESCO publishing, 13–18.

Hibbard, M. J. 1981. The magma mixing origin of mantled feldspars. Contributions to Mineralogy and Petrology 76, 158–170.

Hiekkanen, M. 2018. Suomen keskiajan kivikirkot. (Medieval churches of Finland). 4. painos. Helsinki: Suomalaisen Kirjallisuuden Seura. 654 p. (in Finnish)

Hirn, S. 1963. Strövtåg i Österled. (Wandering eastward bound). Kulturhistoriska studier. Bidrag till kännedom av Finlands natur och folk 108. Helsinki: Finska Vetenskaps-Societeten. 279 p. (in Swedish)

Huotari, T. & Wennerström, M. (eds) 2017. Integroitujen geofysikaalisten ja kallioperägeologisten tutkimusmenetelmien kehittäminen yhdyskuntarakentamisen tarpeisiin. Summary: Development of integrated geophysical and bedrock geological research methods for civil engineering. Geological Survey of Finland, Report of Investigation 231. 140 p. [Accessed 29.11.2019]. Available at: http://tupa.gtk.fi/julkaisu/tutkimusraportti/tr_231.pdf

Huotari, T., Härmä, P., Sutinen, H. & Selonen, O. 2018. Geophysical measurements in a natural stone prospect in the Wiborg rapakivi granite batholith. Geological Survey of Finland, GTK Open File Work Report 84/2018. 41 p. [Accessed 22.10.2019]. Available at: http://tupa.gtk.fi/raportti/arkisto/84_2018.pdf

Ihalainen, P. 1994. Rapautumisen vaikutus eräiden rakennuskivien lujuusominaisuuksiin: tutkimusmenetelmien vertailu. Summary: The effect of weathering on the strength of some building stones. Academic dissertation, Technical University of Tampere. 123 p. (in Finnish with an English summary)

Jodry, C., Palma Lopes, S., Fargier, Y., Sanchez, M. & Côte, P. 2019. 2D-ERT monitoring of soil moisture seasonal behaviour in a river levee: A case study. Journal of Applied Geophysics 167, 140–151.

Karell, F. 2006. Magnetic fabric investigations on rapakivi granites in Finland. In: Kukkonen, I. T., Eklund, O., Korja, T., Pesonen, L. J. & Poutanen, M. (eds) Lithosphere 2006 – Fourth Symposium on the Structure, Composition and Evolution of the Lithosphere in Finland. Programme and extended Abstracts, Espoo, Finland, November 9–10, 2006. Institute of Seismology, University of Helsinki, Report S-46, 51–56.

Karell, F. 2013. Structure-related magnetic fabric studies: Implications for deformed and undeformed Precambrian rocks. Academic dissertation, Åbo Akademi University, Department of natural sciences, geology and mineralogy. Espoo: Geological Survey of Finland. 34 p. [Accessed 22.10.2019]. Available at: http://tupa.gtk.fi/julkaisu/erikoisjulkaisu/ej_087_synopsis.pdf

Karell, F., Ehlers, C. & Airo, M.-L. 2014. Emplacement and magnetic fabrics of rapakivi granite intrusions within Wiborg and Åland rapakivi granite batholiths in Finland. Tectonophysics 614, 31–43.

Karell, F., Ehlers, C., Airo, M.-L. & Selonen, O. 2009. Intrusion mechanisms and magnetic fabrics of the Vehmaa rapakivi granite batholith in SW Finland. Geotectonic Research 96 (1), 53–68.

Kaukiainen, Y. 2016. Punaiset pilarit. Suomalainen graniitti tsaarien Pietarissa. (Red pillars – Finnish granite in St Petersburg). Helsinki: Suomalaisen Kirjallisuuden Seura. 154 p. (in Finnish)

Kejonen, A. 1985. Weathering in the Wyborg rapakivi area, southeastern Finland. Fennia 163 (2), 309–313.

Kivi ry. (KIVI - Stone from Finland). Suomessa louhittavat kivilajit (Stones quarried in Finland). [Accessed 2.12.2019]. Available at: https://kivi.info/louhinta/suomessa-louhittavat-kivilajit/

Kinnunen, K. A. (ed.) 2017. Gemstones of Finland. Espoo: Geological Survey of Finland. 342 p. [Accessed 14.6.2019]. Available at: http://tupa.gtk.fi/julkaisu/erikoisjulkaisu/ej_098.pdf

Korja, A., Korja, T., Luosto, U. & Heikkinen, P. 1993. Seismic and geoelectric evidence for collisional and extensional events in the Fennoscandian Shield implications for Precambrian crustal evolution. Tectonophysics 219, 129–152.

Laitakari, I. & Simonen, A. 1963. Lapinjärven karttaalueen kallioperä. Summary: Pre-Quaternary Rocks of the Lapinjärvi Map-Sheet area. Geological Map of Finland 1:100 000, Explanation to the map of Pre-Quaternary Rocks, Sheet 3022. Geological Survey of Finland. 48 p. (in Finnish with an English summary). [Accessed 13.5.2019]. Available at: http://tupa.gtk.fi/kartta/kallioperakartta100/kps_3022.pdf

Laitala, M. 1984. Pellingin ja Porvoon kartta-alueiden kallioperä. Summary: Pre-Quaternary rocks of the Pellinki and Porvoo map-sheet areas. Geological Map of Finland 1:100 000, Explanation to the maps of Pre-Quaternary rocks, Sheets 3012 and 3021. Geological Survey of Finland. 53 p. (in Finnish with an English summary). [Accessed 13.5.2019]. Available at: http://tupa.gtk.fi/kartta/kallioperakartta100/kps_3012_3021.pdf

Lanne, E. 2007. Geophysical studies at Mutsoiva, Sodankylä, dimension stone deposit in 2005–2006. Geological Survey of Finland, archive report Q19/3731/2007/20/10. 13 p. (in Finnish). [Accessed 23.10.2019]. Available at: http://tupa.gtk.fi/raportti/arkisto/q19_3731_2007_20_10.pdf

Laurén, L. 1970. An Interpretation of the Negative Gravity Anomalies Associated with the Rapakivi Granites

and the Jotnian Sandstone in Southern Finland. Geologiska Föreningen i Stockholm Förhandlingar, 92, 21–34.

Lehijärvi, M. 1964. Lahden kartta-alueen kallioperä. Summary: Pre-Quaternary rocks of the Lahti Map-Sheet area. Geological Map of Finland 1:100 000, Explanation to the Map of Pre.Quaternary Rocks, Sheet 3111. Geological Survey of Finland. 40 p. (in Finnish with an English summary). [Accessed 13.5.2019]. Available at: http://tupa.gtk.fi/kartta/kallioperakartta100/kps_3111.pdf

Lehijärvi, M. & Tyrväinen A. 1969. Vuohijärvi. Geological Map of Finland 1:100 000, Pre-Quaternary Rocks, Sheet 3114. Geological Survey of Finland. [Accessed 13.5.2019]. Available at: http://tupa.gtk.fi/kartta/kallioperakartta100/kp_3114.pdf

Lehtinen, M. 1995. Lappeenrannan Ihalaisten muodostuman mineralogiasta ja geologiasta. (On mineralogy and geology of the Ihalainen deposit in Lappeenranta). Unpublished Lic. thesis, University of Turku, Department of Geology, Geology and Mineralogy, Turku, Finland. 127 p. (in Finnish)

Leinonen, S. 2005. Diamond drilling and core analysis. Promotion of natural stone industry in the Northern areas PNASTINA. Report of PNASTINA project. 16 p.

LiDAR UK. [Accessed 20.3.2019]. Available at: http://www.lidar-uk.com/what-is-lidar/

Loke, M. H. & Barker, R. D. 1996. Rapid least squares inversion of apparent resistivity pseudosections by a quasi-Newton method. Geophysical Prospecting (44), 131–152.

Loorents, K.-J. 2000. Sedimentary characteristics, brittle structures and prospecting methods of the flammet quartzite – a feldspacthic metasandstone in industrial use from the Offerdal Nappe, Swedish Caledonides. Academic dissertation, Earth Science Centre, Göteborg University, A48. 8 p.

Lorenz, W. & Gwosdz, W. 2003. Manual on the geological-technical assessment of mineral construction materials. Hannover: Geologische Jahrbuch, Reihe H, Heft SH 15. 498 p.

Lukkari, S. 2007. Magmatic evolution of topaz-bearing granite stocks within the Wiborg rapakivi granite batholith. Academic dissertation, University of Helsinki, Publications of the Department of Geology, D12. 29 p.

Lukkari, S., Thomas, R. & Haapala, I. 2009. Crystallization of the Kymi topaz granite stock within the Wiborg rapakivi granite batholith, Finland: evidence from melt inclusions. The Canadian Mineralogist 47, 1359–1374.

Lundén, E. 1979. Lappeenrannan Ihalaisten kalkkikiviesiintymän geologiasta. (On geology of the limestone deposit in Ihalainen, Lappeenranta). Vuoriteollisuus – Bergshanteringen 37, 20–23. (in Finnish)

Luodes, H. 2003. Exploration of natural stones in Finland. In: Kuula-Väisänen, P. & Uusinoka, R. (eds) Workshop on building stones. Helsinki, Finland August 7, 2001. Tampere University of Technology, Laboratory of engineering geology, Report 56, 11–13.

Luodes, H. 2007a. Ground penetrating radar in natural stone quality assessment. In: ISCORD, The 8th International Symposium on Cold Region Development, 25–27.9.2007 Tampere, Finland. Symposium proceedings, 257–258.

Luodes, H. 2007b. Natural stone assessment with ground penetrating radar. In: 15th Meeting of the Association of European Geological Societies. Georesources and public policy: research, management, environment, 16-20 September 2007, Tallinn, Estonia: abstracts. Tallinn: Geological Society of Estonia, 31–32.

Luodes, H. 2008. Prospecting of new natural stone types in Finland. In: Dimension stones: XXI century challenges. Proceedings of the Second International Congress, May, 29th–31st 2008, Carrara, Italy, 89–93.

Luodes, H. 2015. Ground penetrating radar and assessment of natural stone. Geological Survey of Finland, Report of Investigation 223. 46 p. [Accessed 12.5.2019]. Available at: http://tupa.gtk.fi/julkaisu/tutkimusraportti/tr_223.pdf

Luodes, H. & Sutinen, H. 2011. Evaluation and modelling of natural stone rock quality using ground penetrating radar (GPR). In: Nenonen, K. & Nurmi, P. A. (eds) Geoscience for Society, 125th Anniversary Volume. Geological Survey of Finland, Special Paper 49, 83–90. [Accessed 12.5.2019]. Available at: http://tupa.gtk.fi/julkaisu/specialpaper/sp_049_pages_083_090.pdf

Luodes, H., Huotari-Halkosaari, T., Sutinen, H., Härmä, P. & Selonen, O. 2014. Document of best practices on natural stone evaluation and research. ENPI report. 24 p. [Accessed 6.11.2019]. Available at: http://newprojects.gtk.fi/export/sites/projects/ENPI/results/documents/Document_of_best_practices_on_natural_stone.pdf

Luodes, H., Selonen, O. & Pääkkönen, K. 2000. Evaluation of dimension stone in gneissic rocks – a case history from southern Finland. Engineering Geology 58, 209–223.

Luodes, H., Sutinen, H., Härmä, P., Pirinen, H. & Selonen, O. 2015. Assessment of potential natural stone deposits. In: Lollino, G., Manconi, A., Guzzetti, F., Culshaw, M., Bobrowsky, P. T. & Luino, F. (eds) Engineering Geology for Society and Territory 5, 243–246.

Luodes, N., Pirinen, H., Bellopede, R. & Selonen, O. 2019. Frost resistance of natural stones – a case study from Finland. Kivi – Stone from Finland, Geotechnical Report 13. 27 p. [Accessed 20.10.2019]. Available at: https://kivi.info/wp/wp-content/uploads/2019/11/geotechnical_report_13_web.pdf

Luosto, U., Tiira, T., Korhonen, H., Azbel, I., Burmin, V., Buyanov, A., Kosminskaya, I., Ionkis, V. & Sharov, N. 1990. Crust and upper mantle structure along the DSS Baltic profile in SE Finland. Geophysical Journal International, 89–110.

Markovaara-Koivisto, M., Hokkanen, T. & Huuskonen-Snicker, E. 2014. The effect of fracture aperture and filling material on GPR signal. Bulletin of Engineering Geology and the Environment 73 (3), 815–823.

Meiser, M. 2019. Lidar Enlightens the Search for Critical Minerals. Using lidar to search for important minerals turns decades of work into a few years. [Accessed 5.8.2019]. Available at: https://lidarmag.com/2019/05/08/lidar-enlightens-the-search-for-critical-minerals/

Meriluoto, A. 2008. Puulan graniitin ja Viipurin rapakivibatoliitin Laapaksen alueen rakennegeologinen tulkinta. (Structural analysis of the Puula granite and the Laapas area in the Wiborg rapakivi granite batholith). Unpublished master's thesis, University of Turku, Department of Geology, Geology and Mineralogy, Turku, Finland. 61 p. (in Finnish)

Muinonen, M. 2014. Stone Town Guide Lappeenranta. ENPI Report. 60 p. [Accessed 30.10.2019]. Available at: http://projects.gtk.fi/export/sites/projects/ENPI/results/documents/lappeenranta_town_guide.pdf

Müller, A. 2007. Rocks explained 1. Rapakivi granites. Geology Today (23), No. 3, 114–120.

Muravyev, L. A., Sapunov, V. A., Narkhov, E. D. & Khasanov, I. M. 2019. Application of Overhauser Magnetometers in the Search for Ore and Placer Gold

and Diamonds Deposits. European Association of Geoscientists & Engineers. Conference Proceedings, Engineering and Mining Geophysics 2019. 15th Conference and Exhibition, Apr 2019, Volume 2019, 1–10.

Nekvasil, H. 1991. Ascent of felsic magmas and formation of rapakivi. American Mineralogist 76, 1279–1290.

Nishiyama, T. & Kusuda, H. 1996. Application of a fluorescent technique to the study of the weathering process. Engineering Geology 43 (4), 247–253.

Nykänen, O. & Meriläinen, K. 1991. Imatran kartta-alueen kallioperä. Summary: Pre-Quaternary Rocks of the Imatra Map-Sheet area. Geological Map of Finland 1:100 000, Explanation to the Maps of Pre-Quaternary Rocks, Sheets 4111, 4112. Geological Survey of Finland. 44 p. (in Finnish with an English summary). [Accessed 13.5.2019]. Available at: http://tupa.gtk.fi/kartta/kallioperakartta100/kps_4112_4111.pdf

Nyström, A. & Selonen, 0. 2004. Rapakivien rapautumisprosessissa liukenevat aineet. (Dilution of substances during weathering of rapakivi granite). Geologi 56, 208–212. (in Finnish)

Okko, O., Front, K. & Anttila, P. 2003. Low-angle fracture zones in rapakivi granite at Hästholmen, southern Finland. Engineering Geology 69, 171–191.

Ollier, C. 1984. Weathering. Second edition. Harlow: Longman Group. 270 p.

Paajanen, I. 2014. Stone Town Guide Kotka. ENPI Report. 44 p. [Accessed 30.10.2019]. Available at: http://projects.gtk.fi/export/sites/projects/ENPI/results/documents/kotka_town_guide.pdf

Palmu, J.-P. & Nenonen, K. 2015. Maaston laserkeilausaineistot maa- ja kallioperän korkokuvan ja rakenteiden heijastajana. Geologi 67, 18–25. (in Finnish)

Parkkinen, J. & Huomo, P. 1978. Viipurin massiivi, rakennetulkinta. (The Wiborg massif, a structural interpretation). Geologi 7, 57–62. (in Finnish)

Pirhonen, V. 1990. Porosity and focused dissolution of granitic rocks in two study areas in southern Finland. Aspects of methodology. Academic dissertation, Technical Research Centre of Finland, Publications 69. 109 p.

Pirinen, H., Leinonen, S. & Selonen, O. 2018. Soapstone from eastern Finland – characteristics and use. Geotechnical report 11. The Finnish Natural Stone Association. Helsinki, Finland. 33 p. [Accessed 20.10.2019]. Available at: https://kivi.info/wp/wp-content/uploads/2019/10/Soapstone-from-eastern-Finland-_-characteristics-and-use.pdf

Přikryl, R. & Smith, B. J. (eds) 2007. Building Stone Decay: From Diagnosis to Conservation. Geological Society, Special Publications. London: Geological Society of London. Volume 271. 339 p.

Puntanen, P. & Talka, A. 1999. Ylämaan historia. (The history of Ylämaa). Jyväskylä: Gummerus Kirjapaino Oy. 155 p. (in Finnish)

Rämö, O. T. 1991. Petrogenesis of the Proterozoic rapakivi granites and related basic rocks of southeastern Fennoscandia: Nd and Pb isotopic and general geochemical constraints. Geological Survey of Finland, Bulletin 355. 161 p. [Accessed 14.6.2019]. Available at: http://tupa.gtk.fi/julkaisu/bulletin/bt_355.pdf

Rämö, O. T. & Haapala, I. 1995. One hundred years of Rapakivi Granite. Mineralogy and Petrology 52, 129–185.

Rämö, O. T. & Haapala, I. 2005. Rapakivi granites. In: Lehtinen, M., Nurmi, P. A. & Rämö, O. T. (eds) Precambrian Geology of Finland – Key to the Evolution of the Fennoscandian Shield. Amsterdam: Elsevier B.V., 533–562.

Rämö, O. T., Turkki, V., Mänttäri, I., Heinonen, A., Larjamo, K. & Lahaye, Y. 2014. Age and isotopic fingerprints of some plutonic rocks in the Wiborg rapakivi granite batholith with special reference to the dark wiborgite of the Ristisaari Island. Bulletin of the Geological Society of Finland 86, 71–91.

Romu, I. (ed.) 2014. Best environmental practices (BEP) for natural stone production. The Finnish Environment 5/2014. Helsinki: Ministry of Environment. 133 p. (in Finnish with an English and a Swedish summary)

Sederholm, J. J. 1891. Über die finnländischen Rapakivigesteine. (On Finnish rapakivi granites). Tschermak's Mineralogische und Petrographische Mittheilungen 12, 1–31. (in German)

Selonen, O. 1998. Exploration for dimension stone – geological aspects. Academic dissertation, Åbo Akademi University, Department of geology and mineralogy. 64 p.

Selonen, O. & Härmä, P. 2003. Stone resources and distribution: Finland. In: Selonen, O. & Suominen, V. (eds) Nordic Stone. Geological Science series. Paris: Unesco publishing, 19–29.

Selonen, O. & Heldal, T. 2003. Technologies. In: Selonen, O. & Suominen, V. (eds) Nordic Stone. Geological Science series. Paris: Unesco publishing, 42–50.

Selonen, O., Ehlers, C., Härmä, P. & Nyman, R. 2012. Natural stone deposits in an assemblage of subhorizontal intrusions – The Kuru granite batholith. Bulletin of the Geological Society of Finland 84 (2), 167–174.

Selonen, O., Ehlers C., Luodes H. & Härmä, P. 2014. Exploration methods for granitic natural stones – geological and topographical aspects from case studies in Finland. Bulletin of the Geological Society of Finland 86, 5–22.

Selonen, O., Ehlers C., Luodes, H. & Karell, F. 2011. Magmatic constraints on localization of natural stone deposits in the Vehmaa rapakivi granite batholith, southwestern Finland. Bulletin of the Geological Society of Finland 83, 25–39.

Selonen, O., Ehlers, C., Luodes, H. & Lerssi, J. 2005. The Vehmaa rapakivi granite batholith – an assemblage of successive intrusions indicating a piston-type collapsing centre. Bulletin of the Geological Society of Finland 77, 65–70.

Selonen, O., Jauhiainen, P. & Härmä, P. 2018. Luonnonkiviteollisuuden eurooppalaiset standardit ja CE-merkintä. (European standards and CE marking for natural stone products). Tekninen Tiedote (Technical communication) Nro 5. Helsinki: The Finnish Natural Stone Association. 13 p. (in Finnish). [Accessed 5.11.2019]. Available at: https://kivi.info/wp/wp-content/uploads/2019/10/LUONNONKIVITEOLLISUUDEN-EUROOPPALAISET-STANDARDIT-JA-CE-MERKINT%c3%84.pdf

Selonen, O., Luodes, H. & Ehlers, C. 2000. Exploration for dimensional stone — implications and examples from the Precambrian of southern Finland. Engineering Geology 56, 275–291.

Shadmon, A. 1996. Stone: an introduction. Second edition. London: Intermediate Technology Publications. 172 p.

Shekov, V. 2015. Free of stress massif as a source for dimensional stone deposits. Proceedings of 15th International Multidisciplinary Scientific Geoconference SGEM 2015, Science and Technology in Geology, Exploration and Mining, Vol. III, 313–321.

Sibul, I., Plado, J. & Jõeleht, A. 2017. Ground-penetrating radar and electrical resistivity tomography for mapping bedrock topography and fracture zones: a case study in Viru-Nigula, NE Estonia. Estonian Journal of Earth Sciences 66 (3), 142–151.

Siegesmund, S. & Snethlake, R. (eds) 2014. Stone in architecture. Properties, durability. 5th edition. Berlin Heidelberg: Springer-Verlag. 550 p.

Simonen, A. 1973. Hamina. Geological Map of Finland 1:100 000, Pre-Quaternary Rocks, Sheet 3042. Geological Survey of Finland. [Accessed 13.5.2019]. Available at: http://tupa.gtk.fi/kartta/kallioperakartta100/kp_3042.pdf

Simonen, A. 1987. Kaakkois-Suomen rapakivimassiivin kartta-alueiden kallioperä. Summary: Pre-Quaternary Rocks of the Map-Sheet areas of the rapakivi massif in SE Finland. Geological Map of Finland 1:100 000, Explanation to the Maps of Pre-Quaternary Rocks, Sheets 3023 + 3014, 3024, 3041, 3042, 3044, 3113, 3131 and 3133. Geological Survey of Finland. 49 p. (in Finnish with an English summary). [Accessed 13.5.2019]. Available at: http://tupa.gtk.fi/kartta/kallioperakartta100/kps_3023_3014_3024_3041_3042_3044_3113_3131_3133.pdf

Simonen, A. & Tyrväinen, A. 1981. Savitaipaleen kartta-alueen kallioperä. Summary: Pre-Quaternary Rocks of the Savitaipale Map-Sheet area. Geological Map of Finland 1:100 000, Explanation to the Maps of Pre-Quaternary Rocks, Sheet 3132. Geological Survey of Finland. 29 p. (in Finnish with an English summary). [Accessed 13.5.2019]. Available at: http://tupa.gtk.fi/kartta/kallioperakartta100/kps_3132.pdf

Slater, L. D. & Lesmes, D. 2002. IP interpretation in environmental investigations. Geophysics 67, No. 1, 77–88.

Stan, D. & Stan-Kłeczek, I. 2014. Application of electrical resistivity tomography to map lithological differences and subsurface structures (Eastern Sudetes, Czech Republic). Geomorphology 221, 113–123.

Stevens, R. 2010. Mineral Exploration and Mining Essentials. Port Coquitlam: Pakawau GeoManagement Inc. 322 p.

Stimac, J. A. & Wark, D. A. 1992. Plagioclase mantles on sanidine in silicic lavas, Clear Lake, California: implications for the origin of rapakivi texture. Geological Society of America Bulletin 104, 728–744.

Suhonen, V.-P. 2007. Loviisan Bastion von Rosenin arkeologiset tutkimukset vuonna 2007. (Studies on Bastion von Rosen of the Loviisa fortress in 2007). Helsinki: Museovirasto, rakennushistorian osaston arkisto. 27 p. (in Finnish)

Suhonen, V.-P. (ed.) 2011. Suomalaiset linnoitukset 1720-luvulta 1850-luvulle. (The Finnish fortresses from 1720's to 1850's). Helsinki: Suomalaisen Kirjallisuuden Seura. 349 p. (in Finnish)

Sundblad, K., Cook, N. J., Nygård, R., Eklund, O., Valkama, M., Penttinen, K., Nygård, N., Rimaila, R., Paadar, J., Lammi, M., Seifert, T., Karell, F., Huhma, H. & Airo, M.-L. 2008. Polymetallic Metallogeny in the Wiborg Batholith, Fennoscandia Shield. 33rd International Geological Congress, Oslo, August 6th-14th 2008, Abstract CD-ROM.

Suominen, V. 1980. Loviisan Hästholmenin kallioperän rakoilusta. (On fracturing of bedrock in Hästholmen, Loviisa). Ydinjätteiden sijoitustutkimukset, Tiedonanto - Nuclear waste disposal study project, Communications 13. 17 p. (in Finnish)

Suominen, V. 1981. Loviisan Hästholmenin rapakiven petrografia ja raontäytemineraalit kallionäytekairauksien Y1 ja Y2 perusteella. (Petrography of rapakivi granites and filling minerals in fractures based on diamond core drillings Y1 and Y2). Ydinjätteiden sijoitustutkimukset, Tiedonanto - Nuclear waste disposal study project, Communications 19. 26 p. (in Finnish)

Tahvanainen, T., Heikkinen, E., Niemi, M., Saksa, P. & Vuento, A. 2013. Geofysikaalisten mittaustulosten ja louhinnan aikaisten havaintojen vertailu graniittilouhimolla. (Comparison of geophysical measurements and observations during quarrying at granite quarry). Saimaan ammattikorkeakoulun julkaisuja Sarja A: Raportteja ja tutkimuksia A 37. 39 p. (in Finnish)

Uhlemann, S., Chambers, J., Falck, W., Tirado Alonso, A., Fernández González, J. & Espín de Gea, A. 2018. Applying Electrical Resistivity Tomography in Ornamental Stone Mining: Challenges and Solutions. Minerals 8. 491 p. [Accessed 11.12.2019]. Available at: http://www.mdpi.com/journal/minerals

Ungureanu, C., Priceputu, A., Liviu Bugea, A. & Chirică, A. 2017. Use of electric resistivity tomography (ERT) for detecting underground voids on highly anthropized urban construction sites. Procedia Engineering 209, 202–209.

Uusinoka, R. 1983. Rapautumisilmiöt kallioperässä. (Weathering of bedrock). Rakennusgeologinen yhdistys - Byggnadsgeologiska föreningen ry. Julkaisuja 15. Papers of the Engineering Geologcial Society of Finland, 15. 28 p.

Valkama, M. 2019. Rapakivi-related In-rich mineralisations in southeastern Fennoscandia. Doctoral Dissertation, Turun yliopiston julkaisuja – Annales Universitatis Turkuensis sarja – ser. AII, Osa – tom. 352. 132 p.

Valkama, M., Sundblad, K., Nygård, R. & Cook, N. 2016. Mineralogy and geochemistry of indium-bearing polymetallic veins in the Sarvlaxviken area, Lovisa, Finland. Ore Geology Reviews 75, 206–219.

Vallius, P. 1995. The Suitability of Rapakivi Granite Varieties of the Wiborg Batholith for the Production of Asphalt Pavements. Academic dissertation, University of Helsinki, Department of geology, FinnRA research reports 1/1995. Helsinki: Finnish National Road Administration. 109 p.

Vanhala, H. 1997. Mapping oil-contaminated sand and till with the spectral induced polarization (SIP) method. Geophysical Prospecting 45, 303–326.

Vanhala, H. & Peltoniemi, M. 1992. Spectral lP studies of Finnish ore prospects. Geophysics 57, No. 12, 1545–1555.

Vartiainen, R. 2017. Evaluation of a natural stone prospect in Finnish Lapland – the Mutsoiva massive-type mica schist. Geotechnical report 5. Helsinki: The Finnish Natural Stone Association. 25 p. [Accessed 25.11.2019]. Available at: https://kivi.info/wp/wp-content/uploads/2019/10/Evaluation-of-a-natural-stone-prospect-in-Finnish-Lapland.pdf

Vernon, R. H. 2016. Rapakivi granite problems: plagioclase mantles and ovoid megacrysts. Australian Journal of Earth Sciences 63, 675–700.

Villar, A. 2017. Thermal and hydrothermal influence of rapakivi igneous activity on Late-Svecofennian granites in southeastern Finland. Unpublished master's thesis. University of Turku, Faculty of Mathematics and Natural Sciences, Department of Geography and Geology. 159 p.

Vorma, A. 1965. Lappeenrannan kartta-alueen kallioperä. Summary: Pre-Quaternary Rocks of the Lappeenranta Map-Sheet area. Geological Map of Finland 1:100 000, Explanation to the Map of Pre-Quaternary Rocks, Sheet 3134. Geological Survey of Finland. 72 p. (in Finnish with an English summary). [Accessed 13.5.2019]. Available at: http://tupa.gtk.fi/kartta/kallioperakartta100/kps_3134.pdf

Vorma, A. 1971. Alkali feldspars of the Wiborg rapakivi massif in southeastern Finland. Bulletin de la Commission géologique de Finlande 246. 72 p.

Vorma, A. 1972. On the contact aureole of the Wiborg rapakivi granite massif in southeastern Finland. Geological Survey of Finland, Bulletin 255. 28 p. [Accessed 14.6.2019]. Available at: http://tupa.gtk.fi/julkaisu/bulletin/bt_255.pdf

Vuorinen, A., Mantere-Alhonen, S., Uusinoka, R. & Alhonen, P. 1981. Bacterial weathering of rapakivi granite. Geomicrobiology Journal, 2, 317–325.

Wahl, W. 1925. Die Gesteine des wiborger Rapakiwigebietes. (The rocks of the Wiborg rapakivi area). Fennia 45 (20). 127 p.

Wark, D. A. & Stimac, J. A. 1992. Origin of mantled (rapakivi) feldspars: experimental evidence of a dissolution- and diffusion-controlled mechanism. Contributions to Mineralogy and Petrology 111, 345–361.

Zang, A. & Stephansson, O. 2010. Stress Field of the Earth's Crust. Book. Dordrecht: Springer Netherlands. 322 p.

Zhdanov, M. S. 2018. Foundations of Geophysical Electromagnetic Theory and Methods. 2nd edition. Amsterdam: Elsevier. 804 p.

All GTK's publications online at hakku.gtk.fi

This PhD thesis is a monograph that examines the surficial weathering of rapakivi granites in the classic Wiborg batholith of southeastern Finland and its impact on the exploration process for natural stone. The lithology, fracturing and outcrop weathering of the batholith were defined. In addition, the applicability of geophysical methods in natural stone exploration was tested in detecting weathered zones. The potentiality of the different rapakivi granite types of the Wiborg batholith for natural stone extraction was also evaluated. The lithological assemblage of the Wiborg rapakivi granite batholith is divided into seven main granite types. The fracture pattern in the rapakivi granite types is mainly orthogonal, but in the southeastern part of the batholith, diagonal patterns are also found. The upper parts of the rapakivi granites can be weathered down to a depth of 1–2 metres. The colour of the weathered and stained surface parts of the granite does not represent the real colour of the fresh rock, and the soundness of the rock is diminished. Core drilling is an essential method for determining the colour and soundness of the rock, but it is the most costly one. Of the non-invasive geophysical methods, electrical resistivity tomography (ERT) and induced polarization (IP) successfully exposed a ca. 1-m-thick weathered surficial zone of rapakivi granites and should be applied in the exploration of the Wiborg batholith. Based on the results of this study, a revised exploration process for natural stone, especially suited to the weathered rapakivi granites in the Wiborg batholith, is proposed, comprising a comprehensive set of desk study steps, regional mapping and detailed target studies. This study demonstrated that the natural stone potential for future quarrying in the Wiborg batholith is good.

gtk.fi

ISBN 978-952-217-405-5 (pdf)
ISBN 978-952-217-406-2 (paperback)
ISSN 0367-522X (print)
ISSN 2489-639X (online)